

**GENETIC ANALYSIS OF SIGNALING PATHWAYS MEDIATED BY
RECEPTOR LIKE PROTEIN SNC2 AND TRANSCRIPTION FACTOR SARD1
IN *ARABIDOPSIS THALIANA***

by

Weijie Huang

B. Sc., Sun Yat-sen University, 2015

A THESIS SUBMITTED IN PARTIAL FULFILLMENT OF
THE REQUIREMENTS FOR THE DEGREE OF

DOCTOR OF PHILOSOPHY

in

THE FACULTY OF GRADUATE AND POSTDOCTORAL STUDIES
(Botany)

THE UNIVERSITY OF BRITISH COLUMBIA
(Vancouver)

October 2022

© Weijie Huang, 2022

The following individuals certify that they have read, and recommend to the Faculty of Graduate and Postdoctoral Studies for acceptance, the dissertation entitled:

Genetic analysis of signaling pathways mediated by receptor like protein SNC2 and transcription factor SARD1 in *Arabidopsis thaliana*

submitted by Weijie Huang in partial fulfilment of the requirements for

the degree of Doctor of Philosophy

in Botany

Examining Committee:

Yuelin Zhang, Professor, Botany, UBC
Supervisor

James Kronstad, Professor, Microbiology and Immunology, UBC
Supervisory Committee Member

Siyun Wang, Associate Professor, Food Safety Engineering, UBC
University Examiner

Simone Diego Castellarin, Associate Professor, Land and Food Systems, UBC
University Examiner

Additional Supervisory Committee Members:

Xin Li, Professor, Botany, UBC
Supervisory Committee Member

Ivo Feussner, Professor, Plant Biochemistry, Georg-August-Universität Göttingen
Supervisory Committee Member

Abstract

Plant immune responses against pathogen infections can be activated by different receptors at the site of infection. Activation of local immune responses leads to establishment of systemic acquired resistance (SAR) at distal part of host plant. Salicylic acid (SA) and N-hydroxyphenylacetic acid (NHP) are two critical signaling molecules in plant immunity. Pathogen-induced increase of SA and NHP levels relies on their biosynthetic genes, which are transcriptionally regulated by two transcription factors, SAR Deficient 1 (SARD1) and CaM-Binding Protein 60 g (CBP60g). *Arabidopsis snc2-1D* (for *suppressor of npr1-1, constitute 2D*) is an autoimmune mutant carrying a gain-of-function mutation in the receptor-like protein SNC2. The constitutively activated defense responses in *snc2-1D* can be partially suppressed by *cbp60g*, and almost completely suppressed by *sard1 cbp60g*, suggesting that SARD1 and CBP60g are activated downstream of SNC2. My Ph. D. research aims to identify immune regulators downstream of SNC2 that lead to *SARD1* activation.

In a genetic screen searching for suppressors of *cbp60g-1 snc2-1D*, I identified a *bda7* mutant. Mapping-by-sequencing revealed that *BDA7* encodes the transcription factor CBP60b. Loss of *CBP60b* function causes partial suppression of the *cbp60g-1 snc2-1D* autoimmunity, including the elevated expression of *SARD1* in *cbp60g-1 snc2-1D*. Transient expression of *CBP60b* and a reporter gene driven by the *SARD1* promoter in *Nicotiana benthamiana* showed that *SARD1* expression can be activated by co-expression of *CBP60b*. Chromatin immunoprecipitation assay revealed that CBP60b directly targets *SARD1* promoter. In addition, *Arabidopsis* overexpression lines of *CBP60b* exhibit increased *SARD1* expression level and enhanced disease resistance.

These findings suggest that CBP60b functions downstream of SNC2 to activate *SARD1* expression.

Mutants of *BDA6* were also identified from the *cbp60g-1 snc2-1D* suppressor screen. Mapping-by-sequencing showed that *bda6* mutants carry mutations in the gene *Adaptor Protein 4 μ subunit (AP4M)*. Loss-of-function mutations in *AP4M* suppress the autoimmunity of *cbp60g-1 snc2-1D*, suggesting that the AP4 complex is required for defense responses mediated by SNC2. In addition, various receptor mediated immune responses are compromised in deletion mutants of *AP4M*, indicating that the AP4 complex plays broad roles in plant immunity.

Altogether, studies in this dissertation provide new insights on the regulation of SNC2-mediated immunity.

Lay Summary

Plants are not always healthy. Pathogen infections on crop plants can cause disasters like the great famine. Plants have evolved an immune system to recognize and react to pathogens. Recognition of pathogens leads to activation of a series of defense responses, including defense-related genes expression and accumulation of signaling molecules such as salicylic acid (SA) and N-hydroxyphenylacetic acid (NHP). To develop better strategies to enhance plant disease resistance, it is of great importance to study how plant defense responses are activated. Research in this dissertation identified two positive immune regulators in the model plant *Arabidopsis thaliana*. One of them is Calmodulin-Binding Protein 60 b, which is involved in promoting the biosynthesis of SA and NHP. Another is the Adaptor Protein 4 μ subunit, which likely contributes to the regulation of the subcellular localization of defense-related proteins. These discoveries improve our understanding on how plants regulate defense responses upon pathogen attack.

Preface

The work described in this thesis is the culmination of research from September 2015 through April 2022. Chapter 1 is the general introduction of plant immunity. Chapter 2 and Chapter 3 describes two research projects.

Part of Chapter 1 is modified from a published manuscript as below.

Weijie Huang*, Yiran Wang*, Xin Li and Yuelin Zhang. Biosynthesis and Regulation of Salicylic Acid and N-Hydroxypipicolinic Acid in Plant Immunity. (2020). *Mol. Plant*. 13, 31–41, <https://doi.org/10.1016/j.molp.2019.12.008> (*These authors contributed equally to this article.)

- The candidate and Yiran Wang drafted the manuscript. Xin Li and Yuelin Zhang edited the manuscript.

Chapter 2: *Arabidopsis* CALMODULIN-BINDING PROTEIN 60b plays dual roles in plant immunity was based on the following published manuscript:

Weijie Huang, Zhongshou Wu, Hainan Tian, Xin Li and Yuelin Zhang. *Arabidopsis* CALMODULIN-BINDING PROTEIN 60b plays dual roles in plant immunity, *Plant Communications* (2021), <https://doi.org/10.1016/j.xplc.2021.100213>

- The candidate performed most of the experiments. Zhongshou Wu helped with generating higher order mutants and co-immunoprecipitation assays. Hainan Tian helped with salicylic acid measurement. The candidate together with Xin Li, and Yuelin Zhang analyzed the data and wrote the manuscript. Yuelin Zhang designed and supervised the study.

Chapter 3: The ADAPTOR PROTEIN 4 complex is required for SNC2-mediated immunity

and pattern-triggered immunity was based on the following unpublished manuscript:

Weijie Huang, Hainan Tian and Yuelin Zhang.

- The candidate conducted most of the experiments. Hainan Tian helped with salicylic acid measurements. The candidate and Yuelin Zhang designed the experiments and analyzed the data. The candidate drafted and Yuelin Zhang edited the manuscript.

Table of Contents

Abstract	iii
Lay Summary.....	v
Preface.....	vi
Table of Contents	viii
List of Figures	xi
List of Abbreviations	xii
Acknowledgements	xix
Chapter 1: Introduction.....	1
1.1 Plant diseases.....	1
1.2 Plant innate immunity.....	2
1.2.1 PAMP-triggered immunity.....	2
1.2.1.1 PAMPs and Pattern recognition receptors	2
1.2.1.2 Activation of the PRR complexes	4
1.2.1.3 Defense responses downstream of PRR complexes.....	5
1.2.2 Effector triggered susceptibility	8
1.2.3 Effector-triggered immunity	10
1.2.3.1 Nucleotide-binding leucine-rich repeat receptors	10
1.2.3.2 Perception of pathogen effectors by plant NLRs.....	10
1.2.3.3 NLRs-mediated immune responses.....	12
1.3 Systemic acquired resistance.....	13
1.3.1 Signaling molecules in SAR.....	14
1.4 Biosynthesis and regulation of SA and NHP.....	15
1.4.1 SA biosynthesis in plants	16
1.4.2 Transcriptional regulation of SA biosynthetic genes	17
1.4.3 SA perception and downstream signaling.....	19
1.4.4 NHP biosynthesis.....	19
1.4.5 Transcriptional regulation of NHP biosynthetic genes	20
1.5 SARD1 and CBP60g.....	21
1.5.1 Regulation of SARD1 and CBP60g	21
1.6 SNC2-mediated immune pathways	22
1.7 Thesis objectives	25
Chapter 2: <i>Arabidopsis</i> CALMODULIN-BINDING PROTEIN 60b plays dual roles in plant immunity ...	27
2.1 Summary	27
2.2 Introduction	28
2.3 Materials and Methods.....	30
2.3.1 Plant materials and growth conditions	30
2.3.2 Constructs for generation of deletion mutants and transgenic plants.....	31
2.3.3 Mutagenesis and suppressor screen.....	32
2.3.4 Genetic mapping, mapping by sequencing and identification of <i>bda7-1</i>	33
2.3.5 Chromatin immunoprecipitation (ChIP) analysis	34
2.3.6 Dual reporter assay	34
2.3.7 RNA extraction, reverse transcription and qPCR	35
2.3.8 SA extraction and quantification	35
2.3.9 Pathogen infection assay	36

2.3.10	Statistical analysis.....	36
2.4	Results.....	37
2.4.1	Identification and characterization of <i>bda7-1 cbp60g-1 snc2-1D</i>	37
2.4.2	Map-based cloning of <i>BDA7</i>	39
2.4.3	Loss of <i>CBP60b</i> suppresses the autoimmunity of <i>cbp60g-1 snc2-1D</i>	39
2.4.4	<i>CBP60b</i> regulates <i>SARD1</i> expression.....	42
2.4.5	Overexpression of <i>CBP60b</i> leads to up-regulation of <i>SARD1</i> and enhanced disease resistance in <i>Arabidopsis</i>	44
2.4.6	<i>cbp60b</i> single mutants exhibit constitutively activated immune responses.....	46
2.5	Discussion.....	50
Chapter 3: The adaptor protein 4 complex contributes to plant immune regulation.....		54
3.1	Summary.....	54
3.2	Introduction.....	54
3.3	Materials and methods.....	58
3.3.1	Plant materials and growth conditions.....	58
3.3.2	Plasmid constructs and generation of transgenic plants and deletion mutants.....	59
3.3.3	Mutagenesis and suppressor screen.....	60
3.3.4	Genetic mapping, mapping-by-sequencing, and identification of <i>bda6</i>	60
3.3.5	RNA extraction, reverse transcription and qPCR.....	61
3.3.6	Co-immunoprecipitation analysis.....	61
3.3.7	Pathogen infection assay.....	62
3.3.8	Statistical analysis.....	63
3.4	Results.....	64
3.4.1	Identification and characterization of <i>bda6-1</i> , <i>bda6-2</i> and <i>bda6-3</i> from the <i>cbp60g-1 snc2-1D</i> suppressor screen.....	64
3.4.2	Map-based cloning of <i>BDA6</i>	66
3.4.3	Loss of AP4M suppresses the autoimmunity of <i>cbp60g-1 snc2-1D</i>	67
3.4.4	Mutations in AP4 subunits suppress the autoimmunity of <i>cbp60g-1 snc2-1D</i>	69
3.4.5	AP4 μ interacts with <i>BDA1</i> , a downstream regulator required for <i>SNC2</i> -mediated immunity.....	70
3.4.6	AP4 μ is required for both ETI and PTI.....	72
3.5	Discussion.....	75
Chapter 4: Conclusions and future directions.....		78
4.1	Conclusions.....	78
4.2	Future directions.....	80
4.2.1	<i>CBP60b</i> as a positive regulator in plant immunity.....	80
4.2.2	<i>CBP60b</i> in TNL-mediated immunity.....	81
4.2.3	Function of AP4 in plant immunity.....	82
4.2.4	Signaling partner(s) of <i>SNC2</i> in plant immunity.....	84
Bibliography.....		86
Appendices.....		103
Appendix A - Supplementary figures of Chapter 2.....		103
A.1	<i>bda7-1</i> is recessive.....	103
A.2	Map position and the mutation in <i>bda7-1</i>	103
A.3	Dot plots of frequency (f) of SNP mutations on five chromosomes in <i>bda7-1 cbp60g-1 snc2-1D</i> , as derived from Illumina sequencing.....	104
A.4	Sequences of deletion mutations in <i>CBP60b</i> generated by CRISPR/Cas9.....	105
A.5	Free and total SA levels in wild type (Col-0), <i>cbp60g-1 snc2-1D</i> , <i>bda7-1 cbp60g-1 snc2-1D</i> , and two CRISPR lines of <i>AT5G57580</i> in <i>cbp60g-1 snc2-1D</i> background (#4 and #1).	106
A.6	<i>bda7-1</i> can be complemented by <i>AT5G57580-3HA</i> driven by its native promoter.	106

A.7	Mutations in the conserved region around Leu148 affecting the functions of CBP60b and SARD1.	107
A.8	CBP60b protein levels in the three-week-old soil-grown overexpression lines. The loading is shown by Ponceau S staining of a non-specific band. The overexpression lines #21 and #27 were selected for further analysis.	108
A.9	Suppression of the dwarf morphologies of <i>cbp60b-5</i> , <i>cbp60b cbp60g-1</i> and <i>cbp60b cbp60g-1 sard1-1</i> by high temperature.	108
A.10	List of primers used in the study described in chapter 2. Information is assorted by different applications of the primers.	109
Appendix B - Supplementary figures of Chapter 3.....		114
B.1	Dot plots of frequency (f) of SNP mutations on five chromosomes in <i>bda6-1 cbp60g-1 snc2-1D</i> , as derived from Illumina sequencing.	114
B.2	Dot plots of frequency (f) of SNP mutations on five chromosomes in <i>bda6-2 cbp60g-1 snc2-1D</i> , as derived from Illumina sequencing.	115
B.3	Dot plots of frequency (f) of SNP mutations on five chromosomes in <i>bda6-3 cbp60g-1 snc2-1D</i> , as derived from Illumina sequencing.	116
B.4	Sequences of deletion mutations in <i>AP4M</i> and <i>AP4E</i> generated by CRISPR/Cas9.	117
B.5	List of primers used in the study described in Chapter 3. Information is assorted by different applications of the primers.	118

List of Figures

Figure 1.1 SNC2-mediated defense signaling.	24
Figure 2.1 Identification and characterization of <i>bda7-1 cbp60g-1 snc2-1D</i>	38
Figure 2.2 Deletion mutants of <i>AT5G57580</i> suppress the constitutively activated immunity of <i>cbp60g-1 snc2-1D</i>	41
Figure 2.3 Regulation of <i>SARD1</i> expression by CBP60b.	43
Figure 2.4 Overexpression of <i>CBP60b</i> leads to increased <i>SARD1</i> expression and enhanced resistance against <i>Hpa Noco2</i>	45
Figure 2.5 Knocking out <i>CBP60b</i> activates <i>EDS1</i> -dependent defense responses.	50
Figure 2.6 A working model of CBP60b in plant immunity.	53
Figure 3.1 Identification and characterization of <i>bda6 cbp60g-1 snc2-1D</i>	65
Figure 3.2 Map position of the <i>bda6</i> mutations.	67
Figure 3.3 Mutations in <i>AT4g24550</i> suppress autoimmunity of <i>cbp60g-1 snc2-1D</i>	68
Figure 3.4 Deletion mutants of <i>AP4E</i> suppress the dwarf phenotype of <i>cbp60g-1 snc2-1D</i>	69
Figure 3.5 AP4 μ interacts with BDA1.	71
Figure 3.6 Characterization of immune responses in knockout mutants of <i>AP4M</i>	74

List of Abbreviations

2,5-DHBA	2,5-dihydroxybenzoic acid
35S	A strong promoter from cauliflower mosaic virus
<i>A. thaliana</i>	<i>Arabidopsis thaliana</i>
ACD6	Accelerated cell death 6
ACS2/6	1-aminocyclopropane-1-carboxylic acid synthase 2/6
ADP	Adenosine diphosphate
AIM1	Abnormal inflorescence meristem 1
ALD1	AGD2-like Defense Response Protein 1
ANOVA	Analysis of variance
ANP2/3	Mitogen-activated protein kinase kinase kinase 2/3
AP4	Adaptor protein 4
AP4B	The gene that encodes AP4 β subunit
AP4E	The gene that encodes AP4 ϵ subunit
AP4M	The gene that encodes AP4 μ subunit
AP4S	The gene that encodes AP4 σ subunit
ATG9A	Autophagy related 9a
ATR1	An avirulence gene from <i>Hyaloperonospora arabidopsidis</i>
AvrE	An avirulence gene from <i>Pseudomonas syringae</i> pv. tomato DC3000
AvrPi-Ta	An avirulence gene from <i>Magnaporthe grisea</i>
AvrPphB	An avirulence gene from <i>Pseudomonas syringae</i> pv. tomato DC3000
AvrPto	An avirulence gene from <i>Pseudomonas syringae</i> pv. tomato DC3000
AvrPtoB	An avirulence gene from <i>Pseudomonas syringae</i> pv. tomato DC3000
AvrRpm1	An avirulence gene from <i>Pseudomonas syringae</i> pv. tomato DC3000
AvrRps4	An avirulence gene from <i>Pseudomonas syringae</i> pv. tomato DC3000
AvrRpt2	An avirulence gene from <i>Pseudomonas syringae</i> pv. tomato DC3000
BA	Benzoic acid
BAK1	BRI1-associated kinase 1
BDA1	Bian Da 1; Bian Da means “becoming big” in Chinese
<i>bda6</i>	<i>bian da 6</i> ; <i>bian da</i> means “becoming big” in Chinese

<i>bda7</i>	<i>bian da 7</i> ; <i>bian da</i> means “becoming big” in Chinese
BIK1	Botrytis-induced kinase 1
BOR1	Borate exporter 1
BRI1	Brassinosteroid insensitive 1
BSK1	Brassinosteroid-signaling kinase 1
CA	Cinnamic acid
CaM	Calmodulin
Cas9	CRISPR-associated 9
CBP60a	Calmodulin binding protein 60 a
CBP60b	Calmodulin binding protein 60 b
CBP60g	Calmodulin binding protein 60 g
CC domain	Coiled-Coil domain
CERK1	Chitin elicitor receptor kinase 1
cfu	Colony-forming unit
ChIP	Chromatin immunoprecipitation
CNGC	Cyclic nucleotide-gated channel protein
CNL	CC-NB-LRR protein
CPK5	Calmodulin-domain protein kinase 5
CRISPR	Clustered regularly interspaced short palindromic repeats
DEGs	Differentially expressed genes
DNA	Deoxyribonucleic acid
<i>E. coli</i>	<i>Escherichia coli</i>
EDS1	Enhanced disease susceptibility 1
EDS5	Enhanced disease susceptibility 5
EF-hand	A helix–loop–helix structural domain found in a large family of calcium-binding proteins
EF-Tu	Elongation factor thermo unstable
EFR	EF-Tu receptor
elf18	The peptide consisting of the first 18 amino acid of EF-Tu from <i>Escherichia coli</i>
EMS	Ethyl methanesulfonate

EMSA	Electrophoretic mobility shift assay
ETI	Effector-triggered immunity
ETS	Effector-triggered susceptibility
FLAG	An epitope protein tag composed of DYKDDDDK
flg22	A short peptide of the bacterial flagellin protein
FLS2	Flagellin-sensitive 2
FMO1	Flavin-dependent monooxygenase 1
FRK1	Flg22-induced receptor-like kinase 1
GATK	Genome analysis toolkit
GFP	Green fluorescent protein
GTL1	GT2-like 1
HA	An epitope protein tag composed of YPYDVPDYA from hemagglutinin
HopAI1	An avirulence gene from <i>Pseudomonas syringae</i> pv. tomato DC3000
HopF2	An avirulence gene from <i>Pseudomonas syringae</i> pv. tomato DC3000
<i>Hpa</i>	<i>Hyaloperonospora arabidopsidis</i>
HPCA1	Hydrogen-peroxide-induced Ca ²⁺ increases 1
HSD	Honestly significant difference
ICS	Isochorismate synthase
INA	2,6-dichloroisonicotinic acid
LB	Luria broth
<i>Ler</i>	Landsberg <i>erecta</i>
LRR	Leucine rich repeat
LYK5	Lysin motif-containing receptor kinase 5
LysM	Lysin motif
<i>M. oryzae</i>	<i>Magnaporthe oryzae</i>
MAPK	Mitogen-activated protein kinase
MAPKKK	Mitogen-activated protein kinase kinase kinase
MATE transporter	Multidrug and toxic compound extrusion transporter
MEKK1	Mitogen-activated protein kinase kinase kinase 1
MKK	Mitogen-activated protein kinase kinase

MKS1	Map kinase substrate 1
MPK	Mitogen-activated protein kinase
MS	Murashige and Skoog
<i>N. benthamiana</i>	<i>Nicotiana benthamiana</i>
NAD ⁺	Nicotinamide adenine dinucleotide
NADases	NAD ⁺ -cleaving enzymes
nahG	A salicylate hydroxylase identified in bacteria <i>Pseudomonas putida</i>
NB	Nucleotide-binding
NDR1	Non race-specific disease resistance 1
NHP	N-hydroxy-pipecolic acid
NLP	Necrosis and ethylene-inducing peptide 1-like protein
nlp20	A 20 amino acid peptide of Necrosis and Ethylene-Inducing Peptide 1-Like Protein
NLR	Nucleotide-Binding Leucine-Rich Repeats receptors
NPR	Non-Expresser of PR Genes
NRAMP3/4	Natural resistance-associated macrophage protein 3/4
NUDT	Nudix hydrolase
OD	Optical density
OsCEBiP	Rice chitin-elicitor binding protein
<i>P. syringae</i>	<i>Pseudomonas syringae</i>
P2C	Δ1-piperidine-2-carboxylic acid
PAD4	Phytoalexin deficient 4
PAL	Phenylalanine ammonia-lyase
PAMP	Pathogen-associated molecular pattern
PBL	PBS1-like protein
PBS1	AvrPphb susceptible 1
PBS3	AvrPphb susceptible 3
PCR	Polymerase chain reaction
PCRK	Pattern-triggered immunity compromised receptor-like cytoplasmic kinase 1

pg13	A 13 amino acid peptide of fungal endopolygalacturonases and the lipopolysaccharide from fungal cell wall component chitin
Phe	Phenylalanine
Pi-Ta	An R protein from rice
Pip	L-pipecolic acid
PopP2	An avirulence gene from <i>Ralstonia solanacearum</i>
<i>PR genes</i>	<i>Pathogenesis-related genes</i>
PRR	Pattern recognition receptor
<i>Psm</i> ES4326	<i>Pseudomonas syringae</i> pv. <i>maculicola</i> ES4326
<i>Pst</i> DC3000	Bacterial pathogen <i>Pseudomonas syringae</i> pv. <i>tomato</i> DC3000
<i>Pst</i> DC3000 <i>avrB</i>	Bacterial pathogen <i>Pseudomonas syringae</i> pv. <i>tomato</i> DC3000 carrying the avirulence gene <i>Avrb</i>
<i>Pst</i> DC3000 <i>avrRpm1</i>	Bacterial pathogen <i>Pseudomonas syringae</i> pv. <i>tomato</i> DC3000 carrying the avirulence gene <i>AvrRpm1</i>
<i>Pst</i> DC3000 <i>avrRpt2</i>	Bacterial pathogen <i>Pseudomonas syringae</i> pv. <i>tomato</i> DC3000 carrying the avirulence gene <i>AvrRpt2</i>
PTI	Pathogen-associated molecular pattern-triggered immunity
qPCR	Quantitative polymerase chain reaction
qRT-PCR	Quantitative reverse transcript-PCR
R proteins	Resistance proteins
RbohD	Respiratory burst oxidase homolog D
RIN4	RPM1 interacting protein 4
RLCK	Receptor-like cytoplasmic kinase
RLK	Receptor-like kinase
RLP	Receptor-like protein
RNA	Ribonucleic acid
ROS	Reactive oxygen species
RPM1	Resistance to <i>Pseudomonas syringae</i> pv. <i>maculicola</i> 1
RPP1	Recognition of <i>Peronospora Parasitica</i> 1
RPS2	Resistance to <i>Pseudomonas syringae</i> 2
RPS4	Recognition of <i>Peronospora parasitica</i> 4

RRS1	Resistance to <i>Ralstonia solanacearum</i> 1
RT-PCR	Reverse transcription PCR
SA	Salicylic acid
SAG	SA O- β -glucoside
SAG101	Senescence-associated gene 101
SAR	Systemic acquired resistance
SARD1	SAR deficient 1
SARD4	SAR deficient 4
SERK	Somatic-embryogenesis receptor-like kinase
SID2	SA induction deficient 2
SNC1	Suppressor of <i>npr1-1</i> , constitutive 1
SNC2	Suppressor of <i>npr1-1</i> , constitutive 2
<i>snc2-1D</i>	<i>suppressor of npr1-1, constitute 2D</i>
SNP	Single nucleotide polymorphism
SOBIR1	Suppressor of BAK1 interacting receptor kinase 1
SSLP	Simple sequence length polymorphism
T3SS	Type III secretion system
TGA	TGACG-binding factor
TGN	Trans-Golgi
TIR domain	Toll/Interleukin 1 Receptor domain
TMV	Tobacco mosaic virus
TNL	TIR-NB-LRR protein
tRNA	Transfer RNA
UGT76B1	UDP-dependent glycosyltransferase 76b1
v-cADPR	Variant-cyclic ADP-ribose
<i>Vd</i>	<i>Verticillium dahlia</i>
VPE	Vacuolar possessing enzyme
WRKY	A protein family of transcription factors containing a conserved heptapeptide motif WRKYGQK at the N-terminus and a novel zinc-finger-like motif at the C-terminus

YXXØ motif A tyrosine-based motif. Y, tyrosine residue; X, any amino acid; and Ø, an amino acid with a bulky hydrophobic side chain

ZAR1 Zygotie arrest 1

Acknowledgements

This thesis is completed with the assistance from many people.

First, I would like to express my gratitude to my supervisor Dr. Yuelin Zhang for his expertise, patience, encouragement, and substantial support during my Ph. D. studies. His intelligence and enthusiasm in research inspired and benefited me a lot. I am very grateful that he was always around and available for offering guidance and feedbacks.

I would like to thank my committee members, Dr. Xin Li, Dr. Ivo Feussner and Dr. James Kronstad for their insightful advice and questions and constructive discussions on my research projects. I would also like to thank Dr. George Haughn and Dr. Craig Berezowsky from Biol 234 teaching group for their thoughtful comments and discussion on teaching and education. My skills in both teaching and scientific presentation markedly improved during my TAship in Biol 234.

I am very grateful to my funding resources. China Scholarship Council financially supported my first four years of study and living in Vancouver. NSERC-PRoTECT provided funding to my research projects. Mitacs Globalink Research Award supported my research exchange in Georg August University of Göttingen, Germany.

I appreciate the cooperation and company with all current and past members of both Zhang lab and Li lab. In addition, I would like to extend my thanks to Lennart Mohnike, Isabel Maurus, Sherry Sun and Zhenxiang Li. I am so grateful that we had lots of unforgettable joyful moments

over my years of study, that we worked or marked at late nights, when we took coffee breaks in afternoons no matter cold or warm, rain or shine, or when we hiked or skied on the mountains, or cycled in the medieval town center of Göttingen, and visited museums in Amsterdam, ... etc. All these experiences cheered me up and kept me moving.

Last but not the least, I would like to thank my grandmother, my parents, uncle and aunt as their foresight and thoughts have deeply influenced me since I was a little child. I am very grateful and appreciate their understanding, great support, and sacrifice for my Ph. D. study. In addition, I would also like to express my appreciation to Serine Dy and her family, and Irene Yuen, for their kindness and consideration.

Chapter 1: Introduction

1.1 Plant diseases

There are about 320,000 species of plants on earth, of which green plants obtain energy from sunlight by photosynthesis and produce oxygen. Plants provide us not only grains, vegetables, and fruits, but also building materials and source of medicines. They are the basis of our daily life, and in a broader manner the fundamental of ecosystems. No matter where they live, trees in the wild, domesticated crops in our farms or even ornamental plants in green houses, they all constantly face various challenges from microbial pathogens, including bacteria, fungi, oomycetes, and viruses. Wide exposure of plants, particularly our monogenic crops, to pathogens can cause disaster like the great famine.

In nature, plants are healthy most of the time. The hydrophobic cuticle layers on epidermis and flexible stomata build up a physical barrier to prevent microbes from potential invasion into interior of plants (Melotto et al. 2017; Serrano et al. 2014). At cellular level, the cell wall also serves as a barrier to protect plant cells. However, adapted pathogens have evolved diverse strategies to overcome these barriers. Pathogenic bacteria such as *Pseudomonas syringae* (*P. syringae*) enter host plants through natural pores like hydathodes and stomata by secreting the toxin molecule coronatine to interfere with stomata closure, and then propagate in the apoplast spaces (Melotto et al. 2017). Fungi and oomycete, like *Magnaporthe oryzae* (*M. oryzae*) and *Hyaloperonospora arabidopsidis* respectively, can penetrate epidermal cells through penetration peg, and gain nutrients from host cells via a feeding structure named haustorium (Ribot et al. 2008; Schlaich and Slusarenko 2008). Successful colonization of plants by pathogen eventually causes plant diseases. For instance, bacterial pathogen *P. syringae* can infect a wide range of

plant species, such as *Arabidopsis thaliana*, *Nicotiana benthamiana*, and tomato. The causal oomycete pathogen of the great famine, *Phytophthora infestans*, colonizes on potato plants and leads to potato blight disease. The rice blast fungus *M. oryzae* also causes great yield loss of rice.

1.2 Plant innate immunity

Plants have evolved a sophisticated innate immune system to recognize their enemies, strengthen defensive structures and fight back. The plant innate immune system is a conceptual two-tiered system (Jones and Dangl 2006). The first tier is known as Pathogen-Associated Molecular Pattern (PAMP)-Triggered Immunity (PTI), in which defense signals are initiated from the plasma membrane-localized receptors. Effector-Triggered Immunity (ETI) is the second tier, which is mediated by intracellular or membrane-localized receptors recognizing effector proteins from pathogens. The two tiers of plant immunity function synergistically to protect plants against pathogens (Ngou, Ding, and Jones 2022).

1.2.1 PAMP -triggered immunity

1.2.1.1 PAMPs and Pattern recognition receptors

PAMPs are conserved molecules associated with groups of pathogens. They are usually part of indispensable proteins or structural components of pathogens which can be sensed by plants as elicitors to activate the defense mechanism (Zipfel 2014). One of the best studied PAMPs is flg22, a short peptide of the bacterial flagellin protein, which forms flagellum to enable movement of bacteria. The conserved 22 amino acid peptide localized at the N-terminus of bacterial flagellin is able to trigger defence responses in plants (Boller and Felix 2009). Another PAMP from bacteria is EF-Tu (for Elongation Factor Thermo Unstable), an abundant and highly

conserved protein in prokaryotes. It functions in translation of protein to transport tRNAs to ribosomes during elongation of the polypeptide chains. The peptide consisting of the first 18 amino acids of EF-Tu from *Escherichia coli* has elicitor activity to induce plant immunity (Boller and Felix 2009). Other examples of PAMPs include nlp20, a 20 amino acid peptide of NLP proteins (for Necrosis and ethylene-inducing peptide 1-Like Protein) produced by bacterial, oomycete and fungal microbes, pg13, a 13 amino acid peptide of fungal endopolygalacturonases and the lipopolysaccharide from fungal cell wall component chitin (Boller and Felix 2009; Zipfel 2014).

As the first step of initiating plant immunity, PAMPs are sensed by plant plasma-membrane localized Pattern Recognition Receptors (PRRs). PRRs can be structurally categorized into two classes, Receptor-Like Kinases (RLKs) and Receptor-Like Proteins (RLPs) (Dangl and Jones 2001). Both RLKs and RLPs carry a single transmembrane domain and extracellular domains which facilitate the perception of microbial PAMPs. RLKs have an intracellular kinase domain that transduce defense signals to its downstream components by protein phosphorylation. RLPs lack the kinase domain, suggesting that they require protein partners, likely RLKs, for signal transduction. Most characterized PRRs carry an extracellular leucine rich repeats (LRRs) domain, which creates an interface for protein-protein interaction or ligand-binding. For example, the extracellular LRR domain of *Arabidopsis* RLK Flagellin-Sensitive 2 (FLS2) can physically interact with bacterial flg22, resulting in recognition of the pathogen and activation of a series of downstream defense responses (Zipfel 2014). Similar to FLS2, the EF-Tu Receptor (EFR) in *Arabidopsis* specifically binds to the PAMP EF-Tu with its extracellular LRR domain and triggers plant immunity (Zipfel 2014). Some RLPs have also been discovered as PRRs.

Among them, *Arabidopsis* RLP23 and RLP42 can sense nlp20 and pg13 respectively (Albert et al. 2015; Zhang et al. 2021). Upon perceiving the corresponding PAMPs, these two RLPs recruit RLKs as partners, also called co-receptors, to form a protein complex to initiate defense signal transduction. Although reported PRRs are over-represented by the LRR type receptors, some other types of receptors were also identified. For instance, the *Arabidopsis* Chitin Elicitor Receptor Kinase 1 (CERK1), Lysin Motif-Containing Receptor Kinase 5 (LYK5) and rice Chitin-Elicitor Binding Protein (OsCEBiP) interact with chitin through their extracellular lysin motif (LysM) domains (Zhou and Zhang 2020; Zipfel 2014).

1.2.1.2 Activation of the PRR complexes

PRRs are immediately activated once they bind to the corresponding PAMPs, after which the PRR complexes are formed with other regulatory components to initiate a series of rapid downstream defense signalling events. During bacteria attack, the ligand-bound FLS2 and EFR undergo a conformation change and then recruit their co-receptors in the Somatic-Embryogenesis Receptor-Like Kinase (SERK) family such as Brassinosteroid Insensitive 1 (BRI1)- Associated Kinase 1 (BAK1), which also contain extracellular LRR domains (Zipfel 2014). Next, the Receptor-Like Cytoplasmic Kinase (RLCK) BIK1 (for Botrytis-Induced Kinase 1) is recruited and phosphorylated by the active FLS2/BAK1 or EFR/BAK1 complex (Lu et al. 2010; Zhou and Zhang 2020). The phosphorylated BIK1 also transphosphorylates FLS2/BAK1 and EFR/BAK1 to propagate the signalling. After activation by PRR complexes, BIK1 directly phosphorylates its downstream regulators such as Respiratory Burst Oxidase Homolog D (RbohD) to produce Reactive Oxygen Species (ROS) (Zhou and Zhang 2020), which have direct antimicrobial properties. The Cyclic Nucleotide-Gated Channel proteins CNGC2 and CNGC4,

which form a heteromeric calcium-permeable channel required for flg22-triggered calcium influx, were also shown to be direct substrates of BIK1. In addition to BIK1, a number of other RLCKs have also been reported as important defense regulators linking PRRs to downstream responses, including PBL1, PBL19, PBL27, BSK1 and PCRKs, etc (Liang and Zhou 2018; Zhou and Zhang 2020).

As RLP-type PRRs lack cytoplasmic kinase domain, they need co-receptors to activate downstream signaling components. For instance, the *Arabidopsis* nlp20 receptor RLP23 form a complex with BAK1 and another LRR receptor kinase SOBIR1 (for Suppressor of BAK1 Interacting Receptor Kinase 1) (Albert et al. 2015). RLP23 is associated with SOBIR1 at its resting status. When it gets activated by interaction with nlp20, RLP23/SOBIR1 recruits BAK1 and form a RLP23-BAK1-SOBIR1 heterotrimer, which then activates the downstream defense responses (Albert et al. 2015).

1.2.1.3 Defense responses downstream of PRR complexes

After PAMP perception, the activated PRR complexes trigger a variety of cellular responses to limit the pathogen growth. Callose deposition has been observed in the infected tissue of plants (Boller and Felix 2009; Luna et al. 2011). Callose, which is made of plant polysaccharide, is produced to repair and fortify cell wall damaged by pathogens. In *Arabidopsis*, the extracellular ROS content increases in minutes after treatment with PAMPs (Boller and Felix 2009; Zhou and Zhang 2020). The plasma-membrane localized NADPH oxidase RbohD is phosphorylated and activated by BIK1 (Kadota, Shirasu, and Zipfel 2015; Zhou and Zhang 2020), and catalyzes the production of ROS such as superoxide and peroxides, which can directly damage microbes in

apoplast. Interestingly, extracellular H₂O₂, a major form of ROS in plants, binds to and activates a LRR type receptor kinase Hydrogen-Peroxide-Induced Ca²⁺ Increases 1 (HPCA1) to promote plant defense responses (Wu et al. 2020), suggesting H₂O₂ is used as a signal for propagation of defense signaling.

Calcium influx happens a few seconds after PAMP treatments, which is dependent on calcium channels like CNGC2 and CNGC4 (Tian et al. 2019; Zhou and Zhang 2020). The increased cytoplasmic calcium concentration may lead to activation of the calcium binding motif-containing proteins. For example, RbohD carries an N-terminal calcium binding EF-hand domain and mutational analysis of this domain showed that RbohD-mediated ROS production requires calcium binding (Kadota et al. 2015). In addition, Calmodulin-domain Protein Kinase 5 (CPK5) is activated by calcium and was reported to phosphorylate RbohD to regulate its activity (Kadota et al. 2015). Transcription factors in the family of Calmodulin (CaM) Binding Protein 60 (CBP60) can bind CaM (Reddy, Ali, and Reddy 2002) and CaM-binding is required for the activity of CBP60g, which functions as a positive regulator of PTI (Wang et al. 2009). Therefore, calcium acts as a secondary messenger in the regulation of plant immunity.

PTI responses occurring within plant cells include activation of Mitogen-Associated Protein Kinase (MAPK) cascades, elevated production of defense hormones ethylene and salicylic acid (SA), and transcriptional re-programing (Boller and Felix 2009). Phosphorylation of MAPKs occurs after a few minutes of PAMP treatment in plants. There are three well-characterized MAPK cascades in plant immunity (Sun and Zhang 2022). One of them consists of MAPKKK3/5-MKK4/5-MPK3/6, activity of which is induced by different PAMPs such as

flg22, elf18 and nlp20. The RLCK PBL19 was shown to connect the chitin receptor CERK1 to this cascade. It was shown to phosphorylate MAPKKK5 and contributes to MAPKKK3/5-MKK4/5-MPK3/6 activation. Activation of MPK3/6 leads to the phosphorylation of the transcription factor WRKY33 leading to defense-related transcriptional reprogramming (Mao et al. 2011). Another known MAPK cascade is composed of MEKK1-MKK1/2-MPK4, which was shown to contribute to basal immunity. Like MPK3/6, MPK4 is activated by elicitors such as flg22. One of the MPK4 substrates is MKS1, a positive regulator in plant immunity (Andreasson et al. 2005). Lately, the MAPKKK ANP2/3 and MKK6 have been identified to function upstream of MPK4, pointing to a third defense-related cascade ANP2/3-MKK6-MPK4 (Lian et al. 2018).

Activation of the MKK4/5-MPK6 cascade by PAMP treatment leads to the phosphorylation of the ethylene biosynthetic enzymes ACS2/6 (1-aminocyclopropane-1-carboxylic acid synthase 2/6), which in turn initiate ethylene biosynthesis and accumulation (Liu and Zhang 2004). Ethylene signalling is important for accumulation of FLS2 and production of ROS (Boutrot et al. 2010; Mersmann et al. 2010; Wi, Ji, and Park 2012). *Arabidopsis* mutants defective in ethylene biosynthesis are compromised in plant immunity, suggesting a positive role of ethylene in plant immunity (Boutrot et al. 2010; Guan et al. 2015; Wi et al. 2012). Ethylene accumulation is one of the PTI responses that can be detected in hours after PAMPs treatments.

SA is another plant hormone accumulated during PTI (Boller and Felix 2009; Zhou and Zhang 2020). It has been known since 1990s that pathogen infection leads to drastic increase of SA levels in different plant species (Malamy et al. 1990; Métraux et al. 1990). Pathogens multiply

significantly more on *Arabidopsis* mutants deficient in SA biosynthesis or perception, implying an important role of SA in plant immunity (Cao et al. 1994; Delaney, Friedrich, and Ryals 1995; Nawrath and Métraux 1999). Treatment of PAMPs such as flg22 was shown to trigger the induction of SA level in plants (Tsuda et al. 2008).

PTI also leads to rapid massive transcriptional reprogramming (Boller and Felix 2009; Zhou and Zhang 2020). A recent transcriptome analysis revealed that PAMP treatments shape the transcriptional landscape in *Arabidopsis*, resulting in ~8,000 differentially expressed genes (DEGs) by flg22 treatment, and ~5,000 DEGs by nlp20 treatment (Bjornson et al. 2021). Around half of these DEGs are up-regulated genes, which include the defense marker genes *Pathogenesis-related (PR)* genes and SA biosynthetic genes. A few of these up-regulated genes have been used as PTI marker genes, such as the *flg22-Induced Receptor-like Kinase 1 (FRK1)* (Asai et al. 2002; De Torres et al. 2003).

1.2.2 Effector triggered susceptibility

Pathogens have evolved different strategies to infect host plant cells. To promote their virulence, pathogens deliver effectors, also named virulence factors, into host cells for suppression of PTI, which results in Effector-Triggered Susceptibility (ETS) in plants (Jones and Dangl 2006).

Pathogenic bacteria inject effectors into plant cells through a needle-like structure such as type III secretion system (T3SS) (Galán and Collmer 1999; Grant et al. 2006). Fungal and oomycete pathogens deliver effectors by the feeding structure haustorium (Ribot et al. 2008; Schlaich and Slusarenko 2008).

Effectors from the bacterial pathogen *P. syringae* were shown to target various PTI regulators including PRR complexes, downstream regulator RLCKs, as well as MAPK modules (Grant et al. 2006; Xin and He 2013). For example, the effector AvrPto targets FLS2-BAK1 and EFR-BAK1 complexes by blocking the kinase activity of FLS2 and EFR. AvrPtoB, which contains an E3 ubiquitin ligase domain, targets FLS2 and CERK1 for their degradation. The RLCK BIK1 and its paralogs are cleavage targets of the cysteine protease effector AvrPphB. PAMP-induced phosphorylation of BIK1 is diminished by effector HopF2, and HopF2 was also shown to target the MAPK cascade component MKK5 to suppress its kinase activity. Another MAPK targeting effector, HopAI1, inhibits MAPK cascade by physically interacting with and removing the phosphate group from MPK3, MPK4 and MPK6 through its phosphothreonine lyase activity.

Besides the critical PTI components, pathogen effectors also target plant regulators of different biological pathways. A phenomenon of aqueous apoplast, also called “water soaking”, in plant leaves is often observed after bacterial infection. Recent studies revealed that effector AvrE secreted by *P. syringae* T3SS, hijacks a negative regulator in abscisic acid pathway, causes the abnormal stomata activity, and consequently creates an aqueous apoplast space for better pathogen virulence and propagation (Hu et al. 2022). In addition, the effector VdSCP41 delivered by fungal pathogen *Verticillium dahlia* through haustorium, targets *Arabidopsis* defense-related master transcription factors SARD1 and CBP60g to inhibit their transcriptional activity (Qin et al. 2018).

1.2.3 Effector-triggered immunity

1.2.3.1 Nucleotide-binding leucine-rich repeat receptors

While pathogens can deliver effectors to suppress PTI, plants have evolved another kind of receptors, also known as resistance (R) proteins, to specifically recognize pathogenic effectors and trigger a robust and prolonged response, called ETI (Jones and Dangl 2006; Ngou et al. 2022). Although some R proteins in the RLP class are localized on plasma membrane, the majority of R proteins recognize effectors in intracellular space. These R proteins were found to possess a Nucleotide-Binding (NB) domain for protein oligomerization, and a Leucine-Rich Repeats (LRR) region believed to be involved in perception of effectors (Ngou et al. 2022; van Wersch et al. 2020). Based on the protein structure, these group of receptors are termed NB-LRR receptors (NLRs).

Plant NLRs are divergent in their N-terminus: some of them carry a Coiled-Coil (CC) domain, and others have a Toll/Interleukin 1 Receptor (TIR) domain. Based on the difference in their N-terminus, NLRs are subdivided into two groups, the CC-NB-LRRs (CNLs) and TIR-NB-LRRs (TNLs). CNL-mediated defense often relies on a membrane-localized protein called Non Race-Specific Disease Resistance 1 (NDR1), whereas signalling downstream of TNLs requires the lipase-like protein Enhanced Disease Susceptibility 1 (EDS1) (Aarts et al. 1998), suggesting two independent signaling mechanisms for the two groups of NLRs.

1.2.3.2 Perception of pathogen effectors by plant NLRs

Recognition of pathogen attack by plant NLRs is through either direct or indirect interaction with effectors. Different models have been proposed to describe how NLRs detect pathogen effectors

(Jones, Vance, and Dangl 2016). Examples such as *Arabidopsis* TNL RPP1 (Recognition of *Peronospora Parasitica* 1) and its cognate oomycete effector ATR1, rice NLR Pi-Ta and its corresponding effector AvrPi-Ta from *M. oryzae* (Krasileva, Dahlbeck, and Staskawicz 2010), fall into the model of direct interaction, where plant NLRs recognise effectors via direct physical interaction.

However, in many cases, direct interaction is not observed between NLRs and effectors. Instead, many NLRs monitor the modifications of host proteins, also known as guardees, which are targets of pathogen effectors (Van Der Hoorn and Kamoun 2008). The *Arabidopsis* RIN4 (RPM1 INTERACTING PROTEIN 4) involved in basal defense is one of the best studied guardees. *P. syringae* delivers effectors AvrRpt2 and AvrRpm1 to modify and de-activate RIN4 by cleavage and phosphorylation respectively (Kim et al. 2005). The resulted modified forms of RIN4 are recognized by two different plant CNLs, RPS2 (Resistance to *P. Syringae* 2) and RPM1 (Resistance to *P. Syringae* pv *Maculicola* 1) respectively, which leads to activation of ETI (Belkhadir et al. 2004; Grant et al. 2006; Mackey et al. 2003). The guard model is used to describe that plant NLRs guard the host defense-related proteins by sensing its modifications altered by effectors.

Researchers noticed that pathogen-secreted effectors do not always target host proteins with a role in disease resistance. In the example given previously, the effector AvrPphB from *P. syringae* cleaves host cytoplasmic kinase PBS1 (Grant et al. 2006; Xin and He 2013). However, mutations in *PBS1* do not lead to enhanced disease susceptibility, which indicates that targeting PBS1 by effectors does not result in improvement of pathogen virulence or fitness. Thus, PBS1

likely has been evolved as a decoy to lure effectors into attacking it instead of other defense-related proteins (Jones et al. 2016). Indeed, PBS1 belongs to the RLCK VII subfamily which has 46 members, and some of them such as BIK1 and PBL1 are important in PTI signaling (Liang and Zhou 2018). This has been described as the decoy model (Van Der Hoorn and Kamoun 2008).

Recently the integrated-decoy model was proposed based on the research of *Arabidopsis* NLR pair RRS1 and RPS4. The plant NLR RRS1 contains a C-terminal WRKY domain, which is a typical DNA-binding domain predominantly found in defense-related transcription factors (Ishihama and Yoshioka 2012). Interaction of effector AvrRps4 or PopP2 with the WRKY domain of RRS1 leads to disassociation of RRS1 and RPS4, leading to immune activation (Cesari et al. 2014; Narusaka et al. 2009). Thus, the WRKY domain of RRS1 serves as an integrated decoy for interaction with effectors.

1.2.3.3 NLRs-mediated immune responses

Perception of pathogenic effectors by plant NLRs triggers activation of defense responses. A recent structural study of the CNL ZAR1 revealed that the oligomerized pentamer structure of activated ZAR1, termed resistosome, is required for resistance. It functions as a calcium permeable channel (Bi et al. 2021). By contrast, upon perception of the corresponding effectors, TIR domain of TNLs, which has NAD⁺-cleaving enzymes (NADases) activity, catalyses the production of several chemicals such as variant-cyclic ADP-ribose (*v*-cADPR) (Horsefield et al. 2019; Wan et al. 2019). The downstream components EDS1-PAD4 and EDS1-SAG101

complexes are believed to sense the signals from these TIR-catalysed chemicals and subsequently activate defense responses (Horsefield et al. 2019; Wan et al. 2019).

The final outcomes of ETI responses are generally similar to those in PTI, including ROS burst, MAPK phosphorylation, elevation of SA levels and transcriptional re-programming, except that immune responses are often more robust and prolonged during ETI (Dangl, Horvath, and Staskawich 2013; Jones and Dangl 2006). Activation of ETI is often accompanied by the program cell death at the infection site, also known as hypersensitive responses, to reduce amount of nutrients available to pathogens and restrict their propagation (Jones and Dangl 2006).

1.3 Systemic acquired resistance

Distinct from human beings, plants do not have adaptive immunity. However, besides PTI and ETI that occur in the local/primary infected tissue, plants have developed an immune response, termed Systemic Acquired Resistance (SAR) (Fu and Dong 2013; Zeier 2013), that establishes a long-lasting resistance to secondary infections. SAR is invoked after a pathogen infection on local leaf, where PTI or ETI is activated by perception of PAMPs or effectors, respectively. A mobile signal is generated at local infection site, and later translocated to distant/systemic leaves to systemically induce SAR, which confers systemic tissue resistance against a broad-spectrum of pathogens (Hartmann and Zeier 2018).

SAR was described as early as 1960s on tobacco plants. After inoculated with tobacco mosaic virus (TMV), tobacco plants subsequently developed an induced resistance against secondary infection on systemic leaves (Ross 1961). Later studies on SAR discovered a number of SAR-

induced genes, including but not limited to *PR* genes (Durrant and Dong 2004). Expression levels of *PR* genes are induced on both local infected tissue and systemic tissue. Some *PR* proteins have been characterized to have antimicrobial function. For instance, *PR1* and *PR5* were reported to have antifungal properties (Sato 1999). *PR* genes have been widely considered as important defense marker genes.

1.3.1 Signaling molecules in SAR

How plants build up SAR in distant tissue after primary infection at local infection site have long been a puzzle since SAR was observed. With the focus on identifying the mobile signaling molecules, many studies have implied several candidates, including SA, methyl salicylate, azelaic acid, L-pipecolic acid (Pip), N-hydroxypipecolic acid (NHP), etc (Cao et al. 1994; Jung et al. 2009; Návarová et al. 2012; Park et al. 2007). Amongst these candidates, SA and NHP have been shown to synergistically orchestrate SAR responses (Hartmann and Zeier 2019; Zeier 2021).

SA is an essential plant defense hormone involved in activation of SAR (Cao et al. 1994; Delaney et al. 1995; Nawrath and Métraux 1999). In 1990s, SA was started to be considered as a signaling molecule in SAR, because its concentration markedly rises in both local infected tissue and systemic tissue (Malamy et al. 1990; Métraux et al. 1990), which correlates with the induction of *PR* gene expression. Exogenous application of either SA or its analogue 2,6-dichloroisonicotinic acid (INA) is sufficient to induce expression of *PR* genes and plant immunity (Cao et al. 1994). Expressing the bacterial salicylate hydroxylase *nahG* in transgenic tobacco and *Arabidopsis* greatly decreases pathogen-induced SA accumulation, and subsequently

results in no induction of *PR* genes and impairment in SAR (Gaffney et al. 1993). These findings indicate an indispensable role of SA in SAR. Even though SA accumulation has been detected in the phloem exudate after pathogen infection, it has been proven that SA is not the mobile signal, because SAR still can be observed on grafted tobacco plants with the *nahG* plant as stock and wild type shoot as scion (Vernooij et al. 1994).

Recent analysis of a group of SAR-deficient mutants that do not affect SA levels or signaling identified Pip and its derivative NHP as two critical metabolites involved in establishment of SAR (Chen et al. 2018; Hartmann et al. 2018; Hartmann and Zeier 2019; Návarová et al. 2012). Blocking Pip or NHP biosynthesis results in total loss of SAR, but with only minor effects on local disease resistance (Jing et al. 2011; Mishina and Zeier 2006; Song, Lu, McDowell, et al. 2004). Latest research on tracking translocation of the exogenously applied NHP or isotope labelled NHP suggested that NHP is transported from local to systemic tissue, indicating that it plays a main role in long-distance signaling (Chen et al. 2018; Mohnike et al. 2021).

In summary, both SA and NHP are increasingly produced after activation of immunity at the local infected site, where NHP translocates to distant tissue to systemically induce SA biosynthesis and *PR* gene expression, subsequently initiating SAR.

1.4 Biosynthesis and regulation of SA and NHP

As introduced above, both SA and NHP play vital roles in SAR. Studies on *Arabidopsis* mutants defective in SA biosynthesis or perception further confirmed the importance of SA in local disease resistance (Cao et al. 1994; Delaney et al. 1995; Nawrath and Métraux 1999). Extensive

genetic and biochemical analysis on *Arabidopsis* SA or NHP deficient mutants have elucidated the biosynthesis and regulation of both SA and NHP.

1.4.1 SA biosynthesis in plants

Plants use two independent routes to produce SA, the isochorismate synthase (ICS) and phenylalanine (Phe) ammonia-lyase (PAL) pathways (Dempsey et al. 2011; Hartmann and Zeier 2019; Zhang and Li 2019), both initiating in plastids from chorismate, a product of the shikimate pathway.

The ICS pathway of SA biosynthesis was originally proposed with the identification of SA Induction Deficient 2 (SID2) as an ICS (Wildermuth et al. 2001). *Arabidopsis* has two ICS genes, *ICS1* and *ICS2*, both localized to the plastids to convert chorismate into isochorismate (Garcion et al. 2008; Wildermuth et al. 2001). In the *sid2/ics1* single mutant, pathogen-induced SA accumulation is largely blocked and SA levels are further reduced in *ics1 ics2* double mutant plants, suggesting that ICS1 plays a major role, whereas ICS2 plays a minor role, in pathogen-induced SA synthesis (Garcion et al. 2008; Nawrath and Métraux 1999). Recently it was shown that the conversion of isochorismate to SA occurs in the cytosol and the MATE transporter Enhanced Disease Susceptibility 5 (EDS5) facilitates the transport of isochorismate from plastids to the cytosol (Rekhter et al. 2019). *avrPphB Susceptible 3 (PBS3)*, which encodes an amidotransferase, catalyzes the conjugation of glutamate to isochorismate in the cytosol (Torrens-Spence et al. 2019). The resulting product isochorismate-9-glutamate spontaneously decays to yield SA.

The PAL pathway has long been known to contribute to SA biosynthesis in tobacco. Isotope labelling experiments showed that SA can be synthesized from Phe via trans-cinnamic acid (CA) and benzoic acid (BA) in tobacco (Ribnicky, Shulaev, and Raskin 1998; Yalpani et al. 1993). PALs convert Phe to CA in higher plants, which is the first step for phenylpropanoid production (Vogt 2010). The hydroxyacyl-CoA hydrolyase Abnormal Inflorescence Meristem 1 (AIM1) mediates the conversion of CA to BA (Xu et al. 2017). A putative BA 2-hydroxylase was proposed to hydroxylate BA to SA (Leon et al. 1995; León, Yalpani, and Lawton 1993), but the gene encoding this enzyme has not been identified yet. In *Arabidopsis*, loss of all four PAL genes leads to ~75% reduction of basal SA and ~50% decrease in pathogen-induced SA production, suggesting that PALs are not only involved in basal SA production but also contribute to pathogen-induced SA biosynthesis (Huang et al. 2010).

Over-accumulation of SA is toxic to plant itself. Most of the produced SA is converted into the inactive 2,5-dihydroxybenzoic acid (2,5-DHBA) by SALICYLIC ACID 5-HYDROXYLASE, or into SA O- β -glucoside (SAG) by SA glucosyltransferases for storage in vacuole, where it may be converted back into SA in response to pathogen attack (Dean, Mohammed, and Fitzpatrick 2005; Lee and Raskin 1999; Zhang et al. 2017).

1.4.2 Transcriptional regulation of SA biosynthetic genes

In *Arabidopsis*, many transcription factors are involved in regulating SA biosynthetic genes. Pathogen-induced *ICS1* expression and SA biosynthesis are mainly controlled by two plant-specific transcription factors, SAR Deficient 1 (SARD1) and CaM-Binding Protein 60 g (CBP60g) (Wang et al. 2011; Zhang, Xu, et al. 2010). Loss of both SARD1 and CBP60g leads to almost

complete block of the induction of *ICS1* and SA accumulation by bacterial pathogen infection (Wang et al. 2011; Zhang, Xu, et al. 2010). Similar to *ICS1*, the induction of *EDS5* and *PBS3* by the bacterial pathogen *Psm* ES4326 is greatly reduced in the *sard1 cbp60g* double mutant (Sun et al. 2015). Chromatin immunoprecipitation (ChIP) analysis has revealed that SARD1 and CBP60g target not only *ICS1*, but also *EDS5* and *PBS3* (Sun et al. 2015), suggesting that genes involved in pathogen-induced SA biosynthesis pathway are directly regulated by SARD1 and CBP60g.

Some transcription factors in the WRKY family have also been identified as positive regulators of SA biosynthesis. Overexpression of *WRKY28* and *WRKY46* in *Arabidopsis* protoplasts resulted in increased *ICS1* expression. EMSA (electrophoretic mobility shift assay) and ChIP assays showed that *WRKY28* binds to the *ICS1* promoter both *in vitro* and *in vivo* (van Verk, Bol, and Linthorst 2011). Transcription factor *WRKY75* also directly binds to the promoter of *ICS1* and promotes *ICS1* expression and SA production during senescence (Guo et al. 2017). The induction of *ICS1* expression by *Pst* DC3000 *avrRpm1*, *avrRpt2* and *avrB*, but not *Pst* DC3000 is greatly reduced in *wrky8* and *wrky48* mutant plants, suggesting that the effector-induced *ICS1* expression is largely dependent on *WRKY8* and *WRKY48* (Gao et al. 2013).

SA biosynthetic genes are also negatively regulated by several transcription factors. Two WRKY transcription factors, *WRKY70* and *WRKY54*, contribute to negative regulation of SA biosynthesis (Wang, Amornsiripanitch, and Dong 2006). In the *wrky54 wrky70* double mutant, basal expression level of *ICS1* is elevated. The SA level in *wrky54 wrky70* plants treated with *Psm* ES4326 *avrRpt2* is also much higher than in wild type plants. A negative regulator in CBP60 family, *CBP60a*, was also shown to regulate SA biosynthesis negatively (Truman et al. 2013).

cbp60a mutant plants display an increase in basal *ICS1* expression and SA levels, suggesting that CBP60a either directly or indirectly affects the expression of *ICS1* and SA biosynthesis.

1.4.3 SA perception and downstream signaling

Biosynthesized SA in *Arabidopsis* is sensed mainly through three protein receptors encoded by *Non-Expresser of PR Genes (NPRs)* (Ding et al. 2018; Wu et al. 2012). Studies on SA insensitive mutants identified several *npr1* mutant alleles which show defects in both SAR and basal resistance (Cao et al. 1997; Ryals et al. 1997; Shah, Tsui, and Klessig 1997). Analysis on NPR1 protein suggested that SA binding to NPR1 leads to induction of defense gene expression, which requires the NPR1-interacting transcription factors TGA2/5/6 (TGACG-Binding Factor 2/5/6) (Cao et al. 1997; Després et al. 2000; Zhang et al. 1999, 2003; Zhou et al. 2000). Two NPR1 paralogs in *Arabidopsis*, NPR3 and NPR4, are also SA receptors (Ding et al. 2018; Fu et al. 2012). Unlike NPR1, NPR3 and NPR4 function as transcriptional co-repressors in suppression of defense gene expression in the absence of SA. Research on a gain-of-function mutant *npr4-4D* showed that binding of SA leads to inhibition of the transcriptional repression activities (Ding et al. 2018). Both NPR3 and NPR4 have high affinity to SA. Upon infection, SA levels are elevated and SA binds to NPR3 and NPR4, which results in the de-repression of plant defense genes. Meanwhile, pathogen-induced SA binds to NPR1, which further induces the expression of defense genes and promotes plant immunity (Ding et al. 2018).

1.4.4 NHP biosynthesis

Studies on *Arabidopsis SAR-deficient (sard)* mutants largely contributed to the elucidation of the NHP biosynthesis pathway. *ALD1 (AGD2-like Defense Response Protein 1)* encodes an

aminotransferase essential for the onset of SAR and was found to be required for production of the immediate precursor of NHP, Pip (Návarová et al. 2012; Song, Lu, McDowell, et al. 2004; Song, Lu, and Greenberg 2004). It uses lysine as a substrate and catalyzes its conversion to ϵ -amino- α -keto caproic acid, which cyclizes spontaneously to form Δ 1-piperidine-2-carboxylic acid (P2C) (Ding et al. 2016; Hartmann et al. 2017). SARD4 catalyzes the reduction of P2C to Pip (Ding et al. 2016; Hartmann et al. 2017). Biochemical analysis on another SAR-deficient mutant *flavin-dependent monooxygenase 1 (fmo1)* revealed that FMO1 catalyzes the N-hydroxylation of Pip, yielding NHP (Chen et al. 2018; Hartmann et al. 2018). It was recently reported that NHP can be further metabolized into NHP-O-glycoside by the glycosyltransferase UGT76B1 (Bauer et al. 2021; Cai et al. 2021; Holmes et al. 2021; Mohnike et al. 2021).

1.4.5 Transcriptional regulation of NHP biosynthetic genes

Similar to SA, NHP biosynthetic genes are also coordinately regulated by SARD1 and CBP60g in *Arabidopsis*. ChIP analysis revealed that SARD1 and CBP60g target not only genes involved in SA biosynthesis, but also the NHP synthetic genes *ALD1*, *SARD4* and *FMO1* (Sun et al. 2015, 2018). In the *sard1 cbp60g* double mutant, the induction of *ALD1*, *SARD4* and *FMO1* by *Psm* ES4326 is greatly reduced, leading to less biosynthesized Pip and NHP (Sun et al. 2018). On the other hand, overexpression of *SARD1* leads to increased *ALD1* and *SARD4* expression and elevated Pip levels, suggesting that SARD1 and CBP60g activate Pip and NHP biosynthesis through up-regulation of their biosynthetic genes (Sun et al. 2018).

WRKY33 is another transcription factor that positively regulates Pip and NHP biosynthesis (Wang et al. 2018). In *wrky33* mutant plants, *Pst* DC3000 *avrRpt2*-induced *ALD1* and *FMO1* expression

as well as Pip accumulation is dramatically reduced (Wang et al. 2018). ChIP-PCR analysis revealed that WRKY33 binds to the promoter of *ALD1*, suggesting that it directly regulates the expression of *ALD1* to promote Pip and NHP biosynthesis.

1.5 SARD1 and CBP60g

As mentioned above, SARD1 and CBP60g are two master transcription factors regulating both SA and NHP biosynthesis. The *Psm* ES4326-inducible SARD1 and CBP60g were initially found to be required for SA biosynthesis and SAR from a SAR-deficient mutant screen (Zhang, Xu, et al. 2010). SAR response is partially compromised in *sard1* and *cbp60g* mutants, even though the defect in the latter is mild. In *sard1 cbp60g* double mutants, pathogen-induced *ICS1* expression and SA accumulation, and SAR responses are mostly blocked, suggesting an additive effect of SARD1 and CBP60g in plant immunity (Zhang, Xu, et al. 2010). ChIP-seq and ChIP-PCR analysis performed on overexpression lines of *SARD1* and *CBP60g* revealed that SARD1 and CBP60g directly regulate a large number of defense-related genes, including but not limited to SA and NHP biosynthetic genes, genes encoding components of PRR complex such as *BAK1* and *BIK1*, genes in MAPK cascades such as *MEKK1* and *MPK3*, and genes required for ETI such as *EDS1* and *PAD4* (Sun et al. 2015).

1.5.1 Regulation of SARD1 and CBP60g

Both SARD1 and CBP60g belong to the CBP60 transcription factor family, which is named by *in vitro* binding activity to CaM. They are the closest members in phylogeny in the family. Both possess the DNA-binding domain in their central region but vary in both N- and C- terminus, indicating they may be differentially regulated. CBP60g has been showed to bind CaM *in vitro*

with its N-terminus (Wang et al. 2009; Zhang, Xu, et al. 2010). Transgenic lines over-expressing *CBP60g* shows a wild type-like phenotype (Zhang, Xu, et al. 2010), suggesting that *CBP60g* may be regulated post-transcriptionally by interacting with CaM. Lacking a similar N-terminal motif as in *CBP60g*, *SARD1* does not bind CaM (Zhang, Xu, et al. 2010). Unlike *CBP60g*, overexpression of *SARD1* is sufficient to constitutively activate defense responses, implying that *SARD1* is mainly regulated through transcription.

Two closely related transcription factors, TGA1 and TGA4, are involved in the induction of *SARD1* and *CBP60g* (Sun et al. 2018). In the *tga1 tga4* double mutant, the induction of *SARD1* and *CBP60g* as well as SA and Pip accumulation are greatly reduced at early stage of plant defense. ChIP-PCR analysis showed that TGA1 binds to the promoter of *SARD1* but not *CBP60g*, suggesting that the TGA transcription factors directly regulate *SARD1* and indirectly regulate *CBP60g* expression. Another transcription factor GT2-like 1 (GTL1) was shown to directly regulate pathogen-induced *CBP60g* expression (Völz et al. 2018).

1.6 SNC2-mediated immune pathways

In 2010, Zhang *et al.* reported an autoimmune mutant *snc2-1D* (for *suppressor of npr1-1, constitute 2D*) from a suppressor screen of *npr1-1* (Zhang, Yang, et al. 2010). *npr1-1* carries a loss-of-function mutation in the SA receptor NPR1 and is insensitive to SA and the SA analogue INA, resulting in the disability in induction of *PR* gene expression during pathogen attack. The gain-of-function substitution of Gly to Arg in the conserved GXXXG motif of the transmembrane domain of SNC2 leads to increased accumulation of SA, elevated expression level of *PR* genes and enhanced disease resistance. Loss of SNC2 function causes enhanced

susceptibility to *Pst* DC3000, indicating that SNC2 is a critical positive defense regulator in *Arabidopsis*. As constitutively activated immunity is energy-consuming, the autoimmune mutant *snc2-1D* has growth defects, exhibiting a dwarf morphology.

SNC2 encodes an RLP that localizes on the plasma membrane. It contains a short extracellular LRR domains, a single transmembrane domain, and a tiny cytoplasmic tail with only four amino acids. With the LRR domains, RLP *SNC2* could be a receptor of an unknown ligand. Due to the lack of a cytoplasmic kinase domain in *SNC2* protein, a yet-to-be identified RLK is predicted to form a complex with *SNC2* for defense signal transduction.

Genetic analysis of *snc2-1D*-mediated autoimmunity found BDA1 (for Bian Da 1, Bian Da means becoming big in Chinese) as a downstream component of *SNC2* (Yang et al. 2012). Loss of BDA1 function leads to complete suppression of *snc2-1D* autoimmunity. With four transmembrane domains, BDA1 is predicted to be localized on plasma membrane, but whether *SNC2* physically interacts with BDA1 remains unknown. With five ankyrin repeats at its N-terminus, BDA1 may interact with other proteins to transduce *SNC2*-mediated defense signal to downstream regulators.

It has been reported that the master transcription factors *SARD1* and *CBP60g* are required for the autoimmunity of *snc2-1D* (Sun et al. 2015). The up-regulation of *ICS1*, *PR1*, *PR2* and increased accumulation of SA in *snc2-1D* are partially suppressed in *cbp60g-1 snc2-1D* and *sard1-1 snc2-1D* double mutant, and completely suppressed in the *cbp60g-1 sard1-1 snc2-1D* triple mutant. As for morphology, *cbp60g-1 snc2-1D* and *sard1-1 snc2-1D* double mutants

display slight suppression of dwarfism of *snc2-1D*, while *cbp60g-1 sard1-1 snc2-1D* triple mutant exhibits wild type morphology. These findings suggest that there are two parallel signaling pathways downstream of SNC2, one requires SARD1 and the other is dependent on CBP60g (Figure 1.1).

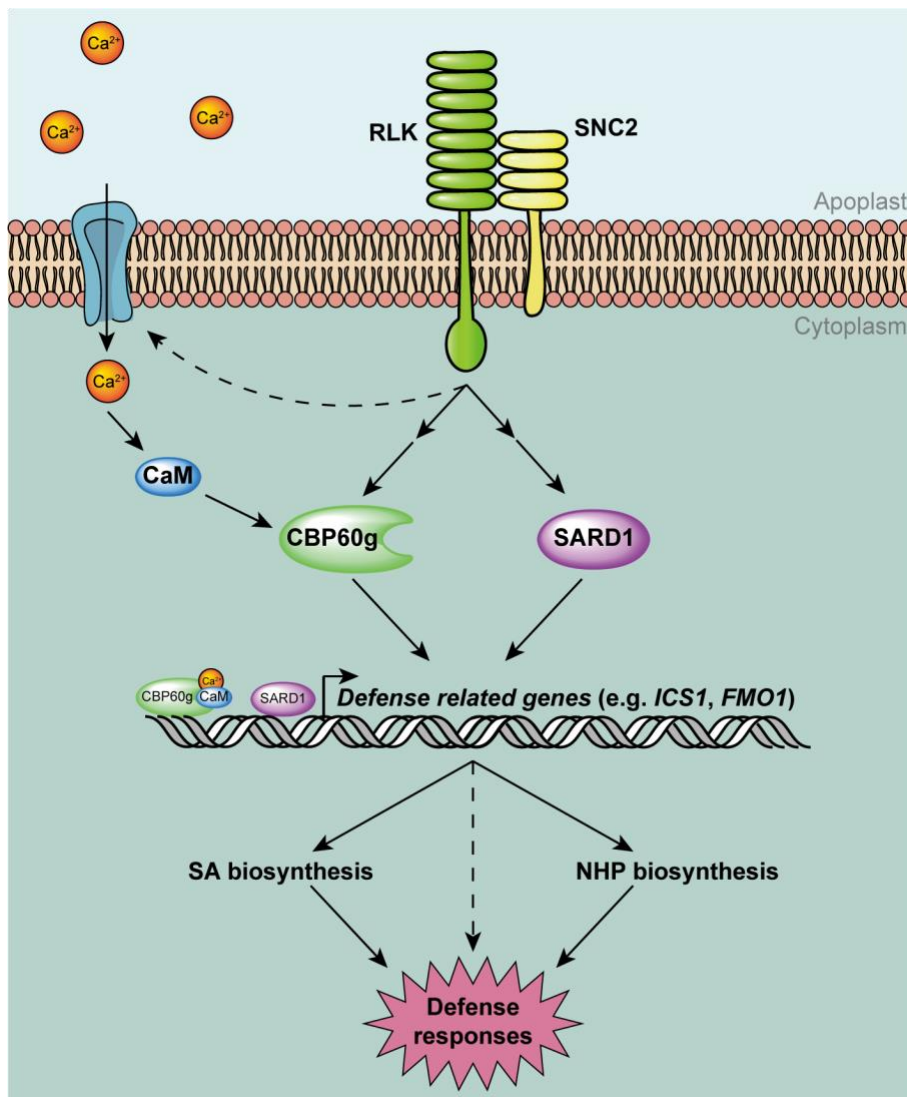


Figure 1.1 SNC2-mediated defense signaling.

A schematic diagram illustrating that transcription factor SARD1 and CBP60g define two parallel pathways downstream of SNC2.

1.7 Thesis objectives

As introduced above, SARD1 and CBP60g are of great importance in transcriptional regulation of defense-related genes. How SARD1 and CBP60g are activated remains largely unknown. The objective of this dissertation is to identify novel upstream regulators of SARD1. Given that SARD1 and CBP60g are both activated in the autoimmune mutant *snc2-1D*, it is practical to search for upstream regulators of SARD1 by performing a *cbp60g-1 snc2-1D* suppressor screen. The identification of regulators downstream of SNC2 would also provide new insights on how SNC2 mediates plant immunity.

In Chapter 2, I describe the identification and characterization of *bda7-1 cbp60g-1 snc2-1D*, a suppressor mutant identified from the suppressor screen performed on *cbp60g-1 snc2-1D*. Using mapping-by-sequencing, a mutation in the transcription factor *CBP60b* was identified to be responsible for phenotypes of *bda7-1 cbp60g-1 snc2-1D*. Further functional analysis showed that *CBP60b* directly regulates expression of *SARD1* by targeting its promoter region. Loss of *CBP60b* function in *Arabidopsis* wild type Col-0 resulted in the EDS1-dependent autoimmunity, indicating that *CBP60b* is required for the expression of a guard/decoy, or a negative regulator of immunity mediated by TNLs. My results in this chapter suggest that *CBP60b* is required for *SNC2*-mediated activation of *SARD1*.

In chapter 3, I describe the identification and characterization of three other suppressors of *cbp60g-1 snc2-1D*, *bda6-1 cbp60g-1 snc2-1D*, *bda6-2 cbp60g-1 snc2-1D* and *bda6-3 cbp60g-1 snc2-1D*. Result of mapping-by-sequencing suggested that *BDA6* is AP4 μ , a subunit of the Adaptor Protein 4 (AP4) complex. AP4 μ can interact with *BDA1* *in vivo*. In addition, I found

that loss-of-function mutations in genes of AP4 subunits lead to compromised basal resistance and PTI. My results here suggest that AP4 complex is generally involved in plant immunity.

Chapter 2: *Arabidopsis* CALMODULIN-BINDING PROTEIN 60b plays dual roles in plant immunity

2.1 Summary

Arabidopsis SYSTEMIC ACQUIRED RESISTANCE DEFICIENT 1 (*SARD1*) and CALMODULIN-BINDING PROTEIN 60g (*CBP60g*) are two master transcription factors that regulate many defense-related genes in plant immunity. They are required for immunity downstream of the receptor-like protein SUPPRESSOR OF NPR1-1, CONSTITUTIVE 2 (*SNC2*). Constitutive defense responses in the gain-of-function autoimmune *snc2-ID* mutant are modestly affected by either *sard1* or *cbp60g* single mutants, but completely suppressed by the *sard1 cbp60g* double mutant. Here we report that *CBP60b*, another member of the *CBP60* family, also functions as a positive regulator of *SNC2*-mediated immunity. Loss-of-function mutations of *CBP60b* suppress the constitutive expression of *SARD1* and enhanced disease resistance in *cbp60g-1 snc2-ID*, whereas over-expression of *CBP60b* leads to elevated *SARD1* expression and constitutive defense responses. In addition, transient expression of *CBP60b* in *Nicotiana benthamiana* activates the expression of the *pSARD1::luciferase* reporter gene. Chromatin immunoprecipitation assay further showed that *CBP60b* is recruited to the promoter region of *SARD1*, suggesting that it directly regulates *SARD1* expression. Interestingly, knocking out *CBP60b* in the wild type background leads to *ENHANCED DISEASE SUSCEPTIBILITY 1* (*EDS1*)-dependent autoimmunity, suggesting that *CBP60b* is required for the expression of a guard/decoy or a negative regulator in immunity mediated by receptors carrying an N-terminal TIR (Toll-interleukin-1 receptor-like) domain.

2.2 Introduction

Plants have evolved sophisticated innate immune systems to fight against various pathogens (Jones and Dangl 2006; Zhou and Zhang 2020). Upon infection, plasma membrane-localized pattern recognition receptors (PRRs) recognize pathogen/microbe-associated molecular patterns (PAMPs or MAMPs), which are conserved molecules associated with groups of pathogens, to initiate pattern-triggered immunity (PTI) (Monaghan and Zipfel 2012). To facilitate colonization, pathogens have evolved various effector proteins to interfere with PTI (Dou and Zhou 2012). Meanwhile, plants evolved resistance (R) proteins, mostly in the nucleotide-binding leucine-rich repeat (NLR) protein family, to perceive the pathogen effectors and activate effector-triggered immunity (ETI) (van Wersch et al. 2020). Activation of PTI and ETI at local infection sites further leads to development of systemic acquired resistance (SAR) in the distal parts of the plants (Sun and Zhang 2021).

One class of plant PRRs belong to the receptor-like protein (RLP) family. RLPs usually have a short cytoplasmic tail, a single transmembrane motif, and an extracellular leucine-rich repeats (LRR) domain involved in binding to ligands. One of the *Arabidopsis* RLPs, SNC2 (SUPPRESSOR OF NPR1-1, CONSTITUTIVE 2), contributes to defense against bacteria (Zhang, Yang, et al. 2010). On one hand, loss of SNC2 results in enhanced susceptibility to bacterial pathogen *Pseudomonas syringae* pv *tomato* (*Pto*) DC3000. On the other hand, a gain-of-function mutation in *snc2-ID* results in constitutive *Pathogenesis-Related* (*PR*) gene expression, elevated levels of the plant defense hormone salicylic acid (SA), and enhanced resistance against the oomycete pathogen *Hyaloperonospora arabidopsidis* (*Hpa*) Noco2

(Zhang, Yang, et al. 2010). Owing to constitutively activated immunity, *snc2-ID* plants exhibit a dwarf morphology.

SAR DEFICIENT 1 (SARD1) and CALMODULIN BINDING PROTEIN 60g (CBP60g) are two master transcription factors in plant immunity (Sun et al. 2015). Induction of SA biosynthetic genes such as *ISOCHORISMATE SYNTHASE 1 (ICS1)*, *ENHANCED DISEASE SUSCEPTIBILITY 5 (EDS5)* and *AVRPPHB SUSCEPTIBLE 3 (PBS3)* during pathogen infection is coordinately regulated by SARD1 and CBP60g (Sun et al. 2015; Wang et al. 2011; Zhang, Xu, et al. 2010). Pathogen-induced SA accumulation is almost completely blocked in *sard1 cbp60g* double mutant plants (Wang et al. 2011; Zhang, Xu, et al. 2010). In addition, SARD1 and CBP60g are also required for activation of the biosynthesis of N-hydroxy-pipecolic acid (NHP), a signaling molecule important for both local resistance and SAR (Sun et al. 2019). They coordinately regulate pathogen-induced expression of NHP biosynthesis genes such as *AGD2-like defense response protein 1 (ALD1)*, *SAR deficient 4 (SARD4)* and *Flavin-dependent monooxygenase 1 (FMO1)* (Sun et al. 2018, 2019). Both SARD1 and CBP60g belong to a small protein family with eight members in *Arabidopsis*. Unlike CBP60g and other members in the family which have calmodulin (CaM)-binding activity (Reddy et al. 2002; Wang et al. 2009), SARD1 does not bind CaM and is primarily regulated at transcriptional level, as overexpression of *SARD1* is sufficient to activate downstream defense gene expression (Zhang, Xu, et al. 2010). Another member of the family, CBP60a, was shown to function as a negative regulator of plant immunity (Truman et al. 2013). How CBP60a negatively regulates plant immunity is unknown.

Both SARD1 and CBP60g contribute to autoimmunity of *snc2-1D* (Sun et al. 2015). Although the up-regulation of *ICS1* and accumulation of SA in *snc2-1D* are only slightly reduced in *cbp60g-1 snc2-1D* and *sard1-1 snc2-1D* double mutants, they are largely blocked in the *cbp60g-1 sard1-1 snc2-1D* triple mutant. *snc2-1D* has a dwarf morphology and is much smaller than wild type. The sizes of *cbp60g-1 snc2-1D* and *sard1-1 snc2-1D* double mutants are slightly larger than *snc2-1D*, whereas the *cbp60g-1 sard1-1 snc2-1D* triple mutant exhibits wild type morphology. These findings suggest that there are two parallel pathways downstream of SNC2, one depending on SARD1 and the other requiring CBP60g (Sun et al. 2015). How the plasma membrane localized SNC2 transduces signals to SARD1 or CBP60g is largely unknown.

To identify components involved in the SARD1-dependent defense signaling downstream of SNC2, we performed a suppressor screen in the *cbp60g-1 snc2-1D* background. Here we report the identification and characterization of one of the suppressors, *bda7-1* (*bian da 7*; *bian da* means “becoming big” in Chinese). Positional cloning revealed that *BDA7* encodes another member of the CBP60 family, CBP60b, which positively regulates the expression of *SARD1*.

2.3 Materials and Methods

2.3.1 Plant materials and growth conditions

All *Arabidopsis thaliana* mutants are in the Col-0 ecotype background unless specified. The *cbp60g-1 snc2-1D*, *cbp60g-1*, *cbp60g-1 sard1-1* plants were described previously (Sun et al. 2015; Zhang, Xu, et al. 2010). *cbp60b-4* and *cbp60b-4 cbp60g-1* plants were isolated from a cross between *cbp60b-4 cbp60g-1 snc2-1D* and Col-0. *cbp60b-5*, *cbp60b-6* are two independent deletion lines generated by CRISPR/Cas9. The *CBP60b-3HA-OX #21* and *#27* are two

independent overexpression lines generated by transforming Col-0 with *Agrobacteria* carrying *pCambia1300-35S-CBP60b-3HA*. *eds1-24* is a CRISPR mutant line with deleting both *EDS1A* and *EDS1B* genes, as described previously (Tian et al. 2021). *cbp60b-5 eds1-24* was obtained from the F2 population of a cross between *cbp60b-5* and *eds1-24*. Primers used for genotyping were listed in Appendix A.10.

Plants were grown on soil under long-day conditions (16-h light/ 8-h dark cycle) with a light intensity of $\sim 100 \mu\text{mol}/\text{m}^2/\text{s}$ of at 22 °C unless specified. Plants for quantitative RT-PCR were grown on plates with $\frac{1}{2}$ Murashige and Skoog (MS) and 1% sucrose for two weeks. Plants used for SA quantification were grown on soil for four weeks under short-day conditions (8-h light/ 16-h dark cycle).

2.3.2 Constructs for generation of deletion mutants and transgenic plants

The CRISPR/Cas9 system used for generating *cbp60b* mutants was described previously (Xing et al. 2014). Two guide RNAs were designed to target *CBP60b* genomic DNA for generation of a deletion of ~ 1 kb in size. A PCR fragment containing the guide RNA sequences was amplified from the *pCBC-DT1T2* vector using primers At5g57580-BsFF0 and At5g57580-BsRR0 and subsequently inserted into the pHEE401 vector using the BsaI site. The derived plasmid was transformed into *E. coli* DH10B and later *Agrobacterium* GV3101 by electroporation.

Arabidopsis plants were transformed with the *Agrobacterium* carrying the plasmid by floral dip method (Clough and Bent 1998). T1 plants were analyzed for deletion in *CBP60b* by PCR with primers listed in Appendix A.10. Homozygous deletion mutants were obtained in the T2 generation.

To overexpress *CBP60b*, *CBP60b* was amplified from genomic DNA using primers AT5G57580-atgKpnI-F and AT5G57580-nstopBamHI-R. The PCR fragment was digested with KpnI and BamHI and afterwards ligated into *pCambia1300-35S-3HA* vector. The derived plasmid was transformed into *E. coli* DH10B and later *Agrobacterium* GV3101. Wild type Col-0 plants were transformed with *Agrobacterium* carrying the plasmid by floral dipping. Homozygous transgenic lines were obtained in the T2 generation.

For transgene complementation, a genomic DNA fragment containing *CBP60b* was amplified with primers AT5G57580-KpnI-F and AT5G57580-nstopBamHI-R. The PCR fragment was inserted into a *pBasta-3HA* vector derived from *pCambia1305* to obtain the *pAt5g57580::At5g57580-3HA* construct. The *pAt5g57580::At5g57580-3HA/cbp60b-4 cbp60g-1 snc2-ID* transgenic lines were obtained by transforming *cbp60b-4 cbp60g-1 snc2-ID* plants with *Agrobacterium* carrying the plasmid of *pAt5g57580::At5g57580-3HA*.

2.3.3 Mutagenesis and suppressor screen

About 5,000 *cbp60g-1 snc2-ID* mutant seeds were mutagenized with 20 mM ethyl methanesulfonate (EMS) as described previously (Li and Zhang 2016). In brief, seeds were soaked in the EMS solution for 16 h. Afterwards, the EMS solution was removed, and the seeds were washed with 100 mM Na₂S₂O₃ three times and then with ddH₂O three more times. The mutagenized seeds were plated on ½ MS plate and later transplanted to soil when the seedlings were about 10-day-old. M2 plants were grown on soil and screened for plants that are larger than *cbp60g-1 snc2-ID*. Any plants with a larger size were collected for further analysis.

2.3.4 Genetic mapping, mapping by sequencing and identification of *bda7-1*

Traditional mapping of *bda7-1* was carried out on the F2 population of a cross between *bda7-1 cbp60g-1 snc2-1D* mutant (in Col-0 background) and Landsberg *erecta* (*Ler*). In F2, any plants homozygous for both *snc2-1D* and *cbp60g-1* were selected for linkage analysis using SSLP markers as previously described (Zhang, Glazebrook, and Li 2007). These plants were first analyzed with markers throughout the five chromosomes, by which *bda7-1* was mapped to the lower arm of chromosome 5. Afterwards, fine mapping was conducted on both F2 and F3 plants with additional markers to narrow down the mapped region to ~0.8 Mb.

For mapping by sequencing, *bda7-1 cbp60g-1 snc2-1D* was backcrossed with *cbp60g-1 snc2-1D*. In the F2 population, about 50 plants that showed similar morphology as *bda7-1 cbp60g-1 snc2-1D* were selected and pooled for genomic DNA extraction. The genomic DNA was subsequently sequenced using the HiSeq-PE150 platform. Single nucleotide polymorphisms (SNPs) were called from the next-generation sequencing data by Genome Analysis Toolkit (GATK v3.5-0) (McKenna et al. 2010) following the variants discovery pipeline from GATK Best Practices suggested by BROAD Institute (Depristo et al. 2011). Briefly, the raw sequence was trimmed and filtered with prinseq lite 0.20.4 to remove any unwanted sequences (Schmieder and Edwards 2011). The sequences were next mapped to Tair10 *Arabidopsis* reference genome with BWA MEM (Li 2013). The alignments were then processed by GATK HaplotypeCaller to call for variants. All variants identified were then merged in PICARD tools (<http://broadinstitute.github.io/picard>). After variants calling, we looked through the ~0.8 Mb

region on chromosome 5, which *bda7-1* was mapped, for homozygous SNPs in the exon of genes to identify the *bda7-1* mutation.

2.3.5 Chromatin immunoprecipitation (ChIP) analysis

ChIP-qPCR assays were performed as previously described (Sun et al. 2015). The chromatin complexes containing CBP60b-3HA were immunoprecipitated using anti-HA antibody (Roche, Basel, Switzerland) and Protein A/G Agarose beads (GE Healthcare, Chicago, United States). The immunoprecipitated DNA was analyzed by qPCR using gene specific primers, which were listed in Appendix A.10.

2.3.6 Dual reporter assay

Dual reporter assay was performed in *Nicotiana (N.) benthamiana* by transforming the reporter constructs together with the different effector constructs. The *pSARD1::Luc* were described previously (Ding et al. 2018). A *pUBQ1*-driven Renilla luciferase reporter was included as internal control. *Agrobacteria* carrying the reporter construct *pSARD1::Luc*, internal control *pUBQ1-Renilla* and effector construct *35S::CBP60b-3HA* or *35S::GFP-3HA* were first cultured in liquid LB and then resuspended in 10 mM MgCl₂. Leaves of *N. benthamiana* were co-infiltrated with *Agrobacteria* carrying the indicated construct combinations with final concentrations of OD₆₀₀ = 0.2 (*pSARD1::Luc*), OD₆₀₀ = 0.05 (*pUBQ1-Renilla*) and OD₆₀₀ = 0.5 (*35S::CBP60b-3HA* or *35S::GFP-3HA*). For imaging the luminescence intensity, *N. benthamiana* leaves was infiltrated with 1 mM luciferin 40 h after inoculation of the *Agrobacteria* and then imaged under the Gel Doc XR+ System (Bio-Rad) with the Bolt mode. For quantification of the promoter activity, areas of *N. benthamiana* leaves inoculated with

Agrobacteria was collected 40 h after inoculation. The Dual-Luciferase® Reporter Assay System (Promega) was used to measure the activity of firefly luciferase and renilla luciferase sequentially using a BioTek™ Synergy™ 2 Multi-Mode Microplate Reader. Relative promoter activities were calculated as the ratio of firefly luciferase/renilla luciferase.

2.3.7 RNA extraction, reverse transcription and qPCR

Plants for gene expression assays were grown on ½ MS plates for 14 days under long-day conditions. Approximately 50 mg plant tissue from 3-4 individual seedlings of the indicated genotypes were collected as a single sample. Three biological replicates were analyzed for each genotype. RNA extraction was performed using the EZ-10 Spin Column Plant RNA Miniprep Kit (Bio Basic Inc., Toronto, Canada). RNAs were reverse transcribed into cDNAs by OneScript Reverse Transcriptase (Applied Biological Materials Inc., Richmond, Canada). qPCR was performed on the total cDNAs using SYBR Premix Ex Taq™ II (Takara, Shiga, Japan). Primers for qPCR are listed in Appendix A.10.

2.3.8 SA extraction and quantification

The procedure of SA extraction and measurement was reported previously (Li et al. 1999). About 100 mg of plant tissue was collected from 2-3 individual plants of the indicated genotypes as a single sample. Plant tissue was ground into fine powder with liquid nitrogen, resuspended with 600 µl 90% methanol and sonicated for 20 min to release SA. After centrifugation at 12,000×g for 10 min, the supernatant was collected, and the pellets underwent a second round of extraction by adding 500 µl of 100% methanol and sonicating for another 20 min. The supernatant from both extractions were combined and dried by vacuum. For free SA

quantification, 500 μ l of 5% (w/v) trichloroacetic acid was added to the dry samples, vortexed and sonicated for 5 min. For total SA measurement, 100 μ l β -Glucosidase solution (80 units/ml in 0.1 M NaAc, pH=5.2) was added to the dried samples, vortexed and sonicated for 5 min, and then incubated at 37 degree for 90 min to cleave SAG into free SA before adding 500 μ l 5% (w/v) trichloroacetic acid. After centrifugation at 12,000 \times *g* for 15 min, the supernatant was collected and extracted with 500 μ l extraction buffer (ethylacetate acid: cyclopentane: isopropanol, 100:99:1, v/v/v) for three times. Each time, after centrifugation at 12,000 \times *g* for 1 min, the organic phase was collected and combined into a new tube. The combined organic phase was then dried by vacuum. The dry sample was next resuspended with 200 μ l mobile phase (0.2M KAc, 0.5mM EDTA pH=5) by vortexing and sonicating for 5 min. After the final centrifugation at 12,000 \times *g* for 5 min, the supernatant was collected and used to determine the amount of SA by high-performance liquid chromatography, as compared with a standard.

2.3.9 Pathogen infection assay

Hpa Noco2 infection was conducted by spray-inoculating two-week-old seedlings with spores in water (50,000 spores/ml). Inoculated seedlings were covered with a transparent lid and grown in a plant chamber at 18 °C with a relative humidity of ~80%. Infection was scored at 7 dpi by counting conidia spores with a hemocytometer. Four - five individual plants were pooled as a single sample. Four biological replicates were included for each genotype.

2.3.10 Statistical analysis

Error bars in all of the figures represent standard deviations. The number of biological replicates is indicated in the figure legends. Statistical comparison among different samples is carried out

by either one-way ANOVA with Tukey's honestly significant difference (HSD) post hoc test or Student's *t*-test, as reported in the figure legends.

2.4 Results

2.4.1 Identification and characterization of *bda7-1 cbp60g-1 snc2-1D*

To identify regulators of SARD1-dependent defense signaling in SNC2-mediated immunity, we mutagenized *cbp60g-1 snc2-1D* and searched for mutants suppressing its dwarf morphology.

bda7-1 was one of the mutants identified. As shown in Figure 2.1A, *bda7-1 cbp60g-1 snc2-1D* has an intermediate size compared with wild type Col-0 and *cbp60g-1 snc2-1D*. Quantitative RT-PCR analysis showed that the elevated expression of *PR1* and *ICS1* in *cbp60g-1 snc2-1D* is fully blocked by *bda7-1* (Figure 2.1B and 2.1C). Consistent with the *ICS1* expression, both free (Figure 2.1D) and total SA (Figure 2.1E) levels in *bda7-1 cbp60g-1 snc2-1D* are considerably lower than in *cbp60g-1 snc2-1D*. In addition, the enhanced resistance against *Hpa Noco2* observed in *cbp60g-1 snc2-1D* is lost in *bda7-1 cbp60g-1 snc2-1D* (Figure 2.1F). Together, these data indicate that *bda7-1* suppresses the autoimmunity of *cbp60g-1 snc2-1D*.

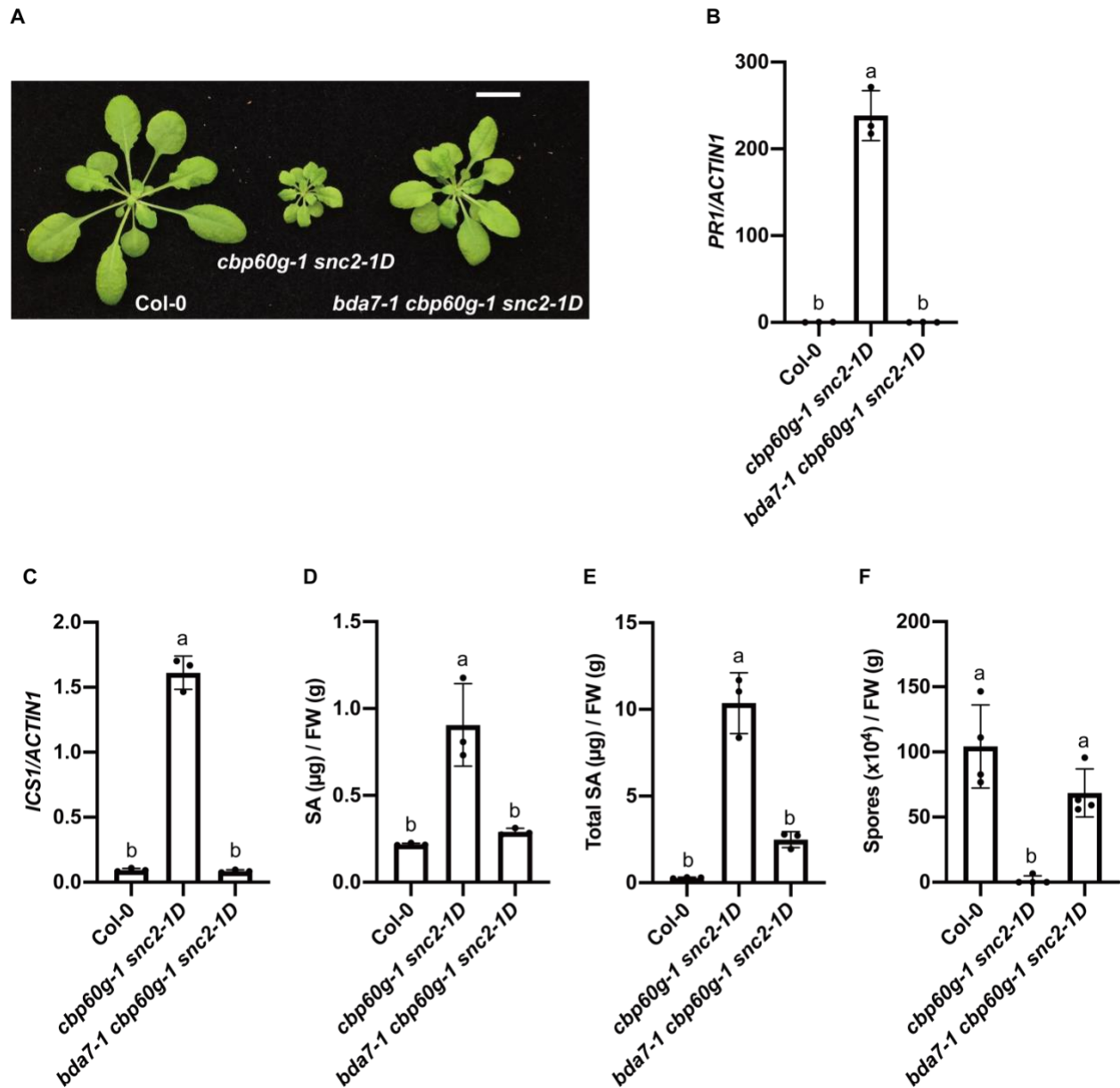


Figure 2.1 Identification and characterization of *bda7-1 cbp60g-1 snc2-1D*.

(A) Morphologies of four-week-old soil-grown plants of Col-0, *cbp60g-1 snc2-1D* and *bda7-1 cbp60g-1 snc2-1D* under long-day condition. Scale bar is 1 cm.

(B and C) Relative expression levels of *PR1* (B) and *ICS1* (C) in the indicated genotypes. Transcript levels were normalized with *ACTIN1*. Error bars represent standard deviations. Letters indicate statistical differences ($P < 0.0001$, one-way ANOVA followed by Tukey's multiple comparisons test; $n = 3$).

(D, E) Free (D) and total SA (E) levels in the indicated genotypes. Error bars represent standard deviations. Letters indicate statistical differences ($P < 0.01$, one-way ANOVA followed by Tukey's multiple comparisons test; $n = 3$).

2.4.2 Map-based cloning of *BDA7*

When *bda7-1 cbp60g-1 snc2-1D* was backcrossed with *cbp60g-1 snc2-1D*, F1 plants showed similar morphology as *cbp60g-1 snc2-1D* (Appendix A.1), indicating that *bda7-1* is recessive. To map *bda7-1*, *bda7-1 cbp60g-1 snc2-1D* (in Col-0 background) was crossed with Landsberg *erecta* (*Ler*). In the F2 population, plants homozygous for both *cbp60g-1* and *snc2-1D* with dwarf morphology were selected for linkage analysis. *bda7-1* was initially mapped to a region between SSLP markers MBG8 and MUB3 on chromosome 5, and subsequently fine-mapped to a ~0.8 Mb region between MUA2 and MMN10 (Appendix A.2).

To identify *BDA7*, DNA from 50 F2 plants with similar size as *bda7-1 cbp60g-1 snc2-1D* obtained from a cross between *bda7-1 cbp60g-1 snc2-1D* and *cbp60g-1 snc2-1D* were pooled and sequenced by Illumina sequencing. A single candidate gene within the ~0.8 Mb mapped region, *AT5G57580*, was found, which carries a homozygous C to T mutation in its coding sequence (Figure 2A and Appendix A.3), resulting in the substitution of Leu148 with Phe (Figure 2.2A).

2.4.3 Loss of *CBP60b* suppresses the autoimmunity of *cbp60g-1 snc2-1D*

To test whether *AT5G57580* is indeed required for the autoimmunity of *cbp60g-1 snc2-1D*, *AT5G57580* was knocked out by CRISPR/Cas9 in the *cbp60g-1 snc2-1D* background. As shown in Figure 2.2B, the newly generated *AT5G57580* CRISPR alleles suppressed *cbp60g-1 snc2-1D* similarly as *bda7-1*. Sanger sequencing confirmed that these lines carry homozygous deletion

mutations in *BDA7* (Appendix A.4). Similar to *bda7-1*, these deletion mutants also suppress the constitutive expression of *PR1* and *ICS1* (Figure 2.2C and 2.2D), elevated SA levels (Appendix A.5) and enhanced resistance against *Hpa Noco2* in *cbp60g-1 snc2-1D* (Figure 2.2E), suggesting that *AT5G57580* is required for the constitutively immune responses in *cbp60g-1 snc2-1D*.

To further confirm that suppression of the *cbp60g-1 snc2-1D* mutant phenotype in *bda7-1 cbp60g-1 snc2-1D* is caused by the mutation in *AT5G57580*, we transformed a construct expressing wild-type *AT5G57580* with a C-terminal 3×HA tag under the control of its native promoter into *bda7-1 cbp60g-1 snc2-1D*. As shown in Appendix A.6, the *AT5G57580-3HA* transgenic lines have similar morphology as *cbp60g-1 snc2-1D*, indicating that *AT5G57580-3HA* can complement the *bda7-1* mutation. Since *AT5G57580* encodes CBP60b, we renamed *bda7-1* as *cbp60b-4*.

The Leu148 residue in CBP60b is highly conserved among all CBP60 family members, except for CBP60a (Appendix A.7A), which functions as a negative regulator of plant immunity (Truman et al. 2013). Notably, from the same *cbp60g-1 snc2-1D* suppressor screen, three *sard1* alleles, which carry mutations on Gly143, were found to suppress the autoimmunity of *cbp60g-1 snc2-1D* (Appendix A.7B). This Gly residue is also highly conserved and is only 2 aa apart from the conserved Leu site. These data suggest that this region with the conserved Leu and Gly residues is critical for the functions of CBP60 family proteins.

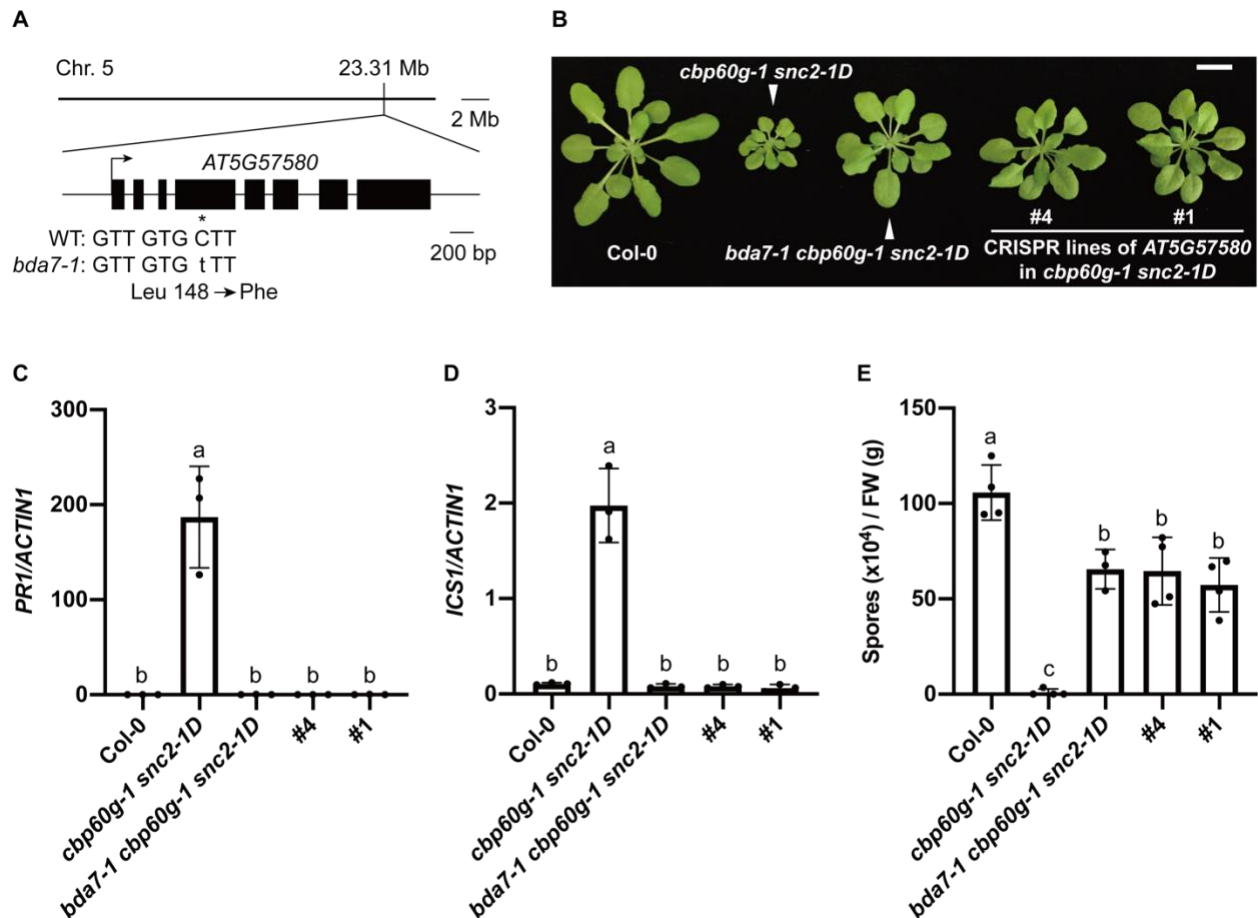


Figure 2.2 Deletion mutants of *AT5G57580* suppress the constitutively activated immunity of *cbp60g-1 snc2-1D*.

(A) Map position and the mutation in *bda7-1*. The asterisk is used to mark the position of *bda7-1*.

(B) Morphologies of four-week-old soil-grown plants of the indicated genotypes under long-day condition. Scale bar is 1 cm.

(C and D) Expression levels of *PR1* (C) and *ICS1* (D) in the indicated genotypes as normalized by *ACTIN1*. Error bars represent standard deviations. Letters indicate statistical differences ($P < 0.01$, one-way ANOVA followed by Tukey's multiple comparisons test; $n = 3$).

(E) Growth of *Hpa Noco2* conidiospores on the indicated genotypes. Error bars represent standard deviations.

Letters indicate statistical differences ($P < 0.01$, one-way ANOVA followed by Tukey's multiple comparisons test; $n = 4$).

2.4.4 CBP60b regulates *SARD1* expression

As the elevated *ICS1* expression and SA levels in *cbp60g-1 snc2-1D* are suppressed by *bda7-1* (Figure 2.1C - 2.1E), we examined whether the expression of *SARD1* is affected in the *cbp60b cbp60g-1 snc2-1D* mutants. As shown in Figure 2.3A, the expression level of *SARD1* is much higher in *cbp60g-1 snc2-1D* than in wild type, and the elevated *SARD1* expression is fully suppressed in *cbp60b cbp60g-1 snc2-1D*, suggesting that CBP60b functions upstream of *SARD1*. We also examined the expression levels of *FMO1*, which is another target gene of *SARD1*. Consistent with the expression levels of *SARD1*, up-regulation of *FMO1* in *cbp60g-1 snc2-1D* is also blocked in *cbp60b cbp60g-1 snc2-1D* (Figure 2.3B). These data suggest that CBP60b functions upstream of *SARD1*.

As CBP60b is predicted to be a transcription factor, we tested whether CBP60b binds to the promoter of *SARD1*. ChIP-qPCR assay was carried out on transgenic plants expressing *CBP60b-3HA* under its own promoter in the *cbp60b-4 cbp60g-1 snc2-1D* background. Compared to the non-transgenic negative control *cbp60g-1 snc2-1D*, ~4.6-fold enrichment of the DNA around 1.0 kb upstream of the start codon and ~2.8-fold enrichment of the DNA around 0.3 kb upstream of the start codon were observed in the samples from the *CBP60b-3HA* transgenic line (Figure 2.3C), indicating that CBP60b is recruited to the *SARD1* promoter region.

To further test whether CBP60b can activate the expression of *SARD1*, a plasmid expressing a luciferase reporter gene under the control of the *SARD1* promoter (*pSARD1::Luc*) was transformed into *Nicotiana (N.) benthamiana*, together with a *35S::CBP60b-3HA* construct. Co-transformation of *35S::CBP60b-3HA* with *pSARD1::Luc* resulted in increased expression of the

luciferase reporter (Figure 2.3D and 2.3E), suggesting that overexpression of *CBP60b* in *N. benthamiana* leads to activation of *SARD1* expression. Together, these data suggest that CBP60b serves as a transcriptional activator of *SARD1*.

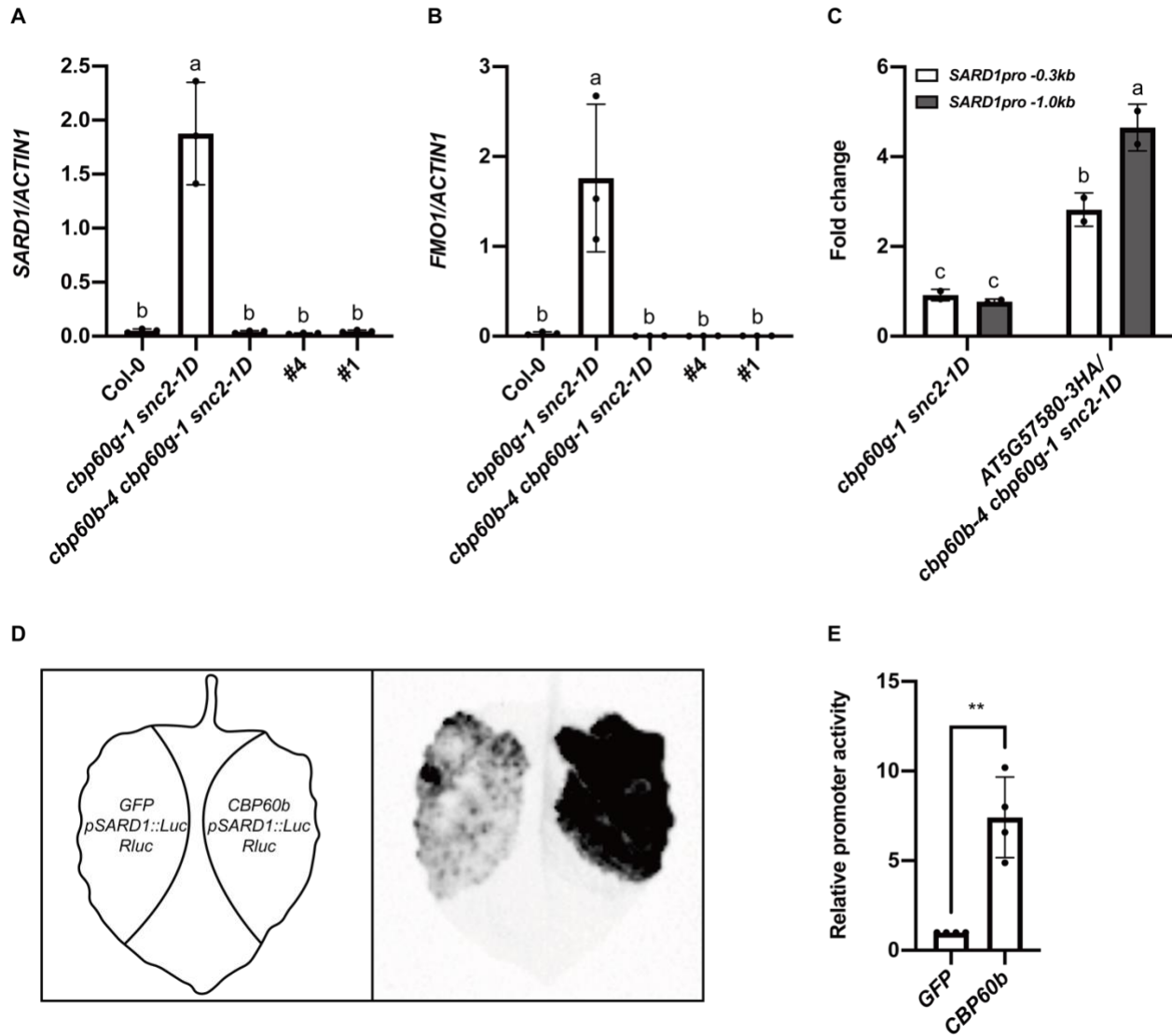


Figure 2.3 Regulation of *SARD1* expression by CBP60b.

(A and B) Expression levels of *SARD1* (A) and *FMO1* (B) in Col-0, *cbp60g-1 snc2-1D*, *cbp60b-4 cbp60g-1 snc2-1D* and two CRISPR lines of *AT5G57580* in *cbp60g-1 snc2-1D* background (#4 and #1) as described in Figure 2B. Expression levels were normalized to those of *ACTIN1*. Error bars represent standard deviations. Letters indicate statistical differences ($P < 0.01$, one-way ANOVA followed by Tukey's multiple comparisons test; $n = 3$).

(C) Binding of CBP60b to the promoter of *SARD1* as determined by ChIP-PCR. Two-week-old seedlings grown on ½ MS plates were sprayed with 1 µM of the elicitor nlp20 5 h before tissue collection. CBP60b-3HA chromatin complexes were immunoprecipitated with anti-HA antibody and protein G agarose beads. Negative control reactions were performed in parallel without adding anti-HA antibody. Immunoprecipitated DNA samples were quantified by qPCR using primers specific to *SARD1* promoter. ChIP results are presented as fold changes by dividing signals from ChIP with the anti-HA antibody by those from no antibody controls. Error bars represent standard deviations. Letters indicate statistical differences ($P < 0.05$, one-way ANOVA followed by Tukey's multiple comparisons test; $n = 2$).

(D) Activation of *pSARD1::Luc* reporter gene expression by CBP60b in *N. benthamiana* leaves. *Agrobacterium* carrying *pSARD1::Luc* ($OD_{600}=0.2$) and *pUBQ1::Rluc* expressing the Renilla luciferase ($OD_{600}=0.05$) were co-infiltrated with *Agrobacterium* carrying *35S::CBP60b* or *35S::GFP* ($OD_{600}=0.5$). The left diagram illustrates the different treatments. 2 days after inoculation, luminescence was detected after infiltration with 1 mM luciferin, as shown in the right image.

(E) Quantification of firefly luciferase activities in *N. benthamiana* leaves co-transformed with the construct combinations as indicated in (D). Relative promoter activity was presented as a ratio of firefly luciferase/renilla luciferase. Relative promoter activity of the GFP control group was set as 1. ** indicates statistical differences ($P < 0.01$, unpaired t test; $n = 4$).

2.4.5 Overexpression of *CBP60b* leads to up-regulation of *SARD1* and enhanced disease resistance in *Arabidopsis*

To further test the hypothesis that CBP60b regulates *SARD1* expression, we overexpressed *CBP60b* under the 35S promoter in wild type Col-0 background. Among a number of *CBP60b* lines with high levels of CBP60b-3HA protein (Appendix A.8), two lines, *CBP60b-3HA-OX #21* and *#27*, were selected for further analysis. Both lines exhibit dwarfism with dark green leaves (Figure 2.4A). The expression levels of *SARD1* are significantly higher in the *CBP60b-3HA* transgenic lines than in the wild type control (Figure 2.4B), further supporting the role of

CBP60b in regulating *SARDI* expression. Consistent with the elevated *SARDI* expression levels, these transgenic lines showed enhanced resistance to *Hpa* Noco2 (Figure 2.4C).

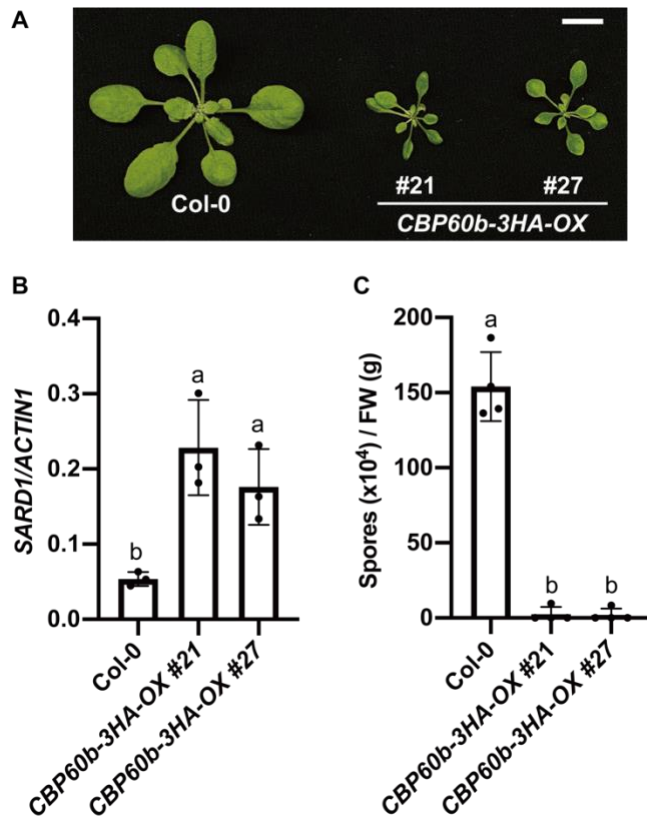


Figure 2.4 Overexpression of *CBP60b* leads to increased *SARDI* expression and enhanced resistance against *Hpa* Noco2.

(A) Morphologies of three-week-old soil-grown plants of the indicated genotypes under long-day condition. Scale bar is 1 cm.

(B) Expression level of *SARDI* in the indicated genotypes as normalized by *ACTIN1*. Error bars represent standard deviations. Letters indicate statistical differences ($P < 0.05$, one-way ANOVA followed by Tukey's multiple comparisons test; $n = 3$).

(C) Growth of *Hpa* Noco2 on the indicated genotypes. Error bars represent standard deviations. Letters indicate statistical differences ($P < 0.0001$, one-way ANOVA followed by Tukey's multiple comparisons test; $n = 4$).

2.4.6 *cbp60b* single mutants exhibit constitutively activated immune responses

The requirement of CBP60b for the constitutive defense responses in *cbp60g-1 snc2-1D* indicates that CBP60b serves as a positive regulator of plant immunity. To our surprise, when we isolated the *cbp60b-4* single mutant from the F2 population of a cross between *cbp60b-4 cbp60g-1 snc2-1D* and Col-0, the *cbp60b-4* plants displayed a dwarf morphology with dark green and abnormal leaves (Figure 2.5A). *cbp60b-4 cbp60g-1* double mutant plants isolated from the same F2 population showed an even more dramatic phenotype, as they were seedling-lethal and grew only two cotyledons at room temperature (Figure 2.5A). To rule out the possibility that the unexpected phenotypes originated from random background mutations in *cbp60b-4 cbp60g-1 snc2-1D*, we generated *cbp60b* deletion mutants in wild type Col-0 and *cbp60g-1* backgrounds by CRISPR/Cas9. The *cbp60b* deletion mutants *cbp60b-5* and *cbp60b-6* showed identical morphology as *cbp60b-4* (Figure 2.5A). In addition, the *cbp60b* deletion mutants in the *cbp60g-1* background exhibited similar morphology as *cbp60b-4 cbp60g-1* (Figure 2.5A). These data confirm that the dwarfism observed in *cbp60b-4* and *cbp60b-4 cbp60g-1* is caused by the mutation in *CBP60b*.

Next, we tested whether defense responses are activated in the *cbp60b* single and *cbp60b cbp60g* double mutants. As shown in Figure 2.5B, the expression levels of *PR1* were dramatically increased in *cbp60b-5* and *cbp60b-6* single mutants, and even higher in the *cbp60b cbp60g-1* double mutants. *cbp60b* and *cbp60b cbp60g-1* mutants also exhibited elevated *ICS1* expression (Figure 2.5C). Consistently, SA levels in *cbp60b* mutants were much higher than in the wild type (Figure 2.5D and 2.5E). In addition, *cbp60b* mutants showed strong resistance against *Hpa*

Noco2 (Figure 2.5F). These observations suggest that knocking out *CBP60b* leads to constitutive activation of defense responses.

We further examined whether mutations in *SARD1* affects the autoimmunity of *cbp60b cbp60g-1*. *cbp60b cbp60g-1 sard1-1* triple mutants were generated through knocking out *CBP60b* in the *cbp60g-1 sard1-1* double mutant by CRISPR/Cas9. Similar to the *cbp60b cbp60g-1* double mutant, *cbp60b cbp60g-1 sard1-1* triple mutants were seedling lethal and grew only two cotyledons (Appendix A.9A). Unlike *cbp60b cbp60g-1*, cotyledons of *cbp60b cbp60g-1 sard1-1* plants also showed visible lesion (Appendix A.9A).

Positive regulators of plant immunity are often monitored/guarded by NLR receptors (Cui, Tsuda, and Parker 2015). To test whether the constitutive defense responses in *cbp60b* is caused by activation of NLR-mediated immunity, we crossed *cbp60b-5* with *eds1-24*, a CRISPR deletion knockout mutant of *EDS1*, a gene known to be required for defense signaling mediated by Toll/interleukin-1 receptor (TIR) domain containing NLRs (TNLs) (Aarts et al. 1998). The *cbp60b-5 eds1-24* double mutant showed wild type-like morphology (Figure 2.5G). In addition, the constitutive *PR1* expression and enhanced resistance to *Hpa* Noco2 are completely suppressed in *cbp60b-5 eds1-24* (Figure 2.5H and 2.5I), indicating that the autoimmunity of *cbp60b* is dependent on *EDS1*, and TNL-mediated immunity is likely activated with loss of *CBP60b* function.

As NLR-mediated autoimmunity can often be suppressed by high temperature (van Wersch, Li, and Zhang 2016), we tested whether the dwarf phenotype of *cbp60b*, *cbp60b cbp60g-1* and

cbp60b cbp60g-1 sard1-1 can be suppressed by growing them at 28 °C. As shown in Appendix A.9B, *cbp60b* exhibited wild type morphology at 28 °C, while *cbp60b cbp60g-1* and *cbp60b cbp60g-1 sard1-1* plants had intermediate size and were able to grow true leaves at 28 °C.

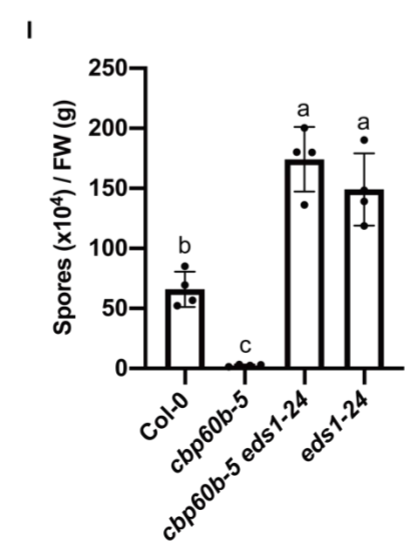
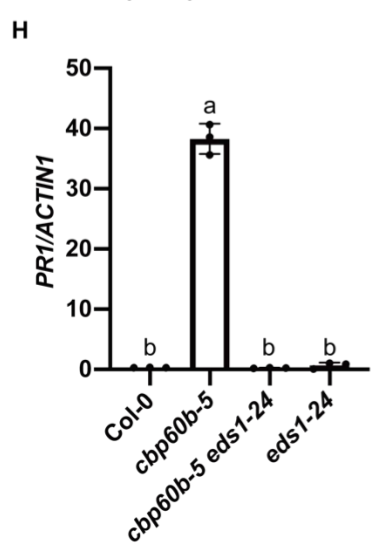
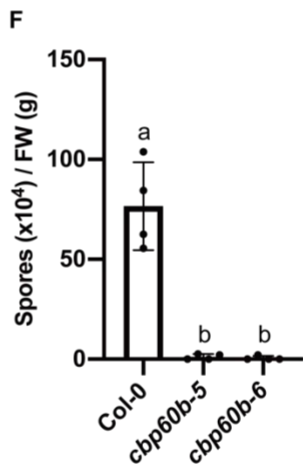
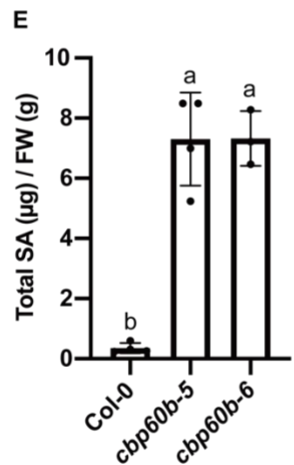
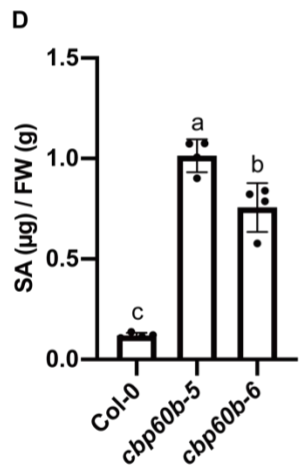
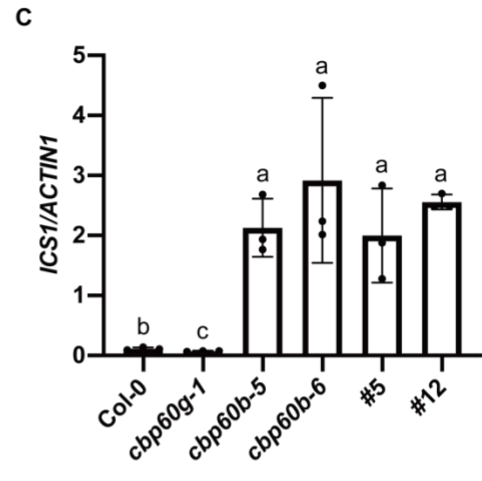
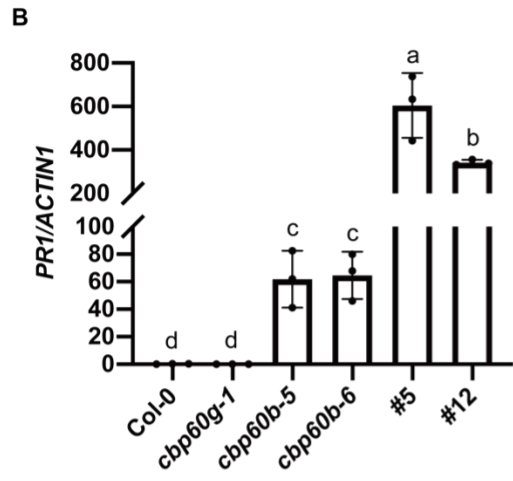
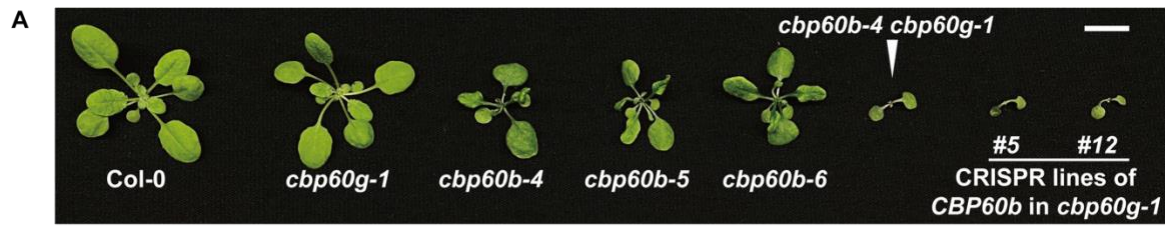


Figure 2.5 Knocking out *CBP60b* activates *EDS1*-dependent defense responses.

(A, G) Morphologies of three-week-old soil-grown plants of the indicated genotypes under long-day condition.

Scale bar is 1 cm.

(B, C) Expression levels of *PR1* (B) and *ICS1*(C) in the indicated genotypes as normalized by those of *ACTIN1*.

Error bars represent standard deviations. Letters indicate statistical differences ($P < 0.05$, Student's t-test; $n = 3$).

(D, E) Free (D) and total SA(E) levels in the indicated genotypes. Error bars represent standard deviations. Letters indicate statistical differences ($P < 0.01$, one-way ANOVA followed by Tukey's multiple comparisons test; $n = 4$).

(F) Growth of *Hpa Noco2* on the indicated genotypes. Error bars represent standard deviations. Letters indicate statistical differences ($P < 0.0001$, one-way ANOVA followed by Tukey's multiple comparisons test; $n = 4$).

(H) Expression levels of *PR1* in the indicated genotypes as normalized by those of *ACTIN1*. Error bars represent standard deviations. Letters indicate statistical differences ($P < 0.0001$, one-way ANOVA followed by Tukey's multiple comparisons test; $n = 3$).

(I) Growth of *Hpa Noco2* on the indicated genotypes. Error bars represent standard deviations. Letters indicate statistical differences ($P < 0.01$, one-way ANOVA followed by Tukey's multiple comparisons test; $n = 4$).

2.5 Discussion

SARD1 and *CBP60g* play critical roles in transcriptional regulation of plant immunity (Sun et al. 2015). Unlike *CBP60g*, which requires binding of CaM for its activation (Wang et al. 2009), *SARD1* is primarily regulated at transcription level. The autoimmune mutant *snc2-ID* provides a unique system to uncover components regulating *SARD1* expression, as the constitutive defense responses in *cbp60g-1 snc2-ID* is mainly dependent on *SARD1* (Sun et al. 2015). From a suppressor screen of *cbp60g-1 snc2-ID*, here we identified *CBP60b* as a positive regulator of *SARD1* transcription. *CBP60b* is targeted to the promoter region of *SARD1* and required for its up-regulation in *cbp60g-1 snc2-ID*. Overexpression of *CBP60b* leads to elevated *SARD1* expression and constitutive defense responses. In addition, transient expression of *CBP60b* in *N.*

benthamiana activates the expression of the *pSARD1-Luc* reporter gene, confirming that CBP60b positively regulates the expression of *SARD1*.

CBP60b belongs to the same protein family as SARD1 and CBP60g (Reddy et al. 2002), which share a highly conserved central domain with DNA-binding activity but have divergent sequences at the N- and C-termini (Wang et al. 2009; Zhang, Xu, et al. 2010). Unlike *SARD1* and *CBP60g*, which are strongly induced during pathogen infection (Wang et al. 2009; Zhang, Xu, et al. 2010), *CBP60b* is constitutive expressed in different tissue (Reddy et al. 2002). CBP60b was identified as a CaM-binding protein, suggesting that its activity might be influenced by Ca²⁺ levels (Reddy et al. 2002). SARD1 was previously shown to activate *ICS1* expression through a GAAATTT motif on its promoter (Sun et al. 2015). CBP60b shares ~80% sequence similarity with SARD1 in the middle domain. Whether it binds to a similar DNA sequence in activating *SARD1* expression remains to be determined.

Surprisingly, defense responses are constitutively activated in the *cbp60b* single mutants. The constitutive defense response in *cbp60b* is blocked by knocking out *EDS1*, suggesting that loss of *CBP60b* leads to activation of TNL-mediated immune signaling. It is possible that CBP60b is required for the expression of a negative regulator of TNL-mediated immune signaling. More likely, CBP60b could be either directly or indirectly monitored by a TNL and loss of its function triggers activation of this unidentified TNL and downstream defense responses, since critical immune regulators are often targeted by pathogen effector proteins and guarded by plant NLR receptors (Cui et al. 2015; Kourelis and Van Der Hoorn 2018). This is supported by the partial requirement of the TNL SNC1 (SUPPRESSOR OF NPR1-1, CONSTITUTIVE 1) for the

autoimmunity of *cbp60b* (Li et al. 2021). Although no pathogen effector has been reported to target CBP60b, SARD1 and CBP60g were shown to be targets of *Verticillium* effector VdSCP4 (Qin et al. 2018).

Compared to *cbp60b*, the autoimmune phenotype of the *cbp60b cbp60g-1* double mutants is even more dramatic, suggesting that *CBP60b* and *CBP60g* play partially redundant roles in transcriptional regulation of the putative guardee/decoy recognized by the unknown TNL. In *cbp60b*, the expression of the putative guardee/decoy is partially blocked, leading to activation of TNL-mediated immunity. Lacking both CBP60b and CBP60g leads to further reduction of its expression and stronger defense responses. Interestingly, the severe dwarf phenotype of *cbp60b cbp60g-1* was not observed in the *snc2-1D* background. It is possible that *snc2-1D* can also activate CBP60b and CBP60g-independent expression of the putative guardee/decoy, which compensates the loss of CBP60b and CBP60g.

A working model is proposed based on our findings (Figure 2.6). CBP60b promotes the expression of *SARD1* and contributes to SNC2-mediated immunity. It is required for the expression of a yet-to-be-identified guardee/decoy of a TNL. Disruption of the expression of the putative guardee/decoy results in activation of TNL-mediated immunity. It is of future interest to identify this guardee/decoy that is guarded by SNC1 and other TNL(s).

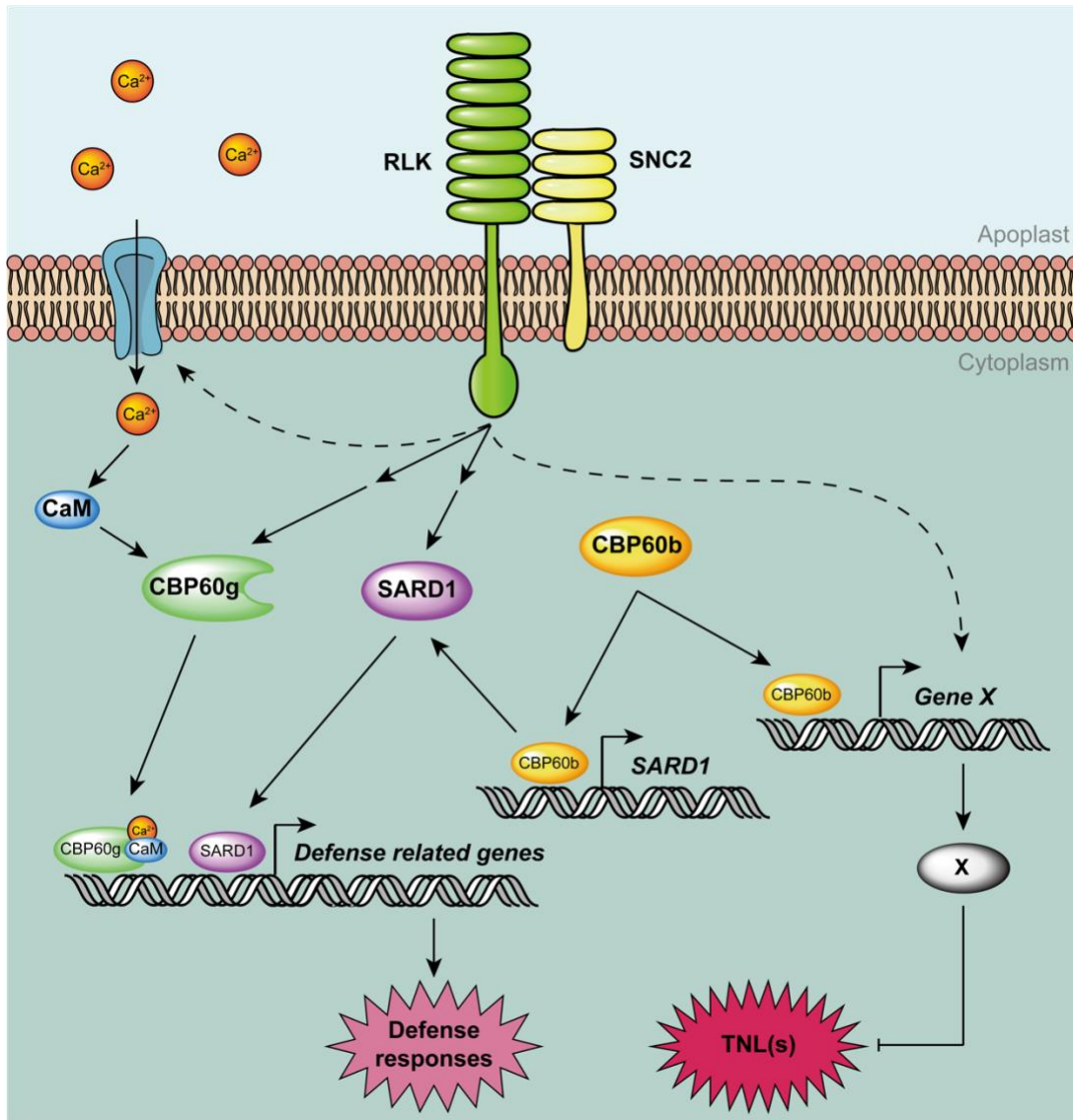


Figure 2.6 A working model of CBP60b in plant immunity.

On one hand, CBP60b contributes to SNC2-mediated immunity by promoting *SARD1* expression. On the other hand, it is also required for the expression of an unknown gene (X), which encodes a guardee/decoy of a TNL(s) or a negative regulator of TIR signaling. Activation of SNC2-mediated defense responses also leads to CBP60b-independent expression of gene X.

Chapter 3: The adaptor protein 4 complex contributes to plant immune regulation

3.1 Summary

The *Arabidopsis* receptor-like protein SUPPRESSOR OF NPR1-1, CONSTITUTIVE 2 (SNC2) is required for basal resistance against pathogenic bacteria. The gain-of-function *snc2-1D* mutant exhibits constitutively activated defense responses. Two transcription factors, SYSTEMIC ACQUIRED RESISTANCE DEFICIENT 1 (SARD1) and CALMODULIN-BINDING PROTEIN 60g (CBP60g), are required for the autoimmunity of *snc2-1D*. Constitutive defense responses in *snc2-1D* are only modestly affected by mutations in *cbp60g*, but completely suppressed by the *sard1 cbp60g* double mutant. Here, we report the identification of the adaptor protein 4 (AP4) complex as an essential component in SNC2-mediated plant immunity. From a suppressor screen using *cbp60g-1 snc2-1D*, mutations in AP4 μ , one of the subunits of AP4 complex, were identified. AP4 complex is involved in target protein sorting in trans-Golgi network (TGN). AP4 μ interacts with BDA1, a transmembrane protein required for SNC2-mediated immunity, suggesting that AP4 complex is likely involved in regulating the subcellular localization of BDA1. In addition, *ap4m* deletion mutants exhibit compromised effector-triggered immunity and pattern-triggered immunity, indicating a broader role of AP4 complex in plant immunity. Thus, the AP4 complex likely contributes to plant immunity regulation through assisting target immune-related proteins for proper subcellular localization.

3.2 Introduction

In nature, plants encounter various microbial pathogens. During co-evolution, plants have evolved a two-tiered immune system to prevent pathogen infection (Jones and Dangl 2006; Ngou

et al. 2022). Pattern recognition receptors (PRRs) localized on plasma membrane can sense conserved pathogen molecules, which are known as pathogen/microbe-associated molecular patterns (PAMPs/MAMPs) (Monaghan and Zipfel 2012; Zhou and Zhang 2020). Perceiving PAMPs by plant PRRs leads to activation of pattern-triggered immunity (PTI), the first tier of plant innate immunity, which protects plants from most pathogens. However, some adapted pathogens can deliver effector proteins into plant cells to interfere with PTI (Jones and Dangl 2006). To restrict the colonization of the pathogens, plants further evolved the immune receptors that specifically recognize pathogen-secreted effectors and thereby initiate the second-tier of immunity named effector-triggered immunity (ETI) (van Wersch et al. 2020). Most of these receptors are intracellular nucleotide-binding leucine-rich-repeat receptor proteins (NLRs). Onset of either PTI or ETI turns on a series of defense responses, including activation of plant defense hormone salicylic acid (SA) biosynthesis and increased expression of the defense marker *pathogenesis-related (PR)* genes.

One group of plant PRRs consists of receptor-like proteins (RLPs), which have a short cytoplasmic tail, a single transmembrane domain, and an extracellular leucine-rich-repeat domain that facilitates the interaction with its corresponding ligand. SNC2 (SUPPRESSOR OF NPR1-1, CONSTITUTIVE 2) is an RLP in *Arabidopsis*. The gain-of-function mutant *snc2-ID* exhibits constitutively activated plant immunity, with increased SA accumulation, *PR* gene expression and resistance against the oomycete pathogen *Hyaloperonospora arabidopsidis (Hpa)* Noco2 (Zhang, Yang, et al. 2010). On the other hand, loss of *SNC2* function leads to enhanced disease susceptibility to the bacterial pathogen *Pseudomonas syringae* pv. *tomato (Pst)* DC3000 (Zhang, Yang, et al. 2010), suggesting that *SNC2* is a critical component of the plant immune

system. Due to a trade-off between immunity and growth, the autoimmune mutant *snc2-ID* has a dwarfed stature.

SAR DEFICIENT 1 (SARD1) and CALMODULIN BINDING PROTEIN 60g (CBP60g) are two master transcription factors in plant immunity (Sun et al. 2015; Wang et al. 2011; Zhang, Xu, et al. 2010). They coordinately regulate pathogen-induced expression of SA biosynthetic genes, such as *ISOCHORISMATE SYNTHASE 1 (ICS1)*, *ENHANCED DISEASE SUSCEPTIBILITY 5 (EDS5)*, and *AVRPPHB SUSCEPTIBLE 3 (PBS3)* (Sun et al. 2015; Zhang, Xu, et al. 2010). The increase in SA levels in response to pathogen infection is almost completely lost in *sard1 cbp60g*, resulting in enhanced susceptibility to pathogens (Zhang, Xu, et al. 2010). SARD1 and CBP60g are required for the autoimmunity in *snc2-ID* (Sun et al. 2015). The elevated *ICS1* expression and SA accumulation in *snc2-ID* are partially suppressed in *sard1-1 snc2-ID* and *cbp60g-1 snc2-ID*, and almost fully blocked in *cbp60g-1 sard1-1 snc2-ID* (Sun et al. 2015). As for plant morphology, the dwarfism observed on *snc2-ID* is slightly attenuated in *sard1-1 snc2-ID* and *cbp60g-1 snc2-ID*, whereas *cbp60g-1 sard1-1 snc2-ID* is almost wild type-like (Sun et al. 2015). These findings indicate two parallel pathways downstream of SNC2, one requiring SARD1 and the other dependent on CBP60g. How SNC2 activates SARD1 and CBP60g requires further study.

Vacuole, a plant organelle for storage of proteins and metabolites, is involved in plant immunity (Hara-Nishimura and Hatsugai 2011; Madina et al. 2019; Shimada et al. 2018). A number of hydrolytic enzymes and defense-related proteins are localized in vacuoles, including some cysteine proteinases and chitinases, which have either direct antimicrobial properties or play a

role in growth restriction of pathogens (Boller and Vögeli 1984; Madina et al. 2019; Neuhaus et al. 1991; Shimada et al. 2018). A fusion of vacuolar membrane and plasma membrane has been observed in *Arabidopsis* cells after inoculation of avirulent *Pst* DC3000 strains carrying *avrRpm1* or *avrRpt2*, which allows direct discharge of the antimicrobial substances from vacuole to extracellular space where bacteria propagate (Hatsugai et al. 2009, 2018). *Arabidopsis* mutants defective in the fusion formation lost ETI-induced cell death and display enhanced disease susceptibility, suggesting that the vacuole-plasma membrane fusion contributes to activation of plant cell death during ETI (Hara-Nishimura and Hatsugai 2011; Hatsugai et al. 2009). However, it remains largely unknown how this fusion structure is formed during pathogen attack.

Studies on *Arabidopsis* mutants deficient in sorting vacuolar proteins showed that the adapter protein 4 (AP4) complex is crucial in vacuolar protein sorting (Fuji et al. 2016; Law, Chung, and Zhuang 2022). The AP4 complex is composed of four subunits, AP4 ϵ , β , μ and σ , which is located on trans-Golgi network (TGN). The *Arabidopsis* AP4 complex was suggested to export target proteins from TGN into multivesicular body/pre-vacuolar compartment, and subsequently to vacuole (Law et al. 2022). In human, the AP4 complex is involved in autophagosome formation by transport of a critical autophagy protein ATG9A from TGN to preautophagosomal structure (Mattera et al. 2017). AP4 complex deficiency is associated with a number of human diseases (Abou Jamra et al. 2011; Moreno-De-Luca et al. 2011; Verkerk et al. 2009). There are very few studies on the plant AP4 complex. *Arabidopsis* mutants of two AP4 subunits, *ap4b* and *ap4e* (for subunit AP4 β and AP4 ϵ respectively), were recently found to be defective in plant cell death induced by avirulent bacteria (Hatsugai et al. 2018). In addition, *ap4b* and *ap4e* mutants are also defective in the aforementioned vacuole-plasma membrane fusion formation, suggesting

that the AP4 complex may mediate avirulent bacteria-induced plant cell death by regulating the fusion formation (Hatsugai et al. 2018).

To identify regulators required for SARD1-dependent defense responses downstream of SNC2, a suppressor screen was performed in the *cbp60g-1 snc2-ID* background. Here, we report the identification and characterization of three suppressors: *bda6-1* (*bian da 6*; *bian da* means “becoming big” in Chinese), *bda6-2* and *bda6-3*. Map-based cloning revealed that they carry different mutations in the AP4 subunit AP4 μ . Further analysis showed that AP4 μ is involved in regulating SNC2-mediated immune responses by interacting with the previously identified BDA1 protein.

3.3 Materials and methods

3.3.1 Plant materials and growth conditions

All *Arabidopsis* mutants are in the Col-0 ecotype background unless specified. The *cbp60g-1 snc2-ID* plants were described previously (Sun et al. 2015). Plants were grown on soil under long-day conditions (16-h light/ 8-h dark cycle) with a light intensity of $\sim 100 \mu\text{mol}/\text{m}^2/\text{s}$ at 22 °C unless specified. Plants for quantitative RT-PCR were grown on plates with $\frac{1}{2}$ Murashige and Skoog (MS) and 1% sucrose for 2 weeks. Plants used for SA quantification were grown on soil for 4 weeks under short-day conditions (8-h light/ 16-h dark cycle). Plants used for bacterial infection assay were grown on soil under short-day conditions for 3 weeks.

3.3.2 Plasmid constructs and generation of transgenic plants and deletion mutants

The CRISPR/Cas9 system used for generating *AP4M* and *AP4E* deletion mutants was described previously (Xing et al. 2014). In short, two guide RNAs were designed to target genomic DNA of the designated gene for generation of a deletion of ~1 kb in size. A PCR fragment containing the guide RNA sequences was amplified from the *pCBC-DT1T2* vector using primers listed in Appendix B.5, and subsequently inserted into the *pHEE401* or *pBEE401* vectors using the *BsaI* site. The derived plasmid was transformed into *E. coli* DH10B and later *Agrobacterium* GV3101 by electroporation. *Arabidopsis* plants were transformed with the *Agrobacterium* carrying the plasmid by floral dip (Clough and Bent 1998). T1 plants were analyzed for deletion in the target genes by PCR with primers listed in Appendix B.5. Homozygous deletion mutants were obtained in the T2 generation.

A genomic DNA fragment containing *AP4M* gene and its native promoter was cloned into the *pBASTA-np-3HA* vector modified from *pCambia1305*, to obtain *pAP4M::AP4M*. *Agrobacteria* carrying this plasmid was transformed into *bda6-1 cbp60g-1 snc2-1D* to generate transgenic lines of *pAP4M::AP4M/bda6-1 cbp60g-1 snc2-1D*. The genomic DNA fragments of *BDA1* and *AP4M* were also cloned into *pBasta35s::2HA-TurboID* and *pCambia1300-35s-3FLAG* plasmids respectively to express *AP4M-HA-TurboID*, *BDA1-HA-TurboID*, *AP4M-3FLAG* and *BDA1-3FLAG*, by primers listed in Appendix B.5. *Agrobacteria* carrying *pBasta35s::AP4M-HA-TurboID* was transformed into *bda6-1 cbp60g-1 snc2-1D* to obtain transgenic plants of *35s::AP4M-2HA-TurboID/bda6-1 cbp60g-1 snc2-1D*.

3.3.3 Mutagenesis and suppressor screen

About 5,000 *cbp60g-1 snc2-1D* mutant seeds were mutagenized with 20 mM ethyl methanesulfonate (EMS) as described previously (Li and Zhang 2016). In brief, seeds were soaked in the EMS solution for 16 h. Afterwards, the EMS solution was removed, and the seeds were washed with 100 mM Na₂S₂O₃ three times and then with ddH₂O three more times. The mutagenized seeds were plated on ½ MS plate and later transplanted to soil when the seedlings were about 10-day-old. M2 plants were grown on soil and screened for plants that are larger than *cbp60g-1 snc2-1D*. Any plants with a larger size were collected for further analysis.

3.3.4 Genetic mapping, mapping-by-sequencing, and identification of *bda6*

Traditional mapping of *bda6-1* was carried out on an F₂ population from a cross between *bda6-1 cbp60g-1 snc2-1D* mutant (in Col-0 background) and Landsberg *erecta* (*Ler*). All plants homozygous for both *snc2-1D* and *cbp60g-1* were selected for linkage analysis using SSLP markers as previously described (Zhang et al. 2007). As a result, *bda6-1* was mapped to chromosome 4. Afterwards, fine mapping was conducted on both F₂ and F₃ plants with additional markers to narrow down the region where *bda6-1* is located to.

For mapping-by-sequencing, three *bda6 cbp60g-1 snc2-1D* mutants were backcrossed with *cbp60g-1 snc2-1D* respectively. In each F₂ population, about 50 plants that showed similar morphology as original *bda6 cbp60g-1 snc2-1D* mutants were selected and pooled for genomic DNA extraction. The genomic DNA was subsequently sequenced using the HiSeq-PE150 platform. Single nucleotide polymorphisms (SNPs) were called from the next-generation sequencing data by Genome Analysis Toolkit (GATK v3.5-0) (McKenna et al. 2010) following

the variants discovery pipeline from GATK Best Practices (Depristo et al. 2011). Briefly, the raw sequence was trimmed and filtered with prinseq lite 0.20.4 to remove any unwanted sequences (Schmieder and Edwards 2011). The sequences were next mapped to Tair10 *Arabidopsis* reference genome with BWA MEM (Li 2013). The alignments were then processed by GATK HaplotypeCaller to call for variants. All variants identified were then merged in PICARD tools (<http://broadinstitute.github.io/picard>). After variants calling, we searched through the ~1.0 Mb region on chromosome 4 for homozygous SNPs in the exons of genes, and identified *bda6-1*, *bda6-2*, and *bda6-3* mutations as different mutations in the same gene.

3.3.5 RNA extraction, reverse transcription and qPCR

For gene expression analysis, approximately 50 mg plant tissues from 3-4 2-week-old seedlings of the indicated genotypes were collected as a single sample. Three biological replicates were analyzed for each genotype. RNA extraction was performed using the EZ-10 Spin Column Plant RNA Miniprep Kit (Bio Basic Inc., Toronto, Canada). RNAs were reverse transcribed into cDNAs by OneScript Reverse Transcriptase (Applied Biological Materials Inc., Richmond, Canada). qPCR was performed on the total cDNAs using SYBR Premix Ex Taq™ II (Takara, Shiga, Japan). Primers for qPCR are listed in Appendix B.5.

3.3.6 Co-immunoprecipitation analysis

Co-immunoprecipitation (Co-IP) analysis was performed on proteins transiently expressed in four-week-old *N. benthamiana* leaves. *Agrobacterium* carrying the designated constructs were cultured in liquid LB supplemented with appropriate antibiotics at 28 °C overnight before they were collected and resuspended in a buffer containing 10 mM MgCl₂ and 150 μM

acetosyringone. *Agrobacteria* suspensions carrying different constructs were mixed in specified combinations. The final concentration of AP4M-HA-TurboID, BDA1-3FLAG, BDA1-HA-TurboID and AP4M-3FLAG was $OD_{600}=0.4$. The final concentration of GFP-HA-TurboID was $OD_{600}=0.8$. The mixed bacterial suspensions were kept at room temperature for 3 hours before infiltration into leaves of *N. benthamiana*.

Two days after infiltration, about 1.5 gram of plant leaf tissue from the infiltrated area was harvested, frozen with liquid nitrogen and ground into fine powder. The ground tissue was resuspended in 2.5 volumes of the extraction buffer containing 10% glycerol, 25 mM Tris-HCl pH 7.5, 1 mM EDTA, 150 mM NaCl, 1% NP-40, 0.5% Triton X-100, 10 mM DTT, 2% PVPP, 2mM NaF, 1mM PMSF, and 1× protease inhibitor cocktail (Roche). The resuspensions were kept on a rotator at 4 °C for 20 min and afterwards centrifuged at 15,000×g for 10 min. The supernatants were obtained and centrifuged at 15,000×g for two more times. Afterwards, the clear supernatants were incubated with anti-FLAG M2 beads (Sigma-Aldrich) on a rotator at 4 °C for 2 h. Next, beads were collected by centrifugation and washed with 1 volume of extraction buffer without PVPP for four times. Proteins enriched on the beads were subsequently eluted for SDS-PAGE electrophoresis and western blot analysis.

3.3.7 Pathogen infection assay

Hpa Noco2 infection was conducted by spraying 2-week-old seedlings with conidia spores in water (50,000 spores/ml). Inoculated seedlings were covered with a transparent lid and grown in a plant growth chamber at 18 °C with a relative humidity of ~80%. Infection was scored at 7 dpi

by counting conidia spores with a hemocytometer. Four - five individual plants were pooled as a single sample. Four biological replicates were included for each genotype.

For bacterial infection assays, two leaves of each 4-week-old plant grown on soil under short day condition were infiltrated with *Pst* DC3000 or *Pst* DC3000 *AvrRpt2* suspension in 10 mM MgCl₂ at the designated concentration with a needleless syringe. Bacterial growth was scored on the day of infection (Day 0) and 3 days post inoculation (Day 3). Two leaf discs from a single plant were collected as one sample. Six to eight biological replicates were included for each genotype. Leaf samples were ground in 10 mM MgCl₂ solution with glass beads at room temperature. The solution was next diluted and plated on LB agar plates with appropriate antibiotic selection. Bacteria colonies were counted after 1-day incubation at 28 °C and calculated as colony-forming unit (cfu). The final value was presented as cfu/cm².

For flg22- and nlp20-induced resistance assay, two leaves of each *Arabidopsis* plant were first treated with either flg22 or nlp20 at 1μM by infiltration with a needleless syringe. 24 hours later, the pre-treated leaves were inoculated with *Pst* DC3000 suspensions in 10 mM MgCl₂ (OD₆₀₀=0.001). Bacteria growth was scored 3 days post inoculation as described above. Six biological replicates were included for each genotype.

3.3.8 Statistical analysis

Error bars in all figures represent standard deviations. The number of biological replicates is indicated in the figure legends. Statistical comparison among different samples is carried out by

either one-way ANOVA with Tukey's honestly significant difference (HSD) post hoc test or Student's *t*-test, as shown in the figure legends.

3.4 Results

3.4.1 Identification and characterization of *bda6-1*, *bda6-2* and *bda6-3* from the *cbp60g-1 snc2-1D* suppressor screen

To identify regulators of SARD1-dependent defense signaling in SNC2-mediated immunity, we screened for mutants that can suppress the dwarfism of *cbp60g-1 snc2-1D*. Three *bda6 cbp60g-1 snc2-1D* mutants were recovered from the screen. As shown in Figure 3.1A, the *bda6 cbp60g-1 snc2-1D* mutants displayed intermediate plant size compared to wild type Col-0 and *cbp60g-1 snc2-1D*. Quantitative reverse transcript (RT)-PCR analysis showed that the constitutive expression of *PR1* and *ICS1* in *cbp60g-1 snc2-1D* was completely suppressed by *bda6* mutations (Figure 3.1B and 3.1C). Consistent with the *ICS1* expression level, SA levels in the *bda6 cbp60g-1 snc2-1D* mutants were comparable to that in Col-0. Moreover, the enhanced disease resistance against oomycete pathogen *Hpa Noco2* in *cbp60g-1 snc2-1D* was fully blocked by the *bda6* mutations (Figure 3.1D). Together, the *bda6* mutations suppress the autoimmunity of *cbp60g-1 snc2-1D*.

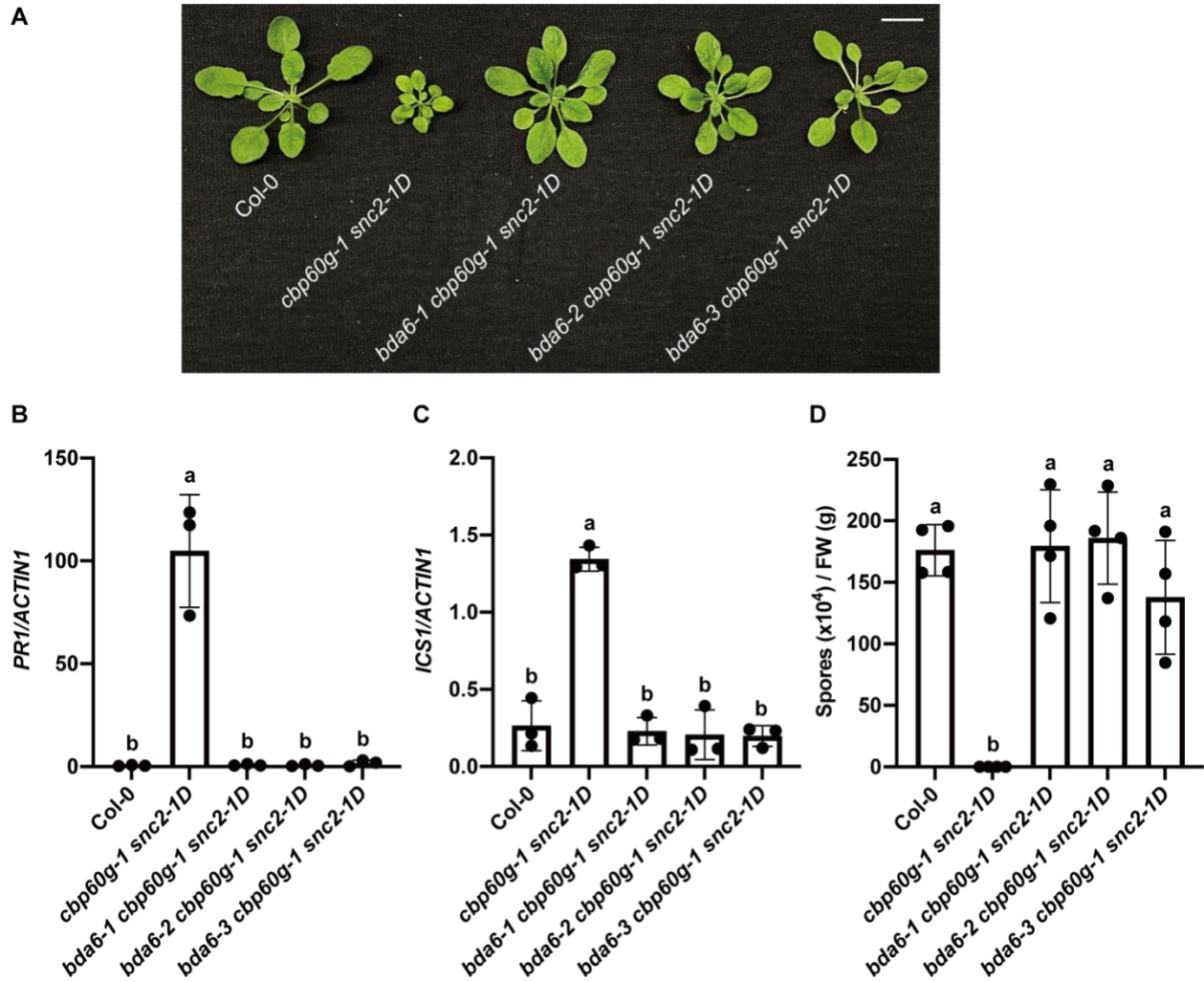


Figure 3.1 Identification and characterization of three alleles of *bda6 cbp60g-1 snc2-1D*.

(A) Morphologies of 3-week-old soil-grown plants of Col-0, *cbp60g-1 snc2-1D*, and three *bda6 cbp60g-1 snc2-1D* mutants. Scale bar, 1 cm.

(B and C) Relative expression levels of *PR1* (B) and *ICSI* (C) in the indicated genotypes. Transcript levels were normalized to those of *ACTIN1*. Error bars represent standard deviations. Letters indicate statistical differences ($P < 0.0001$, one-way ANOVA followed by Tukey's multiple comparison test; $n = 3$).

(D) Growth of *Hpa Noco2* conidiospores on the indicated genotypes. Error bars represent standard deviations.

Letters indicate statistical differences ($P < 0.01$, one-way ANOVA followed by Tukey's multiple comparison test; $n = 4$).

3.4.2 Map-based cloning of *BDA6*

To identify the responsible mutations which cause the suppression of defense responses in *bda6-1 cbp60g-1 snc2-1D*, genetic mapping of *bda6-1* was performed. *bda6-1 cbp60g-1 snc2-1D* was crossed with Landsberg *erecta*. In the F2 population, plants homozygous for *cbp60g-1* and *snc2-1D* loci with dwarf morphology were used for linkage analysis. *bda6-1* was initially found to be genetically linked with the simple sequence length polymorphism marker FIN20 and F19H22 on chromosome 4 (Figure 3.2). Subsequent fine-mapping with F3 population narrowed *bda6-1* to a smaller region of ~ 1.0Mb between T22A6 and M4I22 (Figure 3.2).

Meanwhile, *bda6-1 cbp60g-1 snc2-1D* as well as *bda6-2 cbp60g-1 snc2-1D* and *bda6-3 cbp60g-1 snc2-1D* were backcrossed to *cbp60g-1 snc2-1D* to generate F2 populations for next generation sequencing. F2 plants showed similar morphology to *bda6 cbp60g-1 snc2-1D* were obtained and sequenced by Illumina sequencing. Analysis of the sequencing data showed that all three *bda6* mutants carry different mutations in *At4g24550*, a gene within the ~1.0Mb between T22A6 and M4I22 (Appendix B.1, B.2 and B.3). *bda6-1* and *bda6-3* have the same C-to-T mutation, which creates an early stop codon, whereas *bda6-2* carries a G-to-A mutation at the splicing acceptor site of the sixth intron (Figure 3.2). *At4g24550* is *AP4M*, which encodes the AP4 μ subunit of AP4 complex.

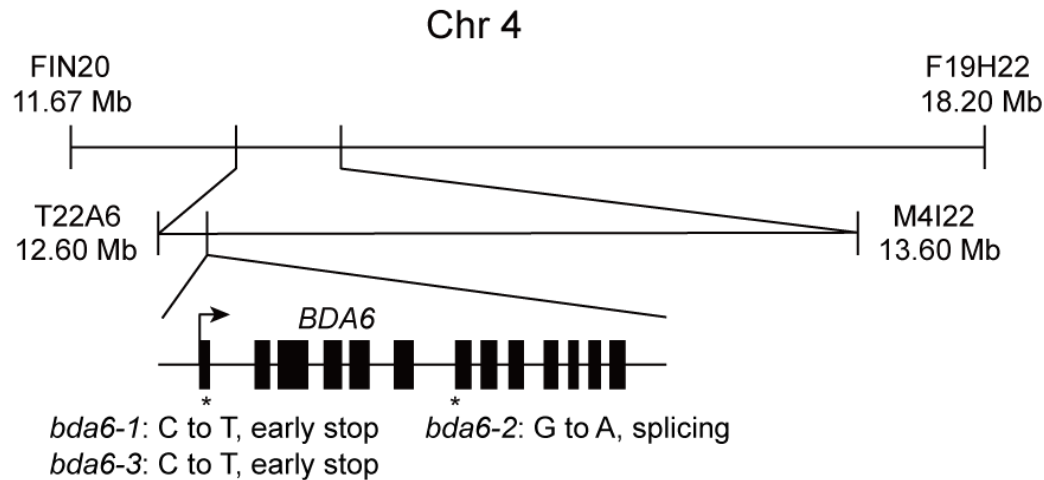


Figure 3.2 Map position of the *bda6* mutations.

The asterisks mark the positions of *bda6* mutations.

3.4.3 Loss of AP4M suppresses the autoimmunity of *cbp60g-1 snz2-1D*

To confirm that the mutations of *AP4M* are responsible for the phenotypes of the *bda6 cbp60g-1 snz2-1D* suppressors, *AP4M* deletion mutants were generated in the *cbp60g-1 snz2-1D* background using CRISPR/Cas9 (Appendix B.4). As shown in Figure 3.3A, two independent deletion lines of *ap4m cbp60g-1 snz2-1D* displayed similar morphology as the *bda6 cbp60g-1 snz2-1D* mutants. Consistently, the constitutive expression of *PR1* and *ICS1* was fully suppressed in *ap4m cbp60g-1 snz2-1D* (Figure 3.3B and 3.3C). In addition, the enhanced disease resistance against *Hpa Noco2* was abolished in these deletion lines (Figure 3.3D), suggesting that *AP4M* is required for the autoimmunity of *cbp60g-1 snz2-1D*.

Furthermore, transforming the wild type *AP4M* under its own promoter into the *bda6-1 cbp60g-1 snz2-1D* background complemented the *bda6-1* mutant phenotype (Figure 3.3E), further confirming that *AP4M* is *BDA6*. Expressing *AP4M* with a C-terminal 2HA-TurboID tag under the *35S* promoter in *bda6-1 cbp60g-1 snz2-1D* also restored the dwarfism of *cbp60g-1 snz2-1D*

(Figure 3.3E), suggesting that the AP4 μ -2HA-TurboID fusion protein function similarly as AP4 μ .

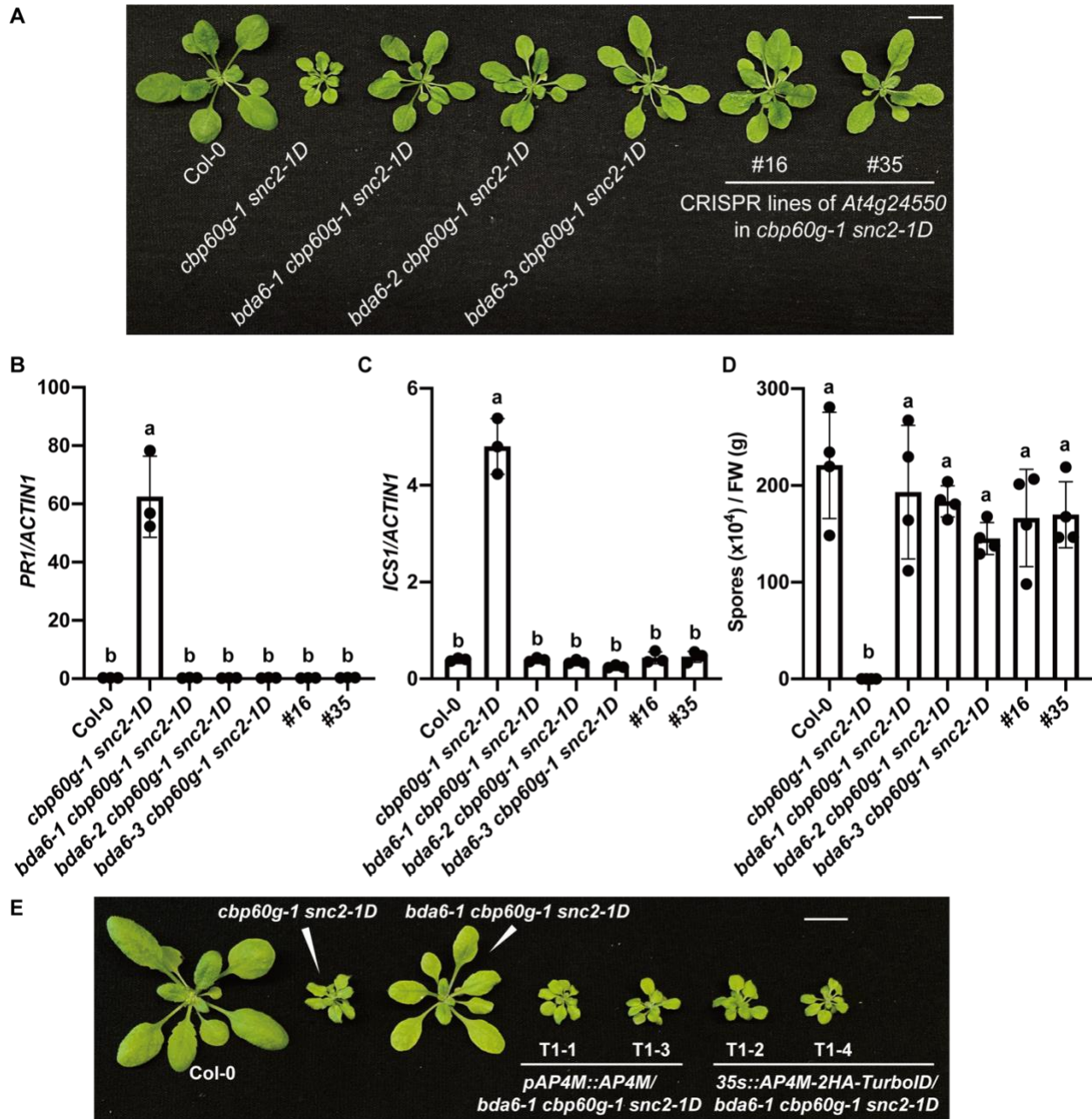


Figure 3.3 Mutations in *AT4g24550* suppress autoimmunity of *cbp60g-1 snc2-1D*.

(A) Morphologies of 3-week-old soil-grown plants of Col-0, *cbp60g-1 snc2-1D*, *bda6 cbp60g-1 snc2-1D* mutants and two CRISPR deletion lines of *At4g24550* in the *cbp60g-1 snc2-1D* background (#16 and #35). Scale bar is 1 cm.

(B and C) Expression levels of *PR1* (B) and *ICS1* (C) in the indicated genotypes as normalized by *ACTIN1*. Error bars represent standard deviations. Letters indicate statistical differences ($P < 0.01$, one-way ANOVA followed by Tukey's multiple comparisons test; $n = 3$).

(D) Growth of *Hpa* Noco2 conidiospores on the indicated genotypes. Error bars represent standard deviations. Letters indicate statistical differences ($P < 0.01$, one-way ANOVA followed by Tukey's multiple comparisons test; $n = 4$).

(E) Morphologies of 4-week-old soil-grown plants of the indicated genotypes. Scale bar is 1 cm.

3.4.4 Mutations in AP4 subunits suppress the autoimmunity of *cbp60g-1 snc2-1D*

Besides AP4 μ , heterotetrametric AP4 complex consists of three other subunits: AP4 ϵ , AP4 β , and AP4 σ . To investigate whether the AP4 complex is required for autoimmunity of *cbp60g-1 snc2-1D*, deletion mutants of *AP4E* (for AP4 ϵ subunit) were generated by CRISPR-Cas9 in *cbp60g-1 snc2-1D* background (Appendix B.4). As shown in Figure 3.4A, loss of *AP4E* also suppressed the dwarfism in *cbp60g-1 snc2-1D*, suggesting that a functional AP4 ϵ subunit is also needed for the constitutively activated immunity of *cbp60g-1 snc2-1D*, which indicates that the AP4 complex is required for the autoimmunity of *cbp60g-1 snc2-1D*.

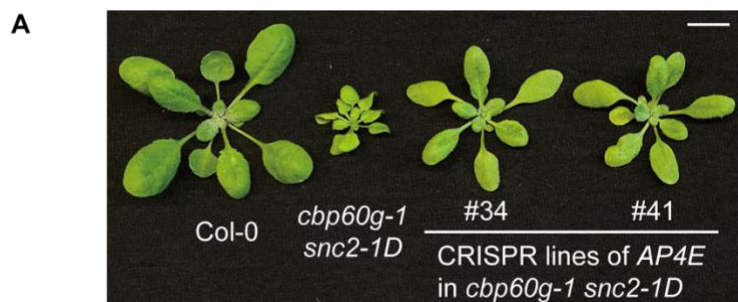


Figure 3.4 Deletion mutants of *AP4E* suppress the dwarf phenotype of *cbp60g-1 snc2-1D*.

Morphologies of 3-week-old soil-grown plants of the indicated genotypes under long-day condition. Scale bar is 1 cm.

3.4.5 AP4 μ interacts with BDA1, a downstream regulator required for SNC2-mediated immunity

It was previously reported that AP4 μ physically interacts with the membrane-bound borate exporter BOR1 through its cytoplasmic tyrosine-based YXX \emptyset motif (Y, tyrosine residue; X, any amino acid; and \emptyset , an amino acid with a bulky hydrophobic side chain) (Yoshinari et al. 2019). BDA1, a transmembrane protein required for SNC2-mediated immunity (Yang et al. 2012), contains five such tyrosine-based motif at its predicted cytoplasmic regions (Figure 3.5A). We therefore tested whether AP4 μ can interact with BDA1 by co-immunoprecipitation analysis. BDA1-3Flag was transiently expressed together with AP4 μ -HA-TurboID or GFP-HA-TurboID in *Nicotiana (N.) benthamiana* leaves. As shown in Figure 3.5B, BDA1-3Flag co-immunoprecipitated with AP4 μ -HA-TurboID but not GFP-HA-TurboID. As AP4 μ -HA-TurboID by itself was not pulled down by anti-Flag beads, there was no non-specific binding of AP4 μ -HA-TurboID to the beads. These data suggest that AP4 μ associates with BDA1 *in vivo*. In addition, BDA1-HA-TurboID could be pulled down by AP4 μ -3Flag in the reciprocal co-immunoprecipitation assay (Figure 3.5C), further confirming the interaction between AP4 μ and BDA1.

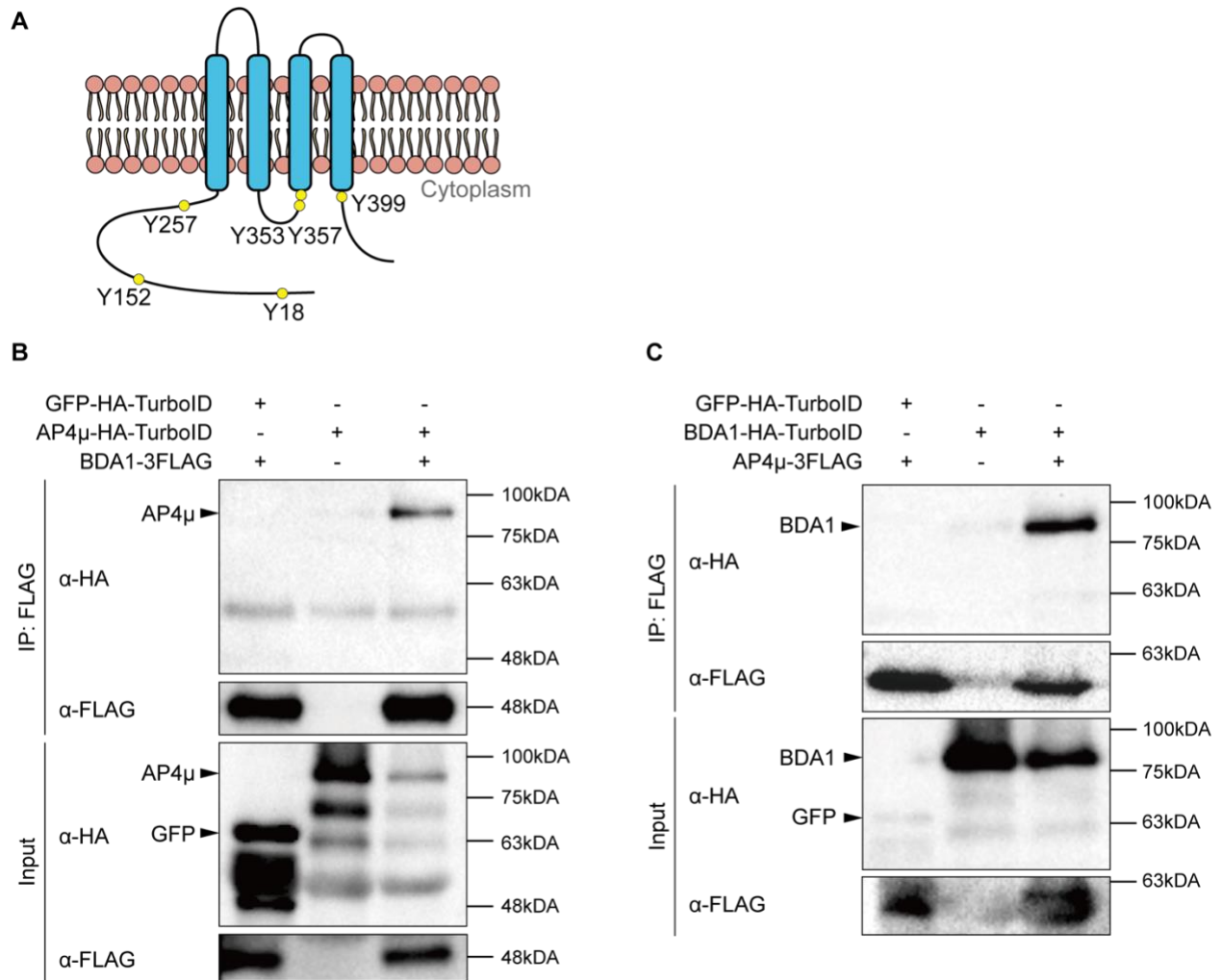


Figure 3.5 AP4 μ interacts with BDA1.

(A) A schematic diagram of BDA1 protein. Blue bars represent transmembrane domains. Yellow dots represent tyrosine residues of the cytoplasmic YXX \emptyset motifs.

(B) Co-immunoprecipitation of BDA1-3FLAG with AP4 μ -HA-TurboID in *N. benthamiana*. GFP-HA-TurboID serves as a negative control. Immunoprecipitation was carried out using anti-FLAG beads.

(C) Co-immunoprecipitation of AP4 μ -3FLAG with BDA1-HA-TurboID in *N. benthamiana*. GFP-HA-TurboID serves as a negative control. Immunoprecipitation was carried out using anti-FLAG beads.

3.4.6 AP4 μ is required for both ETI and PTI

We also generated *ap4m* single mutants using CRISPR/Cas9 (Appendix B.4). *ap4m* mutant plants are slight smaller than wild type, but their leaves are not curly and dark green (Figure 3.6A). Two independent *ap4m* mutants, T1-31 and T1-48, were selected for further analysis (hereafter *ap4m-1* and *ap4m-2*). Analysis of the basal expression level of *PR1* showed that it is comparable in *ap4m* and Col-0 (Figure 3.6B), suggesting that the smaller plant size of *ap4m* is not due to autoimmunity.

Arabidopsis mutants of other AP4 subunits, *ap4b* and *ap4e*, have been reported to be required for resistance against the avirulent *Pst* DC3000 *avrRpt2* (Hatsugai et al. 2018). To test whether AP4 μ also plays a role in resistance against *Pst* DC3000 *avrRpt2*, *ap4m* mutants were challenged with *Pst* DC3000 *avrRpt2*. At day 3 post inoculation, growth of *Pst* DC3000 *avrRpt2* was significantly higher on *ap4m* mutants than on Col-0 (Figure 3.6C), suggesting that AP4 μ is also required for full resistance against *Pst* DC3000 *avrRpt2*.

To investigate whether AP4 μ contributes to basal resistance and PTI, *ap4m* mutants were challenged with *Pst* DC3000 with or without PAMP treatment. As shown in Figure 3.6D, growth of *Pst* DC3000 was significantly higher in *ap4m* mutants than in Col-0, suggesting that basal resistance is compromised in *ap4m* mutants. While pre-treatment of the elicitor flg22 or nlp20 led to substantial reduction of *Pst* DC3000 growth on wild type plants, the flg22- or nlp20-induced protection was almost completely lost in the *ap4m* mutants (Figure 3.6E and 3.6F), indicating a critical role of the AP4 complex in PTI.

To determine whether other PTI responses are influenced in *ap4m* mutants, we test the expression of *FRK1* and MAPK phosphorylation after flg22 and nlp20 treatment. Intriguingly, the flg22- and nlp20-induced *FRK1* expression and MAPK phosphorylation in *ap4m* mutants were similar to those in Col-0 (Figure 3.6G-3.6I), indicating that the AP4 complex may function in a specific pathway downstream of PRRs.

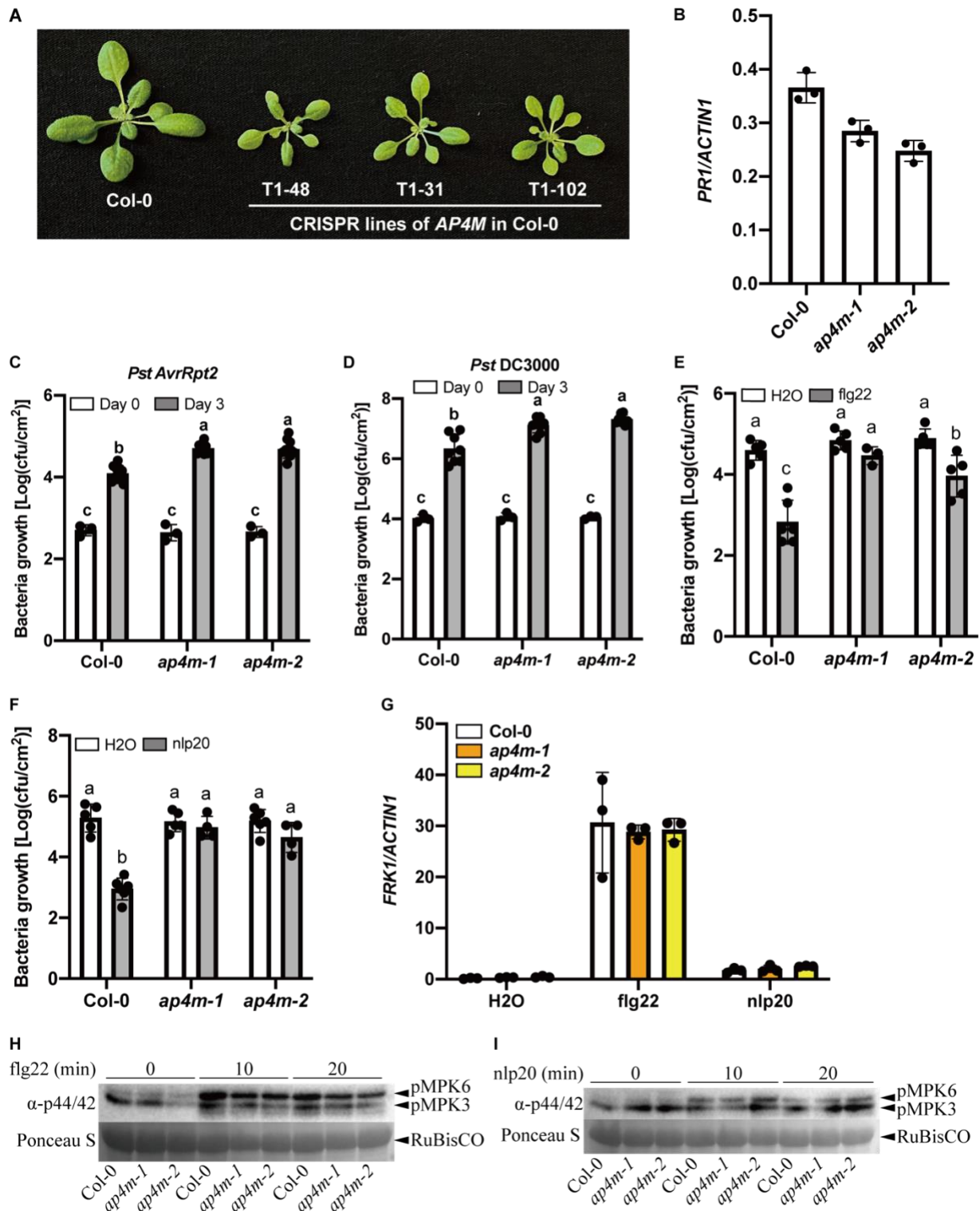


Figure 3.6 Characterization of immune responses in knockout mutants of *AP4M*.

(A) Morphologies of 3-week-old soil-grown plants of the indicated genotypes. Scale bar is 1 cm.

(B) Expression levels of *PRI* in the indicated genotypes as normalized by those of *ACTIN1*. Error bars represent standard deviations. Letters indicate statistical differences ($P < 0.05$, Student's t-test; $n = 3$).

(C and D) Growth of *Pst* DC3000 *AvrRpt2* (C) and *Pst* DC3000 (D) on the indicated genotypes. Error bars represent standard deviations. Letters indicate statistical differences ($P < 0.0001$, one-way ANOVA followed by Tukey's multiple comparisons test; $n = 3$ for Day 0, $n = 8$ for Day 3).

(E and F) Growth of *Pst* DC3000 on the indicated genotypes pre-treated with $1\mu\text{M}$ flg22 (E) or $1\mu\text{M}$ nlp20 (F). Error bars represent standard deviations. Letters indicate statistical differences ($P < 0.0001$, one-way ANOVA followed by Tukey's multiple comparisons test; $n = 6$).

(G) Induction the expression of *FRK1* in the indicated genotypes pre-treated with H_2O , $1\mu\text{M}$ flg22 or $1\mu\text{M}$ nlp20. Values are normalized by those of *ACTIN1*. Error bars represent standard deviations. Letters indicate statistical differences ($P < 0.0001$, one-way ANOVA followed by Tukey's multiple comparisons test; $n = 3$).

(H) and (I) flg22- (H) and nlp20- (I) induced MAPKs activation. 12-day-old seedlings grown on $\frac{1}{2}$ MS medium plates were sprayed with 10 nM flg22 (H) or nlp20 (I). Samples were harvested at 0, 10, 20 min after corresponding treatment. Total proteins from each sample were extracted for western blot analysis with anti-p44/42-ERK antibody. Bands of RuBisCO after Ponceau S staining were shown for equal loading.

3.5 Discussion

The *Arabidopsis* RLP SNC2 is a critical contributor to plant immunity (Zhang, Yang, et al. 2010). The gain-of-function mutant *snc2-ID* constitutively activates defense responses (Zhang, Yang, et al. 2010). How SNC2 activates plant immunity is largely unknown. In this study, we showed that the AP4 complex is required for SNC2-mediated immunity. Mutations in *AP4m* completely suppress the constitutively activated defense responses in *cbp60g-1 snc2-ID*, including the elevated *PRI* and *ICS1* expression and enhanced disease resistance against *Hpa Noco2* (Figure 1). The size of *ap4m cbp60g-1 snc2-ID* is considerably larger than *cbp60g-1 snc2-ID*, but smaller than Col-0 (Figure 1A), which is most likely due to the effect of *ap4m* on plant growth as the *ap4m* single mutant is smaller than Col-0 and *ap4m cbp60g-1 snc2-ID* has

similar size as *ap4m* (Figure 6A). In addition, knocking out *AP4E*, which encodes another subunit of AP4, also leads to suppression of the dwarfism of *cbp60g-1 snc2-1D*, further supporting that the AP4 complex is required for autoimmunity of *cbp60g-1 snc2-1D*.

The AP4 complex has four subunits including AP4 ϵ , β , μ and σ . Among them, AP4 μ serves as the determinant for the transport of target proteins from TGN to vacuole. It was reported to interact with vacuolar sorting receptor 1 to facilitate target proteins sorting (Fuji et al. 2016). In addition, binding of AP4 μ to the iron channel proteins NRAMP3 and NRAMP4 was shown to be critical for their export from TGN to vacuole membrane (Müdsam et al. 2018). As AP4 μ associates with BDA1 *in planta*, it is possible that the AP4 complex regulates SNC2-mediated immunity through BDA1 translocation. Whether the subcellular localization of BDA1 is affected in mutants of the AP4 complex requires further study.

In addition to immunity mediated by SNC2, AP4 μ is also required for PTI induced by flg22 and nlp20, as resistance against *Pst* DC3000 induced by these two elicitors is severely compromised in *ap4m* mutants. How PTI is regulated by the AP4 complex is unclear. It remains to be determined whether any specific responses downstream of PRRs are affected in the *ap4m* mutants and whether the AP4 complex is involved in vacuolar trafficking of any PTI signaling components.

Consistent with a previous report that AP4B and AP4E are required for ETI against avirulent *Pst* DC3000 strains carrying *avrRpm1* or *avrRpt2* (Hatsugai et al. 2018), resistance against *Pst* DC3000 *avrRpt2* is also compromised in the *ap4m* mutant plants. The AP4 complex were shown

to be required ETI-induced vacuolar membrane fusion to the plasma membrane, which may contribute to the inhibition of pathogen growth by the release of the antimicrobial substance to extracellular space (Hatsugai et al. 2004, 2009, 2018). How the AP4 complex regulates cell death during ETI remains to be determined.

Chapter 4: Conclusions and future directions

4.1 Conclusions

SARD1 is a master transcription factor that directly regulates the expression of a number of genes involved in PTI, ETI and SAR (Sun et al. 2015). However, it is largely unclear how SARD1 is regulated. Although SARD1 is a member in CBP60 family, protein structure analysis reveals that SARD1 lacks the CaM binding domain. In addition, over-expression lines of *SARD1* lead to constitutively activated immunity (Zhang, Xu, et al. 2010). These findings lead to the hypothesis that *SARD1* is primarily regulated transcriptionally. In the *Arabidopsis* gain-of-function mutant *snc2-ID*, *SARD1* functions in parallel with CBP60g to regulate immune responses downstream of SNC2 (Sun et al. 2015; Zhang, Yang, et al. 2010). How SARD1 is activated in *snc2-ID* was unknown.

As there are two parallel pathways downstream of SNC2, one requiring SARD1 and the other depending on CBP60g, loss of either SARD1 or CBP60g alone in *snc2-ID* plants can only mildly suppress the autoimmunity of *snc2-ID* (Sun et al. 2015). To better understand how *SARD1* is activated, I performed a forward genetic screen in the *cbp60g-1 snc2-ID* mutant background, considering that loss-of-function mutations in positive regulators upstream of SARD1 could suppress the autoimmune phenotypes of *cbp60g-1 snc2-ID*. In this thesis, I describe the identification and characterization of two groups of suppressors, *bda7 cbp60g-1 snc2-ID* (Chapter 2) and *bda6 cbp60g-1 snc2-ID* (Chapter 3).

Chapter 2 describes the identification and characterization of *bda7 cbp60g-1 snc2-ID*. *bda7 cbp60g-1 snc2-ID* partially suppress the autoimmunity of *cbp60g-1 snc2-ID*. Map-based cloning

and next generation sequencing revealed that *bda7* carries a loss-of-function mutation in *CBP60b*, which encodes a transcription factor. Further analysis revealed that CBP60b can bind to the promoter region of *SARD1* and is required for the up-regulation of *SARD1* level in *cbp60g-1 snc2-1D*. In addition, transiently overexpressing *CBP60b* in *N. benthamiana* activates the expression of the *pSARD1::Luc* reporter genes and over-expressing *CBP60b* in *Arabidopsis* transgenic plants leads to increased *SARD1* expression and constitutive defense responses. These data suggest that CBP60b functions upstream of *SARD1* and directly regulates *SARD1* expression. Thus, findings in chapter 2 answer the question of how *SARD1* is regulated in SNC2-mediated immunity.

Chapter 3 describes the identification and characterization of three *bda6 cbp60g-1 snc2-1D* mutants. Using a combination of genetic mapping, next generation sequencing and complementation test, mutations in *AP4M* were identified to account for the suppression of the phenotypes of *cbp60g-1 snc2-1D*. *AP4M* encodes the μ subunit of the AP4 adapter protein complex which is involved in vacuolar protein sorting. In addition, knockout analysis showed that the other subunits of AP4 complex such as AP4 ϵ are also required for the constitutively activated defense response in *cbp60g-1 snc2-1D*. Thus, AP4-mediated vacuolar protein sorting may be required for SNC2-mediated immunity. Data in chapter 3 identified another layer of regulation of SNC2-mediated immunity. Moreover, as described in chapter 3, *ap4m* mutant plants are defective in flg22- and nlp20-induced resistance against *Pst* DC3000, uncovering a crucial role of the AP4 complex in PTI.

4.2 Future directions

Although studies on the mutants of CBP60b and the AP4 complex improved our understandings of the regulation of the defense signaling downstream of SNC2, many questions remain to be addressed.

4.2.1 CBP60b as a positive regulator in plant immunity

Similar to SARD1 and CBP60g, CBP60b belongs to the CBP60 transcription factor family. CBP60 family members possess a highly conserved central region and divergent sequences at N- and C-termini. The conserved central regions of both SARD1 and CBP60g have been proven to have DNA-binding activity, and both were reported to regulate expression of target genes through the GAAATTT element. CBP60b shares ~80% sequence similarity with SARD1 in the central region. It remains to be determined whether CBP60b binds to a similar DNA element on *SARD1* promoter to regulate its expression. In addition, it will be interesting to test whether CBP60b also regulates genes involved in PTI, ETI and SAR similar to SARD1.

As CBP60b is a transcription factor that functions in the nucleus, we still do not know how the plasma-membrane localized receptor activates CBP60b. Unlike *SARD1* and *CBP60g*, whose expression levels are greatly induced by pathogen infection, *CBP60b* is constitutively expressed in wild type plants, suggesting that activity of CBP60b may be regulated post-transcriptionally. The N-terminal domain of CBP60g can bind to CaM *in vitro*, and three amino acid residues within this domain were shown to be required for CBP60g function (Wang et al. 2009; Zhang, Xu, et al. 2010). In contrast, CBP60b were found to bind CaM *in vitro* via its C-terminal end (Reddy et al. 2002). However, whether the CaM binding is required for the activation of

CBP60b is unknown. It is of future interest to study whether CBP60b is activated and regulated by intracellular calcium signal through CaM binding.

4.2.2 CBP60b in TNL-mediated immunity

Knockout mutants of *CBP60b* display constitutive defense responses which is dependent on the TNL signaling component EDS1, indicating that loss of CBP60b function leads to activation of TNL signaling. As described in Chapter 2, there are two possible explanations.

First, CBP60b could target some negative immune regulators. Losing CBP60b would lower the expression levels of these negative immune regulators, subsequently resulting in activation of immunity. We found that the expression level of *NUDT7*, which encodes a nudix hydrolase involved in negative regulation of plant immunity, is significantly reduced in *cbp60b* mutants (data not shown). Loss of *NUDT7* and its close homolog *NUDT6* constitutively activates EDS1-dependent defense responses (Wang et al. 2013), suggesting that *NUDT7* and *NUDT6* are both negative regulators of TNL-mediated immunity. Whether the decreased *NUDT7* expression in *cbp60b* accounts for its autoimmune phenotypes remains to be determined in the future.

Second, CBP60b could be directly or indirectly monitored by an unknown TNL, as many important immune regulators are guarded by plant NLRs. Indeed, the autoimmunity of *cbp60b* can be partially suppressed by mutations in the TNL gene *SNC1* (Li et al. 2021). However, *SNC1* does not appear to physically interact with CBP60b (data not shown), suggesting that *SNC1* does not directly guard CBP60b. In addition, the partial suppression of *cbp60b*

autoimmunity by loss of SNC1 indicates that other TNLs should be involved in the surveillance of CBP60b activity.

Compared with *cbp60b*, the *cbp60b cbp60g-1* double mutants and *cbp60b cbp60g-1 sard1-1* triple mutants showed an even more dramatic autoimmune phenotype, suggesting that loss of CBP60g and SARD1 enhances TNL-mediated immunity in the *cbp60b* mutant background. Neither *cbp60g* and *sard1* single mutants nor *cbp60g-1 sard1-1* double mutants exhibit autoimmunity phenotypes, suggesting CBP60g and SARD1 are not monitored by TNLs. It is likely that CBP60b, CBP60g and SARD1 play partially redundant roles in the transcriptional regulation of a putative guardee/decoy which is recognized by SNC1 and other unknown TNLs. In *cbp60b*, the expression of the putative guardee/decoy is partially blocked, leading to activation of TNL-mediated immunity. Additional mutations in CBP60g and SARD1 in the *cbp60b* background lead to further reduction in the expression of the guardee/decoy and stronger activation of defense responses. To better understand the autoimmunity caused by loss of function of CBP60b, it is crucial to identify the guardee/decoy monitored by the TNLs.

4.2.3 Function of AP4 in plant immunity

Study in chapter 3 unraveled that AP4 complex is involved in SNC2-mediated immunity. AP4 complex is conserved in plants and mammals. Located on TGN, it mediates the translocation of the autophagy protein ATG9A to cytoplasm to promote autophagosome formation in human neuroglioma cells (Mattera et al. 2017). In *Arabidopsis*, two iron channel proteins NRAMP3 and NRAMP4 are sorted to vacuole membrane through interaction with AP4 μ (Müdsam et al. 2018). AP4M interacts with BDA1, which is a key signaling component downstream of SNC2 (Yang et

al. 2012). BDA1 contains five ankyrin repeats at its N-terminus which is predicted to be involved in protein-protein interaction. It also has four transmembrane domains in its C-terminus and is predicted to localize on plasma membrane. Whether loss of AP4 μ affects the subcellular localization of BDA1 remains to be determined. In order to fully understand the role of AP4M in SNC2-mediated immunity, it is critical to determine how BDA1 functions downstream of SNC2 to transduce defense signals. Recently, another ankyrin-repeat transmembrane domain protein, ACD6, is proposed to function as an ion channel in plant immunity (Zhu et al. 2021). Whether BDA1 has a similar role remains further investigation.

In addition of its role in SNC2-mediated immunity, AP4M is required for cell death and inhibition of bacterial growth during ETI. In plants, a variety of hydrolytic enzymes, proteinases and defense-related proteins are stored in vacuoles, one of such is vacuolar possessing enzyme (VPE). VPE is a proteinase required for tobacco mosaic virus (TMV)-induced plant cell death in *N. benthamiana* plants, by controlling the vacuolar rupture (Hatsugai et al. 2004; Shimada et al. 2018). It was proposed that vacuolar rupture is a crucial event in plant cell death, as the release of those hydrolytic enzymes, proteinases and defense-related proteins from vacuoles to cytosol is thought to limit the virus proliferation (Hara-Nishimura and Hatsugai 2011). However, the vacuolar rupture does not occur during avirulence bacterial infection. Instead, a vacuole-plasma membrane fusion is observed, which connects the vacuole and extracellular space where bacteria propagate (Hatsugai et al. 2009). It was proposed that the discharge of the antimicrobial substance from vacuole to extracellular space through the fusion structure is essential for resistance against avirulence bacteria (Hatsugai et al. 2009). As this fusion formation is

suppressed in mutants of AP4 complex (Hatsugai et al. 2018), it is possible that the AP4 complex contributes to ETI by regulating vacuole-plasma membrane fusion.

In addition to its role in ETI, the AP4 complex is required for PTI, as immunity induced by flg22 and nlp20 against *Pst* DC3000 is severely compromised in *ap4m* mutants. Although infection by the virulent *Pst* DC3000 strain does not induce vacuole-plasma membrane fusion, it is worthwhile to examine whether treatment with elicitors such as flg22 and nlp20 can trigger such membrane fusion, which could lead to the discharge of antimicrobial substances from vacuole to extracellular space to inhibit bacterial growth. To better understand the role of the AP4 complex in PTI, it is important to determine whether it affects PTI signaling and identify PTI signaling components which are regulated by the AP4 complex.

4.2.4 Signaling partner(s) of SNC2 in plant immunity

Although it was long known that SNC2 is critical in basal resistance in *Arabidopsis*, it remains a myth how it transduces defense signal to downstream components to activate defense responses. As RLPs lack a cytoplasmic kinase domain, SNC2 is believed to need at least one kinase-domain containing RLK as its partner for signal transduction. However, the *cbp60g-1 snc2-ID* suppressor screen as well as suppressor screens conducted on other *snc2-ID* mutant backgrounds, such as *snc2-ID npr1-1*, *snc2-ID npr1-1 eds5-3* and *sard1-1 snc2-ID*, failed to identify any RLKs. It is very likely that the co-receptors of SNC2 share functional redundancy. Another possibility is that the SNC2 co-receptor is guarded by an NLR protein. While mutations in the co-receptor suppress the autoimmunity caused by *snc2-ID*, it also triggered activation of

NLR-mediated immunity. Different strategies like reverse genetics or immunoprecipitation-mass spectrometry could help identify of the SNC2 co-receptor(s) in the future.

Bibliography

- Aarts, Nicole, Matthew Metz, Eric Holub, Brian J. Staskawicz, Michael J. Daniels, and Jane E. Parker. 1998. "Different Requirements for EDS1 and NDR1 by Disease Resistance Genes Define at Least Two R Gene-Mediated Signaling Pathways in Arabidopsis." *Proceedings of the National Academy of Sciences of the United States of America* 95(17):10306–11.
- Abou Jamra, Rami, Orianne Philippe, Annick Raas-Rothschild, Sebastian H. Eck, Elisabeth Graf, Rebecca Buchert, Guntram Borck, Arif Ekici, Felix F. Brockschmidt, Markus M. Nöthen, Arnold Munnich, Tim M. Strom, Andre Reis, and Laurence Colleaux. 2011. "Adaptor Protein Complex 4 Deficiency Causes Severe Autosomal-Recessive Intellectual Disability, Progressive Spastic Paraplegia, Shy Character, and Short Stature." *American Journal of Human Genetics* 88(6):788–95.
- Albert, Isabell, Hannah Böhm, Markus Albert, Christina E. Feiler, Julia Imkampe, Niklas Wallmeroth, Caterina Brancato, Tom M. Raaymakers, Stan Oome, Heqiao Zhang, Elzbieta Krol, Christopher Grefen, Andrea A. Gust, Jijie Chai, Rainer Hedrich, Guido Van Den Ackerveken, and Thorsten Nürnberger. 2015. "An RLP23-SOBIR1-BAK1 Complex Mediates NLP-Triggered Immunity." *Nature Plants* 1(October):15140.
- Andreasson, Erik, Thomas Jenkins, Peter Brodersen, Stephan Thorgrimsen, Nikolaj H. T. Petersen, Shijiang Zhu, Jin Long Qiu, Pernille Micheelsen, Anne Rocher, Morten Petersen, Mari Anne Newman, Henrik Björn Nielsen, Heribert Hirt, Imre Somssich, Ole Mattsson, and John Mundy. 2005. "The MAP Kinase Substrate MKS1 Is a Regulator of Plant Defense Responses." *EMBO Journal* 24(14):2579–89.
- Asai, Tsuneaki, Guillaume Tena, Joulia Plotnikova, Matthew R. Willmann, Wan Ling Chiu, Lourdes Gomez-Gomez, Thomas Boller, Frederick M. Ausubel, and Jen Sheen. 2002. "Map Kinase Signalling Cascade in Arabidopsis Innate Immunity." *Nature* 415(6875):977–83.
- Bauer, Sibylle, Dereje W. Mekonnen, Michael Hartmann, Ipek Yildiz, Robert Janowski, Birgit Lange, Birgit Geist, Jürgen Zeier, and Anton R. Schäffner. 2021. "UGT76B1, a Promiscuous Hub of Small Molecule-Based Immune Signaling, Glucosylates N-Hydroxypipicolinic Acid, and Balances Plant Immunity." *Plant Cell* 33(3):714–34.
- Belkhadir, Youssef, Zachary Nimchuk, David A. Hubert, David Mackey, and Jeffery L. Dangl. 2004. "Arabidopsis RIN4 Negatively Regulates Disease Resistance Mediated by RPS2 and RPM1 Downstream or Independent of the NDR1 Signal Modulator and Is Not Required for

- the Virulence Functions of Bacterial Type III Effectors AvrRpt2 or AvrRpm1.” *Plant Cell* 16(10):2822–35.
- Bi, Guozhi, Min Su, Nan Li, Yu Liang, Song Dang, Jiachao Xu, Meijuan Hu, Jizong Wang, Minxia Zou, Yanan Deng, Qiyu Li, Shijia Huang, Jiejie Li, Jijie Chai, Kangmin He, Yu hang Chen, and Jian Min Zhou. 2021. “The ZAR1 Resistosome Is a Calcium-Permeable Channel Triggering Plant Immune Signaling.” *Cell* 184(13):3528-3541.e12.
- Bjornson, Marta, Priya Pimprikar, Thorsten Nürnberger, and Cyril Zipfel. 2021. “The Transcriptional Landscape of Arabidopsis Thaliana Pattern-Triggered Immunity.” *Nature Plants* 7(5):579–86.
- Boller, Thomas and Georg Felix. 2009. “A Renaissance of Elicitors: Perception of Microbe-Associated Molecular Patterns and Danger Signals by Pattern-Recognition Receptors.” *Annual Review of Plant Biology* 60:379–406.
- Boller, Thomas and Urs Vögeli. 1984. “Vacuolar Localization of Ethylene-Induced Chitinase in Bean Leaves.” *Plant Physiology* 74(2):442–44.
- Boutrot, Freddy, Cécile Segonzac, Katherine N. Chang, Hong Qiao, Joseph R. Ecker, Cyril Zipfel, and John P. Rathjen. 2010. “Direct Transcriptional Control of the Arabidopsis Immune Receptor FLS2 by the Ethylene-Dependent Transcription Factors EIN3 and EIL1.” *Proceedings of the National Academy of Sciences of the United States of America* 107(32):14502–7.
- Cai, Jianghua, Adam Jozwiak, Lara Holoïdovsky, Michael M. Meijler, Sagit Meir, Ilana Rogachev, and Asaph Aharoni. 2021. “Glycosylation of N-Hydroxy-Pipecolic Acid Equilibrates between Systemic Acquired Resistance Response and Plant Growth.” *Molecular Plant* 14(3):440–55.
- Cao, Hui, Scott A. Bowling, A. Susan Gordon, and Xinnian Dong. 1994. “Characterization of an Arabidopsis Mutant That Is Nonresponsive to Inducers of Systemic Acquired Resistance.” *Plant Cell* 6(11):1583–92.
- Cao, Hui, Jane Glazebrook, Joseph D. Clarke, Sigrid Volko, and Xinnian Dong. 1997. “The Arabidopsis NPR1 Gene That Controls Systemic Acquired Resistance Encodes a Novel Protein Containing Ankyrin Repeats.” *Cell* 88(1):57–63.
- Cesari, Stella, Maud Bernoux, Philippe Moncuquet, Thomas Kroj, and Peter N. Dodds. 2014. “A Novel Conserved Mechanism for Plant NLR Protein Pairs: The ‘Integrated Decoy’

- Hypothesis.” *Frontiers in Plant Science* 5(NOV):1–10.
- Chen, Yun Chu, Eric C. Holmes, Jakub Rajniak, Jung Gun Kim, Sandy Tang, Curt R. Fischer, Mary Beth Mudgett, and Elizabeth S. Sattely. 2018. “N-Hydroxy-Pipecolic Acid Is a Mobile Metabolite That Induces Systemic Disease Resistance in Arabidopsis.” *Proceedings of the National Academy of Sciences of the United States of America* 115(21):E4920–29.
- Clough, Steven J. and Andrew F. Bent. 1998. “Floral Dip: A Simplified Method for Agrobacterium-Mediated Transformation of Arabidopsis Thaliana.” *Plant Journal* 16(6):735–43.
- Cui, Haitao, Kenichi Tsuda, and Jane E. Parker. 2015. “Effector-Triggered Immunity: From Pathogen Perception to Robust Defense.” *Annual Review of Plant Biology* 66:487–511.
- Dangl, Jeffery L., Diana M. Horvath, and Brian J. Staskawich. 2013. “Pivoting the Plant Immune System.” *Science* 341(August):745–51.
- Dangl, Jeffery L. and Jonathan D. G. Jones. 2001. “Plant Pathogens and Integrated Defence Responses to Infection.” *Nature* 411(June).
- Dean, John V., Leila A. Mohammed, and Terry Fitzpatrick. 2005. “The Formation, Vacuolar Localization, and Tonoplast Transport of Salicylic Acid Glucose Conjugates in Tobacco Cell Suspension Cultures.” *Planta* 221(2):287–96.
- Delaney, T. P., L. Friedrich, and J. A. Ryals. 1995. “Arabidopsis Signal Transduction Mutant Defective in Chemically and Biologically Induced Disease Resistance.” *Proceedings of the National Academy of Sciences of the United States of America* 92(14).
- Dempsey, D’Maris Amick, A. Corina Vlot, Mary C. Wildermuth, and Daniel F. Klessig. 2011. “Salicylic Acid Biosynthesis and Metabolism.” *The Arabidopsis Book* 9:e0156.
- Depristo, Mark A., Eric Banks, Ryan Poplin, Kiran V. Garimella, Jared R. Maguire, Christopher Hartl, Anthony A. Philippakis, Guillermo Del Angel, Manuel A. Rivas, Matt Hanna, Aaron McKenna, Tim J. Fennell, Andrew M. Kernytsky, Andrey Y. Sivachenko, Kristian Cibulskis, Stacey B. Gabriel, David Altshuler, and Mark J. Daly. 2011. “A Framework for Variation Discovery and Genotyping Using Next-Generation DNA Sequencing Data.” *Nature Genetics* 43(5):491–501.
- Després, Charles, Catherine Delong, Sarah Glaze, Enwu Liu, and Pierre R. Fobert. 2000. “The Arabidopsis NPR1/NIM1 Protein Enhances the DNA Binding Activity of a Subgroup of the TGA Family of BZIP Transcription Factors.” *Current Opinion in Plant Biology* 3(3):171.

- Ding, Pingtao, Dmitriy Rekhter, Yuli Ding, Kirstin Feussner, Lucas Busta, Sven Haroth, Shaohua Xu, Xin Li, Reinhard Jetter, Ivo Feussner, and Yuelin Zhang. 2016. "Characterization of a Pipecolic Acid Biosynthesis Pathway Required for Systemic Acquired Resistance." *The Plant Cell* 28(10):2603–15.
- Ding, Yuli, Tongjun Sun, Kevin Ao, Yujun Peng, Yaxi Yuelin Zhang, Xin Li, and Yaxi Yuelin Zhang. 2018. "Opposite Roles of Salicylic Acid Receptors NPR1 and NPR3/NPR4 in Transcriptional Regulation of Plant Immunity." *Cell* 173(6):1454-1467.e10.
- Dou, Daolong and Jian Min Zhou. 2012. "Phytopathogen Effectors Subverting Host Immunity: Different Foes, Similar Battleground." *Cell Host and Microbe* 12(4):484–95.
- Durrant, W. E. and Xinnian Dong. 2004. "SYSTEMIC ACQUIRED RESISTANCE." *Annual Review of Phytopathology* 42(1):185–209.
- Edgar, Robert C. 2004. "MUSCLE: Multiple Sequence Alignment with High Accuracy and High Throughput." *Nucleic Acids Research* 32(5):1792–97.
- Fu, Zheng Qing and Xinnian Dong. 2013. "Systemic Acquired Resistance: Turning Local Infection into Global Defense." *Annual Review of Plant Biology* 64(January):839–63.
- Fu, Zheng Qing, Shunping Yan, Abdelaty Saleh, Wei Wang, James Ruble, Nodoka Oka, Rajinikanth Mohan, Steven H. Spoel, Yasuomi Tada, Ning Zheng, and Xinnian Dong. 2012. "NPR3 and NPR4 Are Receptors for the Immune Signal Salicylic Acid in Plants." *Nature* 486(7402):228–32.
- Fuji, Kentaro, Makoto Shirakawa, Yuki Shimono, Tadashi Kunieda, Yoichiro Fukao, Yasuko Koumoto, Hideyuki Takahashi, Ikuko Hara-Nishimura, and Tomoo Shimada. 2016. "The Adaptor Complex AP-4 Regulates Vacuolar Protein Sorting at the Trans-Golgi Network by Interacting with VACUOLAR SORTING RECEPTOR11." *Plant Physiology* 170(1):211–19.
- Gaffney, Thomas, Leslie Friedrich, Bernard Vernooij, David Negrotto, Gordon Nye, Scott Uknes, Eric Ward, Helmut Kessmann, and John Ryals. 1993. "Requirement of Salicylic Acid for the Induction of Systemic Acquired Resistance." *Science* 261(5122):754–56.
- Galán, Jorge E. and Alan Collmer. 1999. "Type III Secretion Machines: Bacterial Devices for Protein Delivery into Host Cells." *Science* 284(5418):1322–28.
- Gao, Xiquan, Xin Chen, Wenwei Lin, Sixue Chen, Dongping Lu, Yajie Niu, Lei Li, Cheng Cheng, Matthew McCormack, Jen Sheen, Libo Shan, and Ping He. 2013. "Bifurcation of

- Arabidopsis NLR Immune Signaling via Ca²⁺-Dependent Protein Kinases.” *PLoS Pathogens* 9(1).
- Garcion, Christophe, Antje Lohmann, Elisabeth Lamodièrre, Jeremy Catinot, Antony Buchala, Peter Doermann, Metraux, and Jean-Pierre. 2008. “Characterization and Biological Function of the ISOCHORISMATE SYNTHASE2 Gene of Arabidopsis.” *Plant Physiology* 147(July):1279–87.
- Grant, Sarah R., Emily J. Fisher, Jeff H. Chang, Beth M. Mole, and Jeffery L. Dangl. 2006. “Subterfuge and Manipulation: Type III Effector Proteins of Phytopathogenic Bacteria.” *Annual Review of Microbiology* 60:425–49.
- Guan, Rongxia, Jianbin Su, Xiangzong Meng, Sen Li, Yidong Liu, Juan Xu, and Shuqun Zhang. 2015. “Multilayered Regulation of Ethylene Induction Plays a Positive Role in Arabidopsis Resistance against *Pseudomonas Syringae*.” *Plant Physiology* 169(1):299–312.
- Guo, Pengru, Zhonghai Li, Peixin Huang, Bosheng Li, Shuang Fang, Jinfang Chu, and Hongwei Guo. 2017. “A Tripartite Amplification Loop Involving the Transcription Factor WRKY75, Salicylic Acid, and Reactive Oxygen Species Accelerates Leaf Senescence.” *Plant Cell* 29(11):2854–70.
- Hara-Nishimura, I. and N. Hatsugai. 2011. “The Role of Vacuole in Plant Cell Death.” *Cell Death and Differentiation* 18(8):1298–1304.
- Hartmann, Michael, Denis Kim, Friederike Bernsdorff, Ziba Ajami-Rashidi, Nicola Scholten, Stefan Schreiber, Tatyana Zeier, Stefan Schuck, Vanessa Reichel-Deland, and Jürgen Zeier. 2017. “Biochemical Principles and Functional Aspects of Pipecolic Acid Biosynthesis in Plant Immunity.” *Plant Physiology* 174(1):124–53.
- Hartmann, Michael and Jürgen Zeier. 2018. “L-Lysine Metabolism to N-Hydroxypipicolinic Acid: An Integral Immune-Activating Pathway in Plants.” 5–21.
- Hartmann, Michael and Jürgen Zeier. 2019. “N-Hydroxypipicolinic Acid and Salicylic Acid: A Metabolic Duo for Systemic Acquired Resistance.” *Current Opinion in Plant Biology* 50:44–57.
- Hartmann, Michael, Tatyana Zeier, Friederike Bernsdorff, Vanessa Reichel-Deland, Denis Kim, Michele Hohmann, Nicola Scholten, Stefan Schuck, Andrea Bräutigam, Torsten Hölzel, Christian Ganter, and Jürgen Zeier. 2018. “Flavin Monooxygenase-Generated N-Hydroxypipicolinic Acid Is a Critical Element of Plant Systemic Immunity.” *Cell*

173(2):456-469.e16.

- Hatsugai, Noriyuki, Shinji Iwasaki, Kentaro Tamura, Maki Kondo, Kentaro Fuji, Kimi Ogasawara, Mikio Nishimura, and Ikuko Hara-Nishimura. 2009. "A Novel Membrane Fusion-Mediated Plant Immunity against Bacterial Pathogens." *Genes and Development* 23(21):2496–2506.
- Hatsugai, Noriyuki, Miwa Kuroyanagi, Kenji Yamada, Tetsuo Meshi, Shinya Tsuda, Maki Kondo, Mikio Nishimura, and Ikuko Hara-Nishimura. 2004. "A Plant Vacuolar Protease, VPE, Mediates, Virus-Induced Hypersensitive Cell Death." *Science* 305(5685):855–58.
- Hatsugai, Noriyuki, Aya Nakatsuji, Osamu Unten, Kimi Ogasawara, Maki Kondo, Mikio Nishimura, Tomoo Shimada, Fumiaki Katagiri, and Ikuko Hara-Nishimura. 2018. "Involvement of Adapter Protein Complex 4 in Hypersensitive Cell Death Induced by Avirulent Bacteria." *Plant Physiology* 176(2):1824–34.
- Holmes, Eric C., Yun Chu Chen, Mary Beth Mudgett, and Elizabeth S. Sattely. 2021. "Arabidopsis UGT76B1 Glycosylates N-Hydroxy-Pipecolic Acid and Inactivates Systemic Acquired Resistance in Tomato." *Plant Cell* 33(3):750–65.
- Van Der Hoorn, Renier A. L. and Sophien Kamoun. 2008. "From Guard to Decoy: A New Model for Perception of Plant Pathogen Effectors." *Plant Cell* 20(8):2009–17.
- Horsefield, Shane, Hayden Burdett, Xiaoxiao Zhang, Mohammad K. Manik, Yun Shi, Jian Chen, Tiancong Qi, Jonathan Gilley, Jhih Siang Lai, Maxwell X. Rank, Lachlan W. Casey, Weixi Gu, Daniel J. Ericsson, Gabriel Foley, Robert O. Hughes, Todd Bosanac, Mark Von Itzstein, John P. Rathjen, Jeffrey D. Nanson, Mikael Boden, Ian B. Dry, Simon J. Williams, Brian J. Staskawicz, Michael P. Coleman, Thomas Ve, Peter N. Dodds, and Bostjan Kobe. 2019. "NAD⁺ Cleavage Activity by Animal and Plant TIR Domains in Cell Death Pathways." *Science* 365(6455):793–99.
- Hu, Yezhou, Yanxia Ding, Boying Cai, Xiaohui Qin, Jingni Wu, Minhang Yuan, Shiwei Wan, Yang Zhao, and Xiu-Fang Xin. 2022. "Bacterial Effectors Manipulate Plant Abscisic Acid Signaling for Creation of an Aqueous Apoplast." *Cell Host & Microbe* 1–12.
- Huang, Junli, Min Gu, Zhibing Lai, Baofang Fan, Kai Shi, Yan-hong Zhou, Jing-quan Yu, and Zhixiang Chen. 2010. "Functional Analysis of the Arabidopsis PAL Gene Family in Plant Growth, Development, and Response to Environmental Stress." *Plant Physiology* 153(August):1526–38.

- Ishihama, Nobuaki and Hirofumi Yoshioka. 2012. "Post-Translational Regulation of WRKY Transcription Factors in Plant Immunity." *Current Opinion in Plant Biology* 15(4):431–37.
- Jing, Beibei, Shaohua Xu, Mo Xu, Yan Li, Shuxin Li, Jinmei Ding, and Yuelin Zhang. 2011. "Brush and Spray: A High-Throughput Systemic Acquired Resistance Assay Suitable for Large-Scale Genetic Screening." *Plant Physiology* 157(3):973–80.
- Jones, Jonathan D. G. G. and Jeffery L. Dangl. 2006. "The Plant Immune System." *Nature* 444(7117):323–29.
- Jones, Jonathan D. G., Russell e Vance, and Jeffery L. Dangl. 2016. "Intracellular Innate Immune Surveillance Devices in Plants and Animals." *Science* 354(6316).
- Jung, Ho Won, Timothy J. Tschaplinski, Lin Wang, Jane Glazebrook, and Jean T. Greenberg. 2009. "Priming in Systemic Plant Immunity." *Science* 324(5923):89–91.
- Kadota, Yasuhiro, Ken Shirasu, and Cyril Zipfel. 2015. "Regulation of the NADPH Oxidase RBOHD during Plant Immunity." *Plant and Cell Physiology* 56(8):1472–80.
- Kim, Min Gab, Luis Da Cunha, Aidan J. McFall, Youssef Belkhadir, Sruti DebRoy, Jeffrey L. Dangl, and David Mackey. 2005. "Two *Pseudomonas Syringae* Type III Effectors Inhibit RIN4-Regulated Basal Defense in Arabidopsis." *Cell* 121(5):749–59.
- Kourelis, Jiorgos and Renier A. L. Van Der Hoorn. 2018. "Defended to the Nines: 25 Years of Resistance Gene Cloning Identifies Nine Mechanisms for R Protein Function." *Plant Cell* 30(2):285–99.
- Krasileva, Ksenia V., Douglas Dahlbeck, and Brian J. Staskawicz. 2010. "Activation of an Arabidopsis Resistance Protein Is Specified by the in Planta Association of Its Leucine-Rich Repeat Domain with the Cognate Oomycete Effector." *Plant Cell* 22(7):2444–58.
- Law, Kai Ching, Ka Kit Chung, and Xiaohong Zhuang. 2022. "An Update on Coat Protein Complexes for Vesicle Formation in Plant Post-Golgi Trafficking." *Frontiers in Plant Science* 13(February):1–9.
- Lee, Hyung Il and Ilya Raskin. 1999. "Purification, Cloning, and Expression of a Pathogen Inducible UDP- Glucose:Salicylic Acid Glucosyltransferase from Tobacco." *Journal of Biological Chemistry* 274(51):36637–42.
- León, Jose, Nasser Yalpani, and Michael A. Lawton. 1993. "Lnduction of Benzoic Acid 2-Hydroxylase in Virus-Lnoculated Tobacco '." *Plant Physiol* 103:323–28.
- Leon, Josei, Vladimir Shulaev, Nasser Yalpani, Michael A. Lawton, and Ilya Raskint. 1995.

- “Benzoic Acid 2-Hydroxylase , a Soluble Oxygenase from Tobacco , Catalyzes Salicylic Acid Biosynthesis.” *Proc. Natl. Acad. Sci.* 92(October):10413–17.
- Li, Heng. 2013. “Aligning Sequence Reads, Clone Sequences and Assembly Contigs with BWA-MEM.” 00(00):1–3.
- Li, Lu Shen, Jun Ying, En Li, Ting Ma, Min Li, Li Min Gong, Guo Wei, Yan Zhang, and Sha Li. 2021. “Arabidopsis CBP60b Is a Central Transcriptional Activator of Immunity.” *Plant Physiology* 186(3):1645–59.
- Li, Xin and Yuelin Zhang. 2016. *Suppressor Screens in Arabidopsis*. Vol. 1363.
- Li, Xin, Yuelin Zhang, Joseph D. Clarke, Yan Li, and Xinnian Dong. 1999. “Identification and Cloning of a Negative Regulator of Systemic Acquired Resistance, SNI1, through a Screen for Suppressors of Npr1-1.” *Cell* 98(3):329–39.
- Lian, Kehui, Fang Gao, Tongjun Sun, Rowan van Wersch, Kevin Ao, Qing Kong, Yukino Nitta, Di Wu, Patrick Krysan, and Yuelin Zhang. 2018. “MKK6 Functions in Two Parallel MAP Kinase Cascades in Immune Signaling.” *Plant Physiology* 178(3):1284–95.
- Liang, Xiangxiu and Jian Min Zhou. 2018. “Receptor-Like Cytoplasmic Kinases: Central Players in Plant Receptor Kinase-Mediated Signaling.” *Annual Review of Plant Biology* 69:267–99.
- Liu, Yidong and Shuqun Zhang. 2004. “Phosphorylation of 1-Aminocyclopropane-1-Carboxylic Acid Synthase by MPK6, a Stress-Responsive Mitogen-Activated Protein Kinase, Induces Ethylene Biosynthesis in Arabidopsis.” *Plant Cell* 16(12):3386–99.
- Lu, Dongping, Shujing Wu, Xiquan Gao, Yulan Zhang, Libo Shan, and Ping He. 2010. “A Receptor-like Cytoplasmic Kinase, BIK1, Associates with a Flagellin Receptor Complex to Initiate Plant Innate Immunity.” *Proceedings of the National Academy of Sciences of the United States of America* 107(1):496–501.
- Luna, Estrella, Victoria Pastor, Jérôme Robert, Victor Flors, Brigitte Mauch-Mani, and Jurriaan Ton. 2011. “Callose Deposition: A Multifaceted Plant Defense Response.” *Molecular Plant-Microbe Interactions* 24(2):183–93.
- Mackey, David, Youssef Belkhadir, Jose M. Alonso, Joseph R. Ecker, and Jeffery L. Dangl. 2003. “Arabidopsis RIN4 Is a Target of the Type III Virulence Effector AvrRpt2 and Modulates RPS2-Mediated Resistance.” *Cell* 112(3):379–89.
- Maddison, W. P. and D. R. Maddison. 2019. “Mesquite: A Modular System for Evolutionary Analysis. Version 3.61 [Http://Www.Mesquiteproject.Org](http://www.Mesquiteproject.Org).”

- Madina, Mst Hur, Md Saifur Rahman, Huanquan Zheng, and Hugo Germain. 2019. "Vacuolar Membrane Structures and Their Roles in Plant-Pathogen Interactions." *Plant Molecular Biology* 101(4-5):343-54.
- Malamy, Jocelyn, John P. Carr, Daniel F. Klessig, Ilya Raskin, Daniel F. K. Lessig, and Ilya Raskin. 1990. "Salicylic Acid: A Likely Endogenous Signal in the Resistance Response of Tobacco to Viral Infection." *Science* 250(5):1002-4.
- Mao, Guohong, Xiangzong Meng, Yidong Liu, Zuyu Zheng, Zhixiang Chen, and Shuqun Zhang. 2011. "Phosphorylation of a WRKY Transcription Factor by Two Pathogen-Responsive MAPKs Drives Phytoalexin Biosynthesis in Arabidopsis." *Plant Cell* 23(4):1639-53.
- Mattera, Rafael, Sang Yoon Park, Raffaella De Pace, Carlos M. Guardia, and Juan S. Bonifacino. 2017. "AP-4 Mediates Export of ATG9A from the Trans-Golgi Network to Promote Autophagosome Formation." *Proceedings of the National Academy of Sciences of the United States of America* 114(50):E10697-706.
- McKenna, Aaron, Matthew Hanna, Eric Banks, Andrey Sivachenko, Kristian Cibulskis, Andrew Kernytsky, Kiran Garimella, David Altshuler, Stacey Gabriel, Mark Daly, and Mark A. DePristo. 2010. "The Genome Analysis Toolkit: A MapReduce Framework for Analyzing next-Generation DNA Sequencing Data." *Genome Research* 20(9):1297-1303.
- Melotto, Maeli, Li Zhang, Paula R. Oblessuc, and Sheng Yang He. 2017. "Stomatal Defense a Decade Later." *Plant Physiology* 174(2):561-71.
- Mersmann, Sophia, Gildas Bourdais, Steffen Rietz, and Silke Robatzek. 2010. "Ethylene Signaling Regulates Accumulation of the FLS2 Receptor and Is Required for the Oxidative Burst Contributing to Plant Immunity." *Plant Physiology* 154(1):391-400.
- Métraux, J. P., H. Signer, J. Ryals, E. Ward, M. Wyss-Benz, J. Gaudin, K. Raschdorf, E. Schmid, W. Blum, and B. Inverardi. 1990. "Increase in Salicylic Acid at the Onset of Systemic Acquired Resistance in Cucumber." *Science* 250(4983).
- Mishina, Tatiana E. and Jürgen Zeier. 2006. "The Arabidopsis Flavin-Dependent Monooxygenase FMO1 Is an Essential Component of Biologically Induced Systemic Acquired Resistance." *Plant Physiology* 141(4):1666-75.
- Mohnike, Lennart, Dmitriy Rekhter, Weijie Huang, Kirstin Feussner, Hainan Tian, Cornelia Herrfurth, Yuelin Zhang, and Ivo Feussner. 2021. "The Glycosyltransferase UGT76B1 Modulates N-Hydroxy-Pipecolic Acid Homeostasis and Plant Immunity." *Plant Cell*

33(3):735–49.

- Monaghan, Jacqueline and Cyril Zipfel. 2012. “Plant Pattern Recognition Receptor Complexes at the Plasma Membrane.” *Current Opinion in Plant Biology* 15(4):349–57.
- Moreno-De-Luca, Andres, Sandra L. Helmers, Hui Mao, Thomas G. Burns, Amanda M. A. Melton, Karen R. Schmidt, Paul M. Fernhoff, David H. Ledbetter, and Christa L. Martin. 2011. “Adaptor Protein Complex-4 (AP-4) Deficiency Causes a Novel Autosomal Recessive Cerebral Palsy Syndrome with Microcephaly and Intellectual Disability.” *Journal of Medical Genetics* 48(2):141–44.
- Müdsam, Christina, Paul Wollschläger, Norbert Sauer, and Sabine Schneider. 2018. “Sorting of Arabidopsis NRAMP3 and NRAMP4 Depends on Adaptor Protein Complex AP4 and a Dileucine-Based Motif.” *Traffic* 19(7):503–21.
- Narusaka, Mari, Ken Shirasu, Yoshiteru Noutoshi, Yasuyuki Kubo, Tomonori Shiraishi, Masaki Iwabuchi, and Yoshihiro Narusaka. 2009. “RRS1 and RPS4 Provide a Dual Resistance-Gene System against Fungal and Bacterial Pathogens.” *Plant Journal* 60(2):218–26.
- Návarová, Hana, Friederike Bernsdorff, Anne-Christin Döring, and Jürgen Zeier. 2012. “Pipelicolic Acid, an Endogenous Mediator of Defense Amplification and Priming, Is a Critical Regulator of Inducible Plant Immunity.” *The Plant Cell* 24(December):5123–41.
- Nawrath, Christiane and Jean Pierre Métraux. 1999. “Salicylic Acid Induction-Deficient Mutants of Arabidopsis Express PR-2 and PR-5 and Accumulate High Levels of Camalexin after Pathogen Inoculation.” *Plant Cell* 11(8):1393–1404.
- Neuhaus, Jean Marc, Liliane Sticher, Frederick Meins, and Thomas Boller. 1991. “A Short C-Terminal Sequence Is Necessary and Sufficient for the Targeting of Chitinases to the Plant Vacuole.” *Proceedings of the National Academy of Sciences of the United States of America* 88(22):10362–66.
- Ngou, Bruno Pok Man, Pingtao Ding, and Jonathan D. G. Jones. 2022. “Thirty Years of Resistance: Zig-Zag through the Plant Immune System.” *The Plant Cell* 1–32.
- Park, Sang Wook, Evans Kaimoyo, Dharendra Kumar, Stephen Mosher, and Daniel F. Klessig. 2007. “Methyl Salicylate Is a Critical Mobile Signal for Plant Systemic Acquired Resistance.” *Science* 318(5847):113–16.
- Qin, Jun, Kailun Wang, Lifan Sun, Haiying Xing, Sheng Wang, Lin Li, She Chen, Hui Shan Guo, and Jie Zhang. 2018. “The Plant-Specific Transcription Factors CBP60G and SARD1

- Are Targeted by a Verticillium Secretory Protein VDSCP41 to Modulate Immunity.” *ELife* 7:1–25.
- Reddy, Vaka S., Gul S. Ali, and Anireddy S. N. Reddy. 2002. “Genes Encoding Calmodulin-Binding Proteins in the Arabidopsis Genome.” *Journal of Biological Chemistry* 277(12):9840–52.
- Rekhter, Dmitriy, Yuli Ding, Kirstin Feussner, Krzysztof Zienkiewicz, Volker Lipka, Marcel Wiermer, Yuelin Zhang, and Ivo Feussner. 2019. “Isochorismate-Derived Biosynthesis of the Plant Stress Hormone Salicylic Acid.” *Nature* 502(August):498–502.
- Ribnicky, David M., Vladimir Shulaev, and Ilya Raskin. 1998. “Intermediates of Salicylic Acid Biosynthesis in Tobacco.” *Plant Physiol* 118:565–72.
- Ribot, Cécile, Judith Hirsch, Sandrine Balzergue, Didier Tharreau, Jean Loup Nottéghem, Marc Henri Lebrun, and Jean Benoit Morel. 2008. “Susceptibility of Rice to the Blast Fungus, *Magnaporthe Grisea*.” *Journal of Plant Physiology* 165(1):114–24.
- Ross, A. Frank. 1961. “Systemic Acquired Resistance Induced by Localized Virus Infections in Plants.” *Virology* 14(3):340–58.
- Ryals, John, Kris Weymann, Kay Lawton, Leslie Friedrich, Daniel Ellis, Henry York Steiner, Jay Johnson, Terrence P. Delaney, Taco Jesse, Pieter Vos, and Scott Uknes. 1997. “The Arabidopsis NIM1 Protein Shows Homology to the Mammalian Transcription Factor Inhibitor I κ B.” *Plant Cell* 9(3):425–39.
- Sato, Sakihito Kitajima and Fumihiko. 1999. “Plant Pathogenesis-Related Proteins.Pdf.” 125(1):1–8.
- Schlaich, Nikolaus L. and Alan Slusarenko. 2008. “Downy Mildew of Arabidopsis Caused by *Hyaloperonospora Arabidopsidis* (Formerly *Hyaloperonospora Parasitica*).” *Oomycete Genetics and Genomics: Diversity, Interactions, and Research Tools* 4:263–85.
- Schmieder, Robert and Robert Edwards. 2011. “Quality Control and Preprocessing of Metagenomic Datasets.” *Bioinformatics* 27(6):863–64.
- Serrano, Mario, Fania Coluccia, Martha Torres, Floriane L’Haridon, and Jean Pierre Métraux. 2014. “The Cuticle and Plant Defense to Pathogens.” *Frontiers in Plant Science* 5(JUN):1–8.
- Shah, Jyoti, Frank Tsui, and Daniel F. Klessig. 1997. “Characterization of a Salicylic Acid-Insensitive Mutant (Sai1) of Arabidopsis Thaliana, Identified in a Selective Screen Utilizing

- the SA- Inducible Expression of the Tms2 Gene.” *Molecular Plant-Microbe Interactions* 10(1):69–78.
- Shimada, Tomoo, Junpei Takagi, Takuji Ichino, Makoto Shirakawa, and Ikuko Hara-Nishimura. 2018. “Plant Vacuoles.” *Annual Review of Plant Biology* 69(1):123–45.
- Song, Jong Tae, Hua Lu, and Jean T. Greenberg. 2004. “Divergent Roles in Arabidopsis Thaliana Development and Defense of Two Homologous Genes , ABERRANT GROWTH AND DEATH2 and AGD2-LIKE DEFENSE RESPONSE PROTEIN1 , Encoding Novel Aminotransferases.” *The Plant Cell* 16(February):353–66.
- Song, Jong Tae, Hua Lu, John M. McDowell, and Jean T. Greenberg. 2004. “A Key Role for ALD1 in Activation of Local and Systemic Defenses in Arabidopsis.”
- Sun, Tongjun, Lucas Busta, Qian Zhang, Pingtao Ding, Reinhard Jetter, and Yuelin Zhang. 2018. “TGACG-BINDING FACTOR 1 (TGA1) and TGA4 Regulate Salicylic Acid and Piceic Acid Biosynthesis by Modulating the Expression of SYSTEMIC ACQUIRED RESISTANCE DEFICIENT 1 (SARD1) and CALMODULIN-BINDING PROTEIN 60g (CBP60g).” *New Phytologist* 217(1):344–54.
- Sun, Tongjun, Jianhua Huang, Yan Xu, Vani Verma, Beibei Jing, Yulin Sun, Alberto Ruiz Orduna, Hainan Tian, Xingchuan Huang, Shitou Xia, Laurel Schafer, Reinhard Jetter, Yuelin Zhang, and Xin Li. 2019. “Redundant CAMTA Transcription Factors Negatively Regulate the Biosynthesis of Salicylic Acid and N-Hydroxypiceic Acid by Modulating the Expression of SARD1 and CBP60g.” *Molecular Plant* 13(1):144–56.
- Sun, Tongjun, Yaxi Zhang, Yan Li, Qian Zhang, Yuli Ding, and Yuelin Zhang. 2015. “ChIP-Seq Reveals Broad Roles of SARD1 and CBP60g in Regulating Plant Immunity.” *Nature Communications* 6:10159.
- Sun, Tongjun and Yuelin Zhang. 2021. “Short- and Long-Distance Signaling in Plant Defense.” *Plant Journal* 105(2):505–17.
- Sun, Tongjun and Yuelin Zhang. 2022. “MAP Kinase Cascades in Plant Development and Immune Signaling.” *EMBO Reports* 23(2).
- Tian, Hainan, Zhongshou Wu, Siyu Chen, Kevin Ao, Weijie Huang, Hoda Yaghmaiean, Tongjun Sun, Fang Xu, Yanjun Zhang, Shucui Wang, Xin Li, and Yuelin Zhang. 2021. “Activation of TIR Signalling Boosts Pattern-Triggered Immunity.” *Nature* 598(7881):500–503.
- Tian, Wang, Congcong Hou, Zhijie Ren, Chao Wang, Fugeng Zhao, Douglas Dahlbeck,

- Songping Hu, Liying Zhang, Qi Niu, Legong Li, Brian J. Staskawicz, and Sheng Luan. 2019. "A Calmodulin-Gated Calcium Channel Links Pathogen Patterns to Plant Immunity." *Nature* 572(7767):131–35.
- Torrens-Spence, Michael P., Anastassia Bobokalonova, Valentina Carballo, Christopher M. Glinkerman, Tomáš Pluskal, Amber Shen, and Jing Ke Weng. 2019. "PBS3 and EPS1 Complete Salicylic Acid Biosynthesis from Isochorismate in Arabidopsis." *Molecular Plant* 12(12):1577–86.
- De Torres, Marta, Pedro Sanchez, Isabelle Fernandez-Delmond, and Murray Grant. 2003. "Expression Profiling of the Host Response to Bacterial Infection: The Transition from Basal to Induced Defence Responses in RPM1-Mediated Resistance." *Plant Journal* 33(4):665–76.
- Truman, William, Suma Sreekanta, You Lu, Gerit Bethke, Kenichi Tsuda, Fumiaki Katagiri, and Jane Glazebrook. 2013. "The CALMODULIN-BINDING PROTEIN60 Family Includes Both Negative and Positive Regulators of Plant Immunity." *Plant Physiology* 163(4):1741–51.
- Tsuda, Kenichi, Masanao Sato, Jane Glazebrook, Jerry D. Cohen, and Fumiaki Katagiri. 2008. "Interplay between MAMP-Triggered and SA-Mediated Defense Responses." *Plant Journal* 53(5):763–75.
- van Verk, Marcel C., John F. Bol, and Huub J. M. Linthorst. 2011. "WRKY Transcription Factors Involved in Activation of SA Biosynthesis Genes." *BMC Plant Biology* 11:1–12.
- Verkerk, Annemieke J. M. H., Rachel Schot, Belinda Dumeé, Karlijn Schellekens, Sigrid Swagemakers, Aida M. Bertoli-Avella, Maarten H. Lequin, Jeroen Dudink, Paul Govaert, A. L. van Zwol, Jennifer Hirst, Marja W. Wessels, Coriene Catsman-Berrevoets, Frans W. Verheijen, Esther de Graaff, Irenaëus F. M. de Coö, Johan M. Kros, Rob Willemsen, Patrick J. Willems, Peter J. van der Spek, and Grazia M. S. Mancini. 2009. "Mutation in the AP4M1 Gene Provides a Model for Neuroaxonal Injury in Cerebral Palsy." *American Journal of Human Genetics* 85(1):40–52.
- Vernooij, Bernard, Leslie Friedrichya, Roland Reist, Rachida Kolditzjawhar, Eric Ward, Scott Uknes, Helmut Kessmann, and John Ryals. 1994. "Salicylic Acid Is Not the Translocated Signal Responsible for Inducing Systemic Acquired Resistance but Is Required in Signal Transduction." 6(July):959–65.

- Vogt, Thomas. 2010. "Phenylpropanoid Biosynthesis." *Molecular Plant* 3(1):2–20.
- Völz, Ronny, Soon Kap Kim, Jianing Mi, Kiruthiga G. Mariappan, Xiujie Guo, Jean Bigeard, Santiago Alejandro, Delphine Pflieger, Naganand Rayapuram, Salim Al-Babili, and Heribert Hirt. 2018. "The Trihelix Transcription Factor GT2-like 1 (GTL1) Promotes Salicylic Acid Metabolism, and Regulates Bacterial-Triggered Immunity." *PLoS Genetics* 14(10).
- Wan, Li, Kow Essuman, Ryan G. Anderson, Yo Sasaki, Freddy Monteiro, Eui Hwan Chung, Erin Osborne Nishimura, Aaron DiAntonio, Jeffrey Milbrandt, Jeffery L. Dangl, and Marc T. Nishimura. 2019. "TIR Domains of Plant Immune Receptors Are NAD⁺-Cleaving Enzymes That Promote Cell Death." *Science* 365(6455):799–803.
- Wang, Dong, Nita Amornsiripanitch, and Xinnian Dong. 2006. "A Genomic Approach to Identify Regulatory Nodes in the Transcriptional Network of Systemic Acquired Resistance in Plants." *PLoS Pathogens* 2(11):1042–50.
- Wang, Hai, Yuqing Lu, Pei Liu, Wei Wen, Jianhua Zhang, Xiaochun Ge, and Yiji Xia. 2013. "The Ammonium/Nitrate Ratio Is an Input Signal in the Temperature-Modulated, SNC1-Mediated and EDS1-Dependent Autoimmunity of Nudt6-2 Nudt7." *The Plant Journal : For Cell and Molecular Biology* 73(2):262–75.
- Wang, Lin, Kenichi Tsuda, Masanao Sato, Jerry D. Cohen, Fumiaki Katagiri, and Jane Glazebrook. 2009. "Arabidopsis CaM Binding Protein CBP60g Contributes to MAMP-Induced SA Accumulation and Is Involved in Disease Resistance against *Pseudomonas Syringae*." *PLoS Pathogens* 5(2).
- Wang, Lin, Kenichi Tsuda, William Truman, Masanao Sato, Le V. Nguyen, Fumiaki Katagiri, and Jane Glazebrook. 2011. "CBP60g and SARD1 Play Partially Redundant Critical Roles in Salicylic Acid Signaling." *Plant Journal* 67(6):1029–41.
- Wang, Yiming, Stefan Schuck, Jingni Wu, Ping Yang, Anne Christin Döring, Jürgen Zeier, and Kenichi Tsuda. 2018. "A Mpk3/6-Wrky33-Ald1-Pipecolic Acid Regulatory Loop Contributes to Systemic Acquired Resistance[Open]." *Plant Cell* 30(10):2480–94.
- van Wersch, Rowan, Xin Li, and Yuelin Zhang. 2016. "Mighty Dwarfs: Arabidopsis Autoimmune Mutants and Their Usages in Genetic Dissection of Plant Immunity." *Frontiers in Plant Science* 7(NOVEMBER2016):1–8.
- van Wersch, Solveig, Lei Tian, Ryan Hoy, and Xin Li. 2020. "Plant NLRs: The Whistleblowers

- of Plant Immunity.” *Plant Communications* 1(1):100016.
- Wi, Soo Jin, Na Ri Ji, and Ky Young Park. 2012. “Synergistic Biosynthesis of Biphasic Ethylene and Reactive Oxygen Species in Response to Hemibiotrophic *Phytophthora Parasitica* in Tobacco Plants.” *Plant Physiology* 159(1):251–65.
- Wildermuth, Mary C., Julia Dewdney, Gang Wu, and Frederick M. Ausubel. 2001. “Isochorismate Synthase Is Required to Synthesize Salicylic Acid for Plant Defence.” *Nature* 414(November):562–71.
- Wu, Feihua, Yuan Chi, Zhonghao Jiang, Yuanyuan Xu, Ling Xie, Feifei Huang, Di Wan, Jun Ni, Fang Yuan, Xiaomei Wu, Yanyan Zhang, Li Wang, Rui Ye, Benjamin Byeon, Wenhua Wang, Shu Zhang, Matthew Sima, Suping Chen, Minghua Zhu, Jessica Pei, Douglas M. Johnson, Shan Zhu, Xiaoqiang Cao, Christopher Pei, Zijing Zai, Yihao Liu, Tianyi Liu, Gary B. Swift, Weiguo Zhang, Min Yu, Zhangli Hu, James N. Siedow, Xian Chen, and Zhen Ming Pei. 2020. “Hydrogen Peroxide Sensor HPCA1 Is an LRR Receptor Kinase in *Arabidopsis*.” *Nature* 578(7796):577–81.
- Wu, Yue, Di Zhang, Jee Yan Chu, Patrick Boyle, Yong Wang, Ian D. Brindle, Vincenzo De Luca, and Charles Després. 2012. “The *Arabidopsis* NPR1 Protein Is a Receptor for the Plant Defense Hormone Salicylic Acid.” *Cell Reports* 1(6):639–47.
- Xin, Xiu Fang and Sheng Yang He. 2013. “*Pseudomonas Syringae* Pv. Tomato DC3000: A Model Pathogen for Probing Disease Susceptibility and Hormone Signaling in Plants.” *Annual Review of Phytopathology* 51:473–98.
- Xing, Hui-li, Li Dong, Zhi-ping Wang, Hai-yan Zhang, Chun-yan Han, Bing Liu, Xue-chen Wang, and Qi-jun Chen. 2014. “A CRISPR / Cas9 Toolkit for Multiplex Genome Editing in Plants.” *BMC Plant Biology* 14:327.
- Xu, Lei, Hongyu Zhao, Wenyuan Ruan, Minjuan Deng, Fang Wang, Jinrong Peng, Jie Luo, Zhixiang Chen, and Keke Yi. 2017. “ABNORMAL INFLORESCENCE MERISTEM1 Functions in Salicylic Acid Biosynthesis to Maintain Proper Reactive Oxygen Species Levels for Root Meristem Activity in Rice.” *Plant Cell* 29(3):560–74.
- Yalpani, Nasser, Jose León, Michael A. Lawton, and Ilya Raskin. 1993. “Pathway of Salicylic Acid Biosynthesis in Healthy and Virus- Inoculated Tobacco.” *Plant Physiol* 103:315–21.
- Yang, Y., Y. Zhang, P. Ding, K. Johnson, X. Li, and Y. Zhang. 2012. “The Ankyrin-Repeat Transmembrane Protein BDA1 Functions Downstream of the Receptor-Like Protein SNC2

- to Regulate Plant Immunity.” *Plant Physiology* 159(4):1857–65.
- Yoshinari, Akira, Takuya Hosokawa, Taro Amano, Marcel Pascal Beier, Tadashi Kunied, Tomoo Shimada, Ikuko Hara-Nishimur, Satoshi Naito, and Junpei Takano. 2019. “Polar Localization of the Borate Exporter BOR1 Requires AP2-Dependent Endocytosis.” *Plant Physiology* 179(4):1569–80.
- Zeier, Jürgen. 2013. “New Insights into the Regulation of Plant Immunity by Amino Acid Metabolic Pathways.” *Plant, Cell and Environment* 36(12):2085–2103.
- Zeier, Jürgen. 2021. “Metabolic Regulation of Systemic Acquired Resistance.” *Current Opinion in Plant Biology* 62:102050.
- Zhang, Lisha, Chenlei Hua, Rory N. Pruitt, Si Qin, Lei Wang, Isabell Albert, Markus Albert, Jan A. L. van Kan, and Thorsten Nürnberger. 2021. “Distinct Immune Sensor Systems for Fungal Endopolygalacturonases in Closely Related Brassicaceae.” *Nature Plants* 7(9):1254–63.
- Zhang, Yanjun Jun, Li Zhao, Jiangzhe Zhe Zhao, Yujia Jia Li, Jinbin Bin Wang, Rong Guo, Susheng Sheng Gan, Chang-Jun Jun Liu, Kewei Zhang, and Ke Wei Zhanga. 2017. “S5H/DMR6 Encodes a Salicylic Acid 5-Hydroxylase That Fine-Tunes Salicylic Acid Homeostasis.” *Plant Physiology* 175(3):1082–93.
- Zhang, Yaxi, Shaohua Xu, Pingtao Ding, Dongmei Wang, Yu Ti Cheng, Jing He, Minghui Gao, Fang Xu, Yan Li, Zhaohai Zhu, Xin Li, and Yuelin Zhang. 2010. “Control of Salicylic Acid Synthesis and Systemic Acquired Resistance by Two Members of a Plant-Specific Family of Transcription Factors.” *Proceedings of the National Academy of Sciences* 107(42):18220–25.
- Zhang, Yaxi, Yuanai Yang, Bin Fang, Patrick Gannon, Pingtao Ding, Xin Li, and Yuelin Zhang. 2010. “Arabidopsis Snc2-1D Activates Receptor-Like Protein-Mediated Immunity Transduced through WRKY70.” *The Plant Cell* 22(9):3153–63.
- Zhang, Yuelin, Weihua Fan, Mark Kinkema, Xi Li, and Xinnian Dong. 1999. “Interaction of NPR1 with Basic Leucine Zipper Protein Transcription Factors That Bind Sequences Required for Salicylic Acid Induction of the PR-1 Gene.” *Proceedings of the National Academy of Sciences of the United States of America* 96(11):6523–28.
- Zhang, Yuelin, Jane Glazebrook, and Xin Li. 2007. “Identification of Components in Disease-Resistance Signaling in *Arabidopsis* by Map-Based Cloning.” Pp. 69–78 in *Plant-Pathogen*

Interactions. Vol. 1. New Jersey: Humana Press.

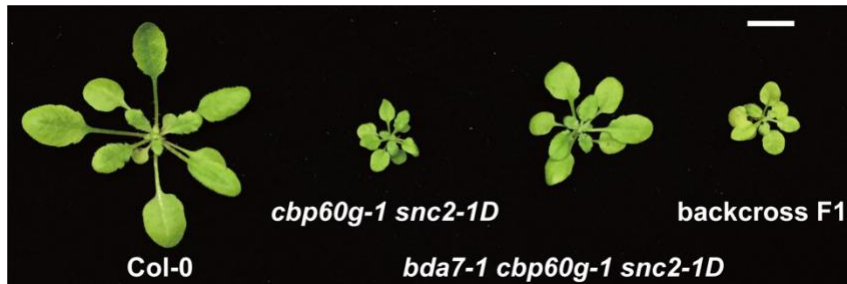
- Zhang, Yuelin and Xin Li. 2019. "Salicylic Acid: Biosynthesis, Perception, and Contributions to Plant Immunity." *Current Opinion in Plant Biology* 50:29–36.
- Zhang, Yuelin, Yuelin Zhang, Mark J. Tessaro, Mark J. Tessaro, Michael Lassner, Michael Lassner, Xin Li, and Xin Li. 2003. "Knockout Analysis of Arabidopsis Transcription Factors TGA2 , TGA5 , and TGA6 Reveals Their Redundant and Essential Roles in Systemic Acquired Resistance." *The Plant Cell* 15(November):2647–53.
- Zhou, Jian Min and Yuelin Zhang. 2020. "Plant Immunity: Danger Perception and Signaling." *Cell* 181(5):978–89.
- Zhou, Jun Ma, Youssef Trifa, Herman Silva, Dominique Pontier, Eric Lam, Jyoti Shah, and Daniel F. Klessig. 2000. "NPR1 Differentially Interacts with Members of the TGA/OBF Family of Transcription Factors That Bind an Element of the PR-1 Gene Required for Induction by Salicylic Acid." *Molecular Plant-Microbe Interactions* 13(2):191–202.
- Zhu, Wangsheng, Lei Li, Benjamin Neuhäuser, Michael Thelen, Mingyu Wang, Junbin Chen, Luyang Wei, Kavita Venkataramani, Moises Exposito-Alonso, Chang Liu, Jakob Keck, A. Cristina Barragan, Rebecca Schwab, Ulrich Lutz, Uwe Ludewig, and Detlef Weigel. 2021. "Small Peptides Modulate the Immune Function of the Ion Channel-like Protein ACD6 in Arabidopsis Thaliana." *BioRxiv* 2021.01.25.428077.
- Zipfel, Cyril. 2014. "Plant Pattern-Recognition Receptors." *Trends in Immunology* 35(7):345–51.

Appendices

Appendix A - Supplementary figures of Chapter 2

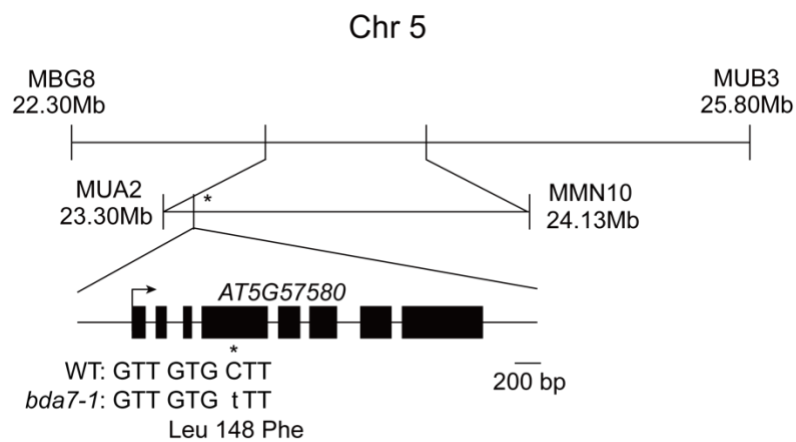
A.1 *bda7-1* is recessive.

Morphologies of 3-week-old soil-grown plants of Col-0, *cbp60g-1 snc2-1D*, *bda7-1 cbp60g-1 snc2-1D* and the backcrossed F1 plant under long-day condition. Scale bar is 1 cm.



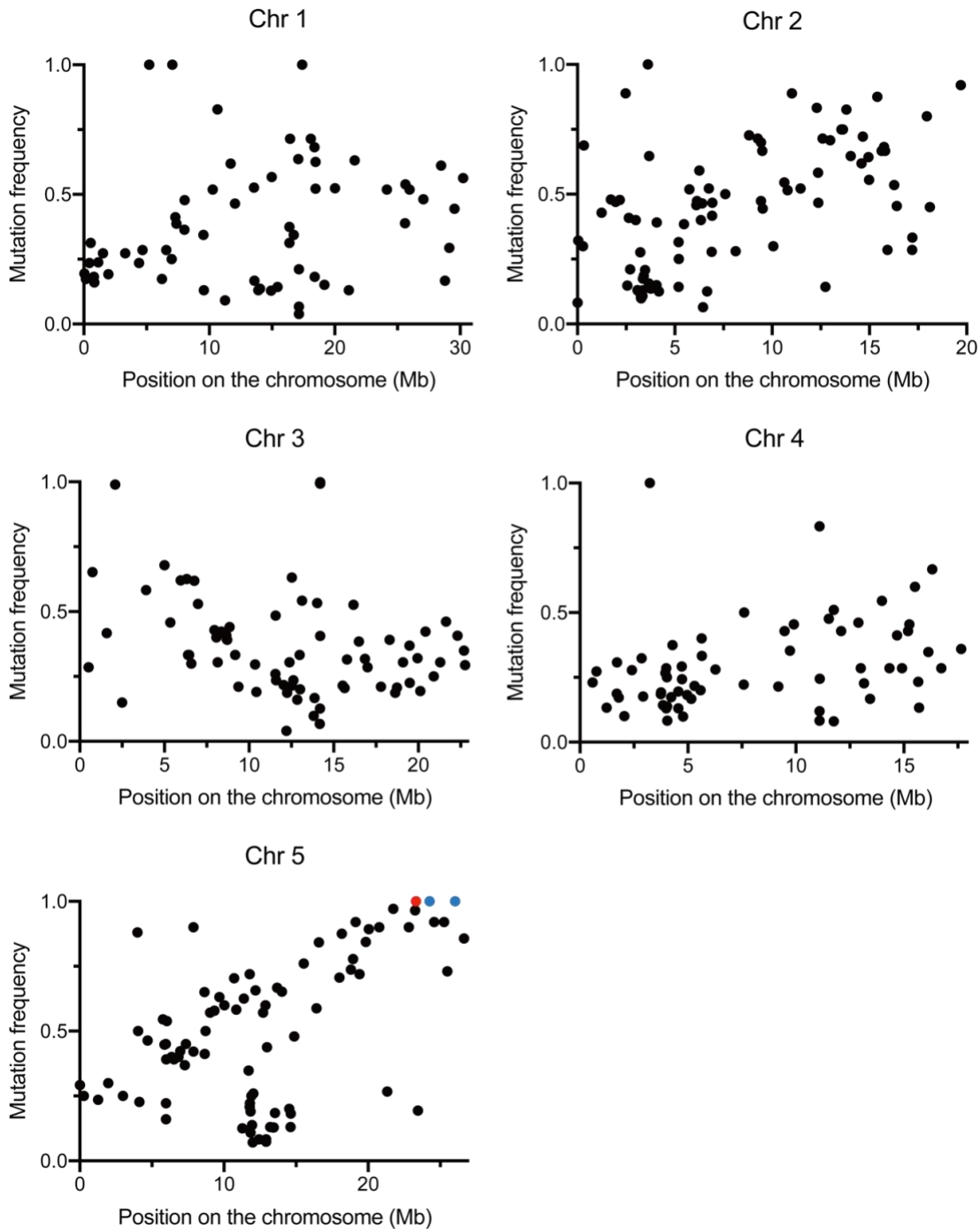
A.2 Map position and the mutation in *bda7-1*.

The asterisk marks the position of *bda7-1*.

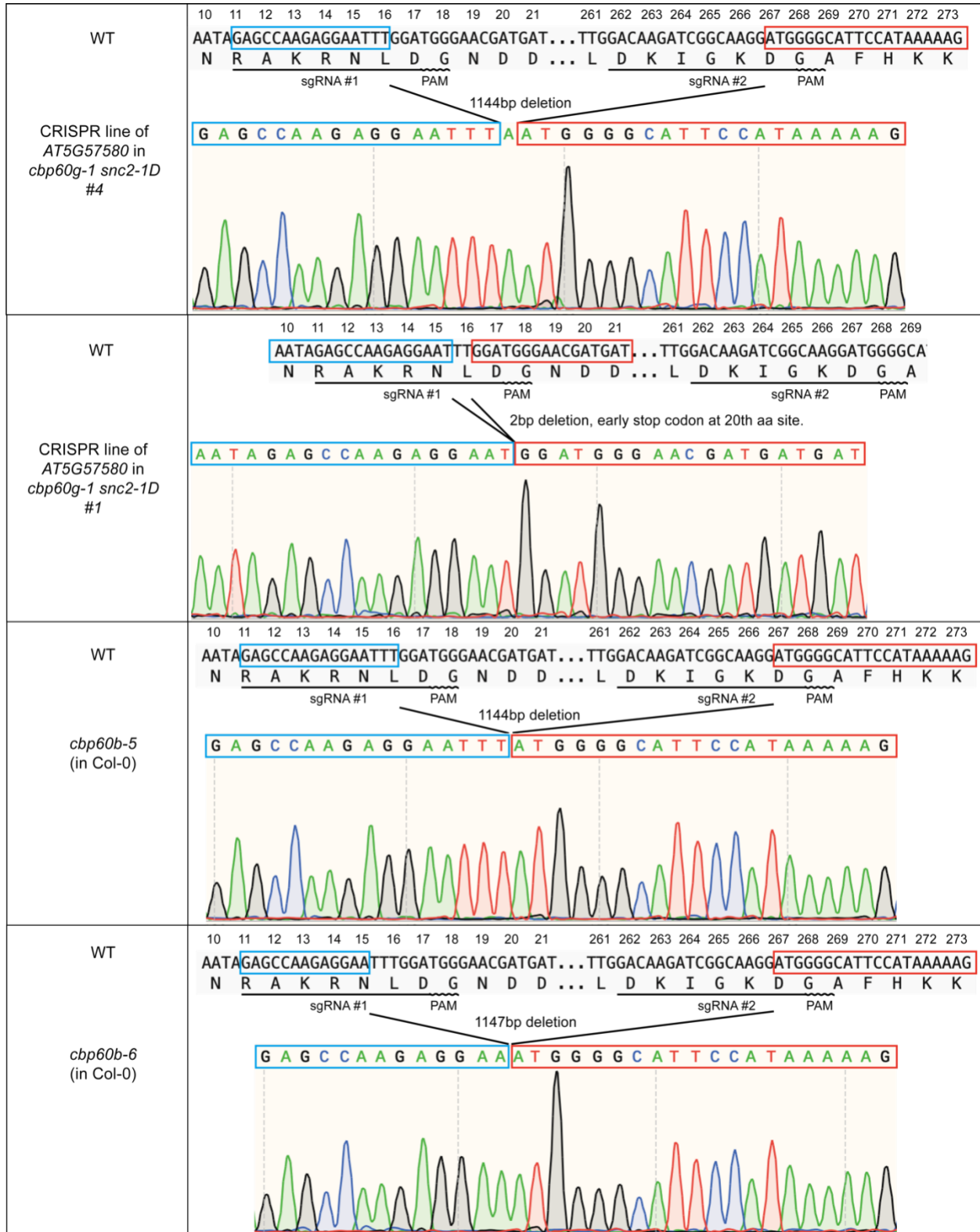


A.3 Dot plots of frequency (f) of SNP mutations on five chromosomes in *bda7-1 cbp60g-1 snc2-ID*, as derived from Illumina sequencing.

Colored dots represent mutations with a $f=1$ on chromosome five. The red dot indicates the mutation with a $f=1$ within the mapped region.

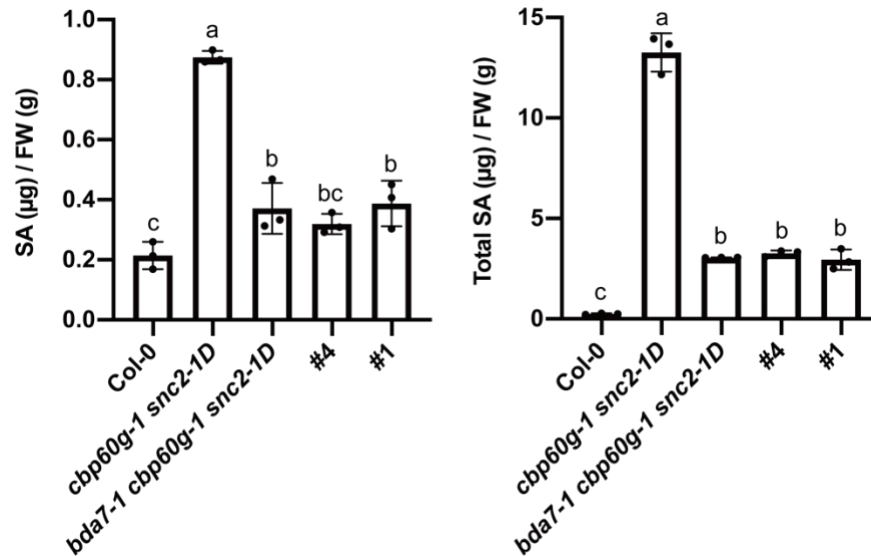


A.4 Sequences of deletion mutations in *CBP60b* generated by CRISPR/Cas9.



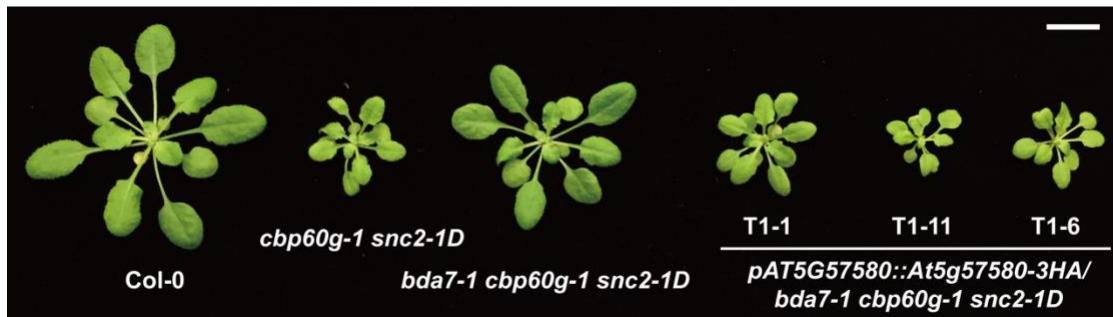
A.5 Free and total SA levels in wild type (Col-0), *cbp60g-1 snc2-1D*, *bda7-1 cbp60g-1 snc2-1D*, and two CRISPR lines of *AT5G57580* in *cbp60g-1 snc2-1D* background (#4 and #1).

Error bars represent standard deviations. Letters indicate statistical differences ($P < 0.05$, one-way ANOVA followed by Tukey's multiple comparisons test; $n = 3$).



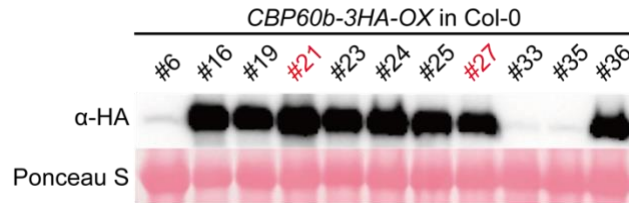
A.6 *bda7-1* can be complemented by *AT5G57580-3HA* driven by its native promoter.

Morphologies of 4-week-old soil-grown plants of the indicated genotypes under long-day condition. Scale bar is 1 cm.



A.8 CBP60b protein levels in the three-week-old soil-grown overexpression lines.

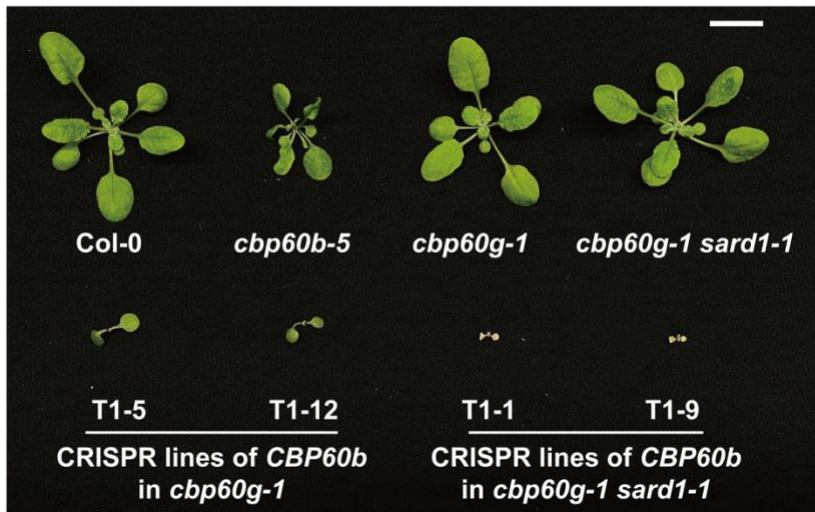
The loading is shown by Ponceau S staining of a non-specific band. The overexpression lines #21 and #27 were selected for further analysis.



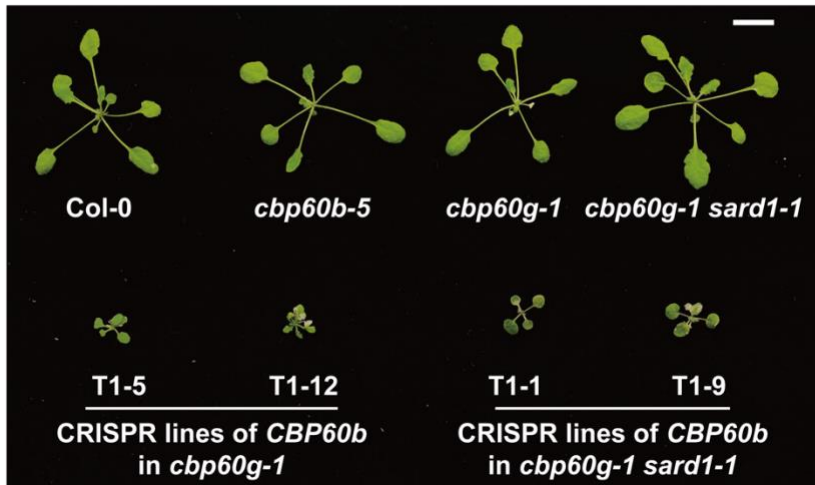
A.9 Suppression of the dwarf morphologies of *cbp60b-5*, *cbp60b cbp60g-1* and *cbp60b cbp60g-1 sard1-1* by high temperature.

Morphologies of 3-week-old soil-grown plants of the indicated genotypes under long-day condition at 22 °C (A) and 28 °C (B). Scale bar is 1 cm.

A



B



A.10 List of primers used in the study described in chapter 2. Information is assorted by different applications of the primers.

Primers for quantitative PCR:

Gene ID	Forward primer	Reverse primer
AT2G37620	ACT1-F: cgatgaagetcaatccaaacga	ACT1-R: cagagtcgagcacaataccg

AT2G14610	PR1-RT-F2: AGGCAACTGCAGACTCATAC	PR1-RT-R2: TTGTTACACCTCACTTTGGC
AT1G74710	ICS1-F101-RT: GTCGTTTCGGTTACAGGTTCC	ICS1-R102-RT: ATTAAACTCAACCTGAGGGAC
AT1G19250	FMO1-F101-RT: GGAGATATTCAGTGGCATGC	FMO1-R102-RT: TTTGGTTAGGCCTATCATGG
AT1G73805	SARD1-RT-NF: TCAAGGCGTTGTGGTTTGTG	SARD1-RT-NR: CGTCAACGACGGATAGTTTC

Primers for genotyping:

Gene ID	Forward primer	Reverse primer	Usage
AT5G57580	AT5G57580-dele-F: gcgagtcattctcgagttgtt	AT5G57580-dele-R: CACAACACCGACATTCCT TG	CBP60b deletion presence
AT5G57580	At5g57580-homo-F: AGGAAAGAGACCGTTGC TGA	AT5G57580-dele-R: CACAACACCGACATTCCT TG	CBP60b deletion homozygosity
AT5G57580	AT5G57580-dele-F: gcgagtcattctcgagttgtt	Bda7-MT-R: TTCAGTGTTAAAGTCACCC TCAtA	cbp60b-4 presence

AT5G57580	Bda7-WT-F: GCAAAGCTTCACATTGT TGTcC	AT5G57580-dele-R: CACAACACCGACATTCCT TG	cbp60b-4 homozygos ity
AT5G26920	CBP60g-TDNA-F: TGTTTCGGTGGACTTGTG AC	CBP60g-TDNA-R: TAAATCCCTCAACGGTCC AG	CBP60g TDNA homozygos ity
AT1G73805	SARD1-TDNA-F: CTTCAGTGTCGGAGTAG TCG	SARD1-TDNA-R: caagacctcttaacctaac	SARD1 TDNA homozygos ity
AT3G48090	EDS1-del-F: AGAACGTAAGACAGGGT TTG	EDS1-del-R: gatggagtctatattaaagagacg	EDS1 deletion presence
AT3G48090	EDS1-del-F: AGAACGTAAGACAGGGT TTG	EDS1-homo-R: CATTCTCCTCTGCGAGAC	EDS1 TDNA homozygos ity

Primers for ChIP-qPCR:

Gene ID	Forward primer	Reverse primer
---------	----------------	----------------

AT1G73805	SARD1pro0.3kb-chipF: ggaaccgtccattgtcaac	SARD1pro0.3kb-chipR: ttcgaagaacgacaaaggaaa
AT1G73805	SARD1pro-1kbF: gcacgacaagtttgagagga	SARD1pro-1kbR: agaaatgtcatgctgtaaaggaa

Primers for cloning:

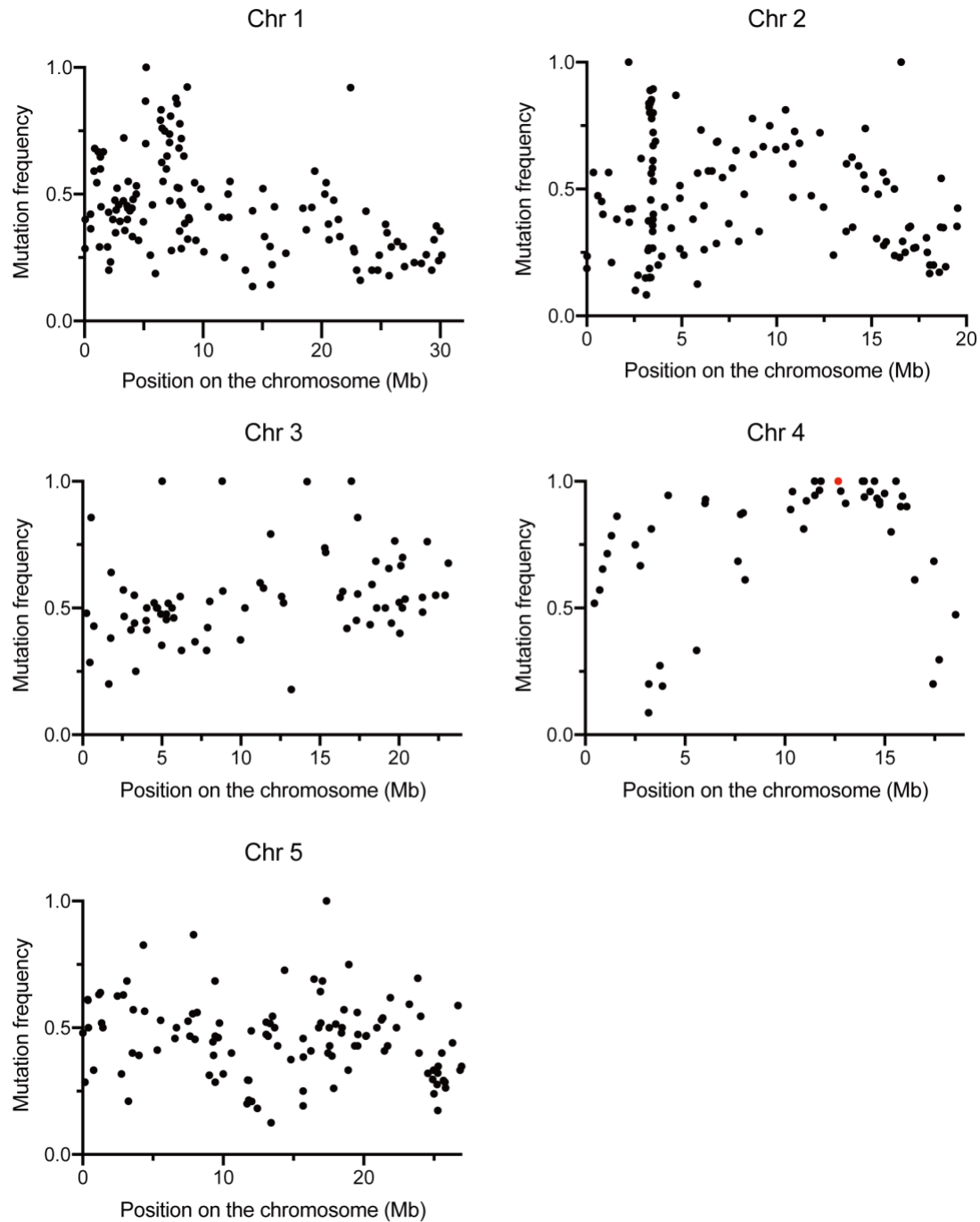
Purpose	Primer	Sequence
CRISPR-deletion (CBP60b)	AT5G57580-T1-BSF	ATATATGGTCTCGATTGGAGCCA AGAGGAATTTGGAGTT
CRISPR-deletion (CBP60b)	AT5G57580-T2-BSR	ATTATTGGTCTCGAAACCATCCTT GCCGATCTTGTC
CRISPR-deletion (CBP60b)	AT5G57580-T1-F0	TGGAGCCAAGAGGAATTTGGAGT TTTAGAGCTAGAAATAGC
CRISPR-deletion (CBP60b)	AT5G57580-T2-R0	AACCATCCTTGCCGATCTTGTC ATCTCTTAGTCGACTCTAC
pCambia1300-35S- At5g57580-3HA	AT5G57580-atgKpnI-F	ccggggtaccggttagATGATGGATAGTG GTAA
pCambia1300-35S- At5g57580-3HA	AT5G57580- nstopBamHi-R	CGCggatccTTCGCCATCTTCATCAT CATC
pBasta- pAt5g57580::At5g57580 -3HA	AT5G57580-KpnI-F	ccggggtaccCTGGCGTCTTGGAGTAG AGg

pBasta- pAt5g57580::At5g57580 -3HA	AT5G57580-PstI-R	AAAActgcagTTCGCCATCTTCATCA TCATC
--	------------------	-------------------------------------

Appendix B - Supplementary figures of Chapter 3

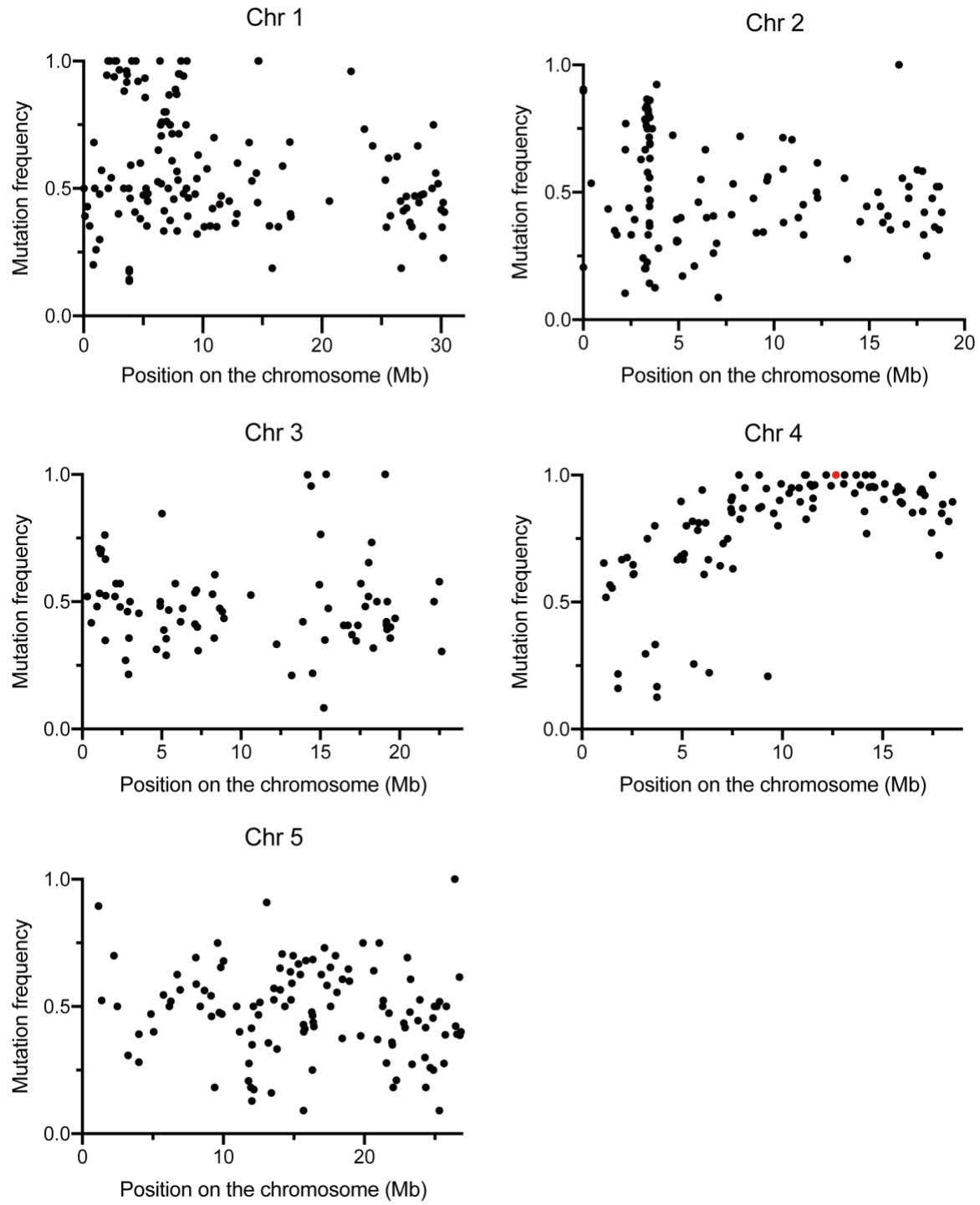
B.1 Dot plots of frequency (f) of SNP mutations on five chromosomes in *bda6-1 cbp60g-1 snz2-1D*, as derived from Illumina sequencing.

The red dot indicates the mutation in *AT4G24550*.



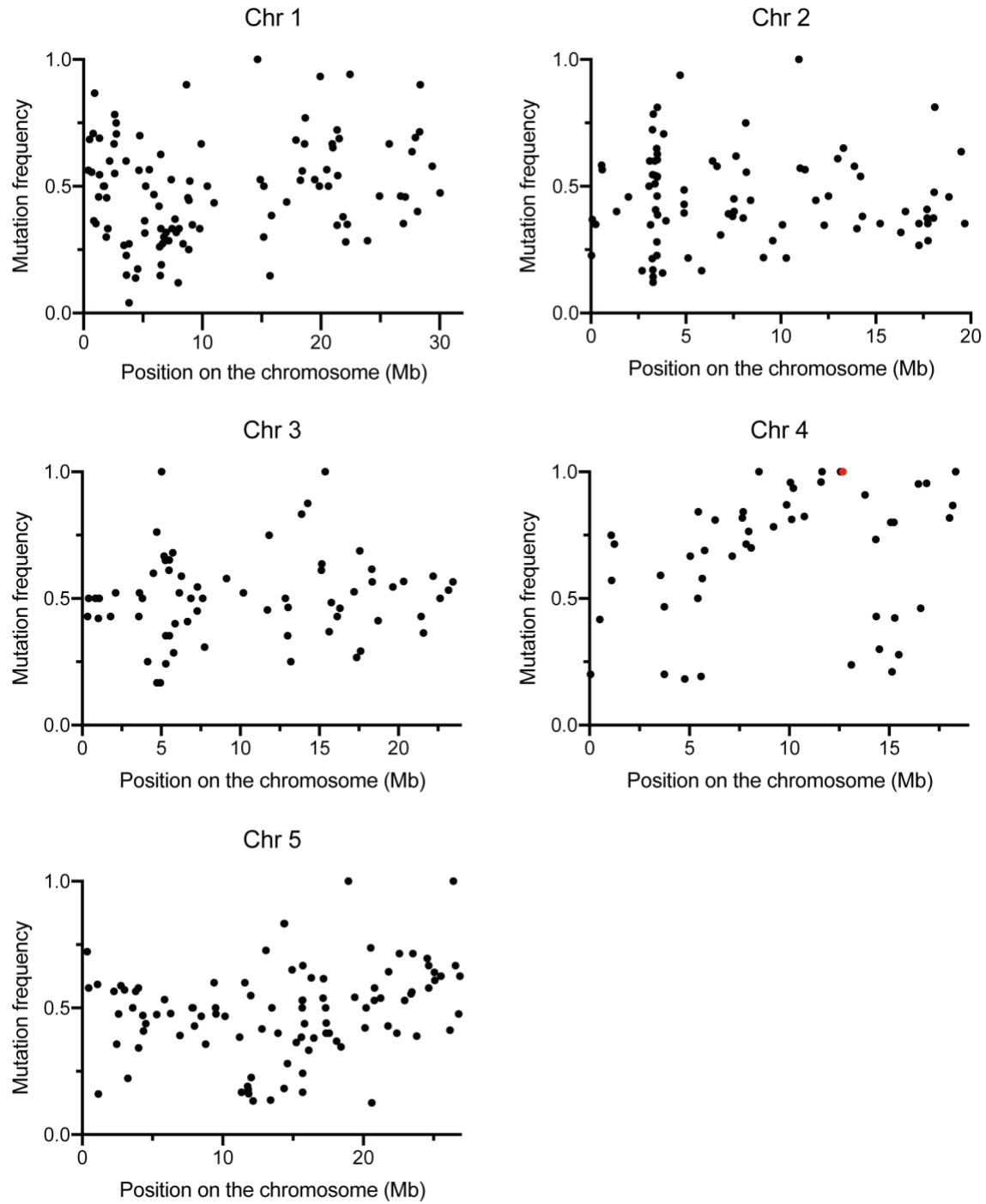
B.2 Dot plots of frequency (f) of SNP mutations on five chromosomes in *bda6-2 cbp60g-1 snc2-ID*, as derived from Illumina sequencing.

The red dot indicates the mutation in *AT4G24550*.

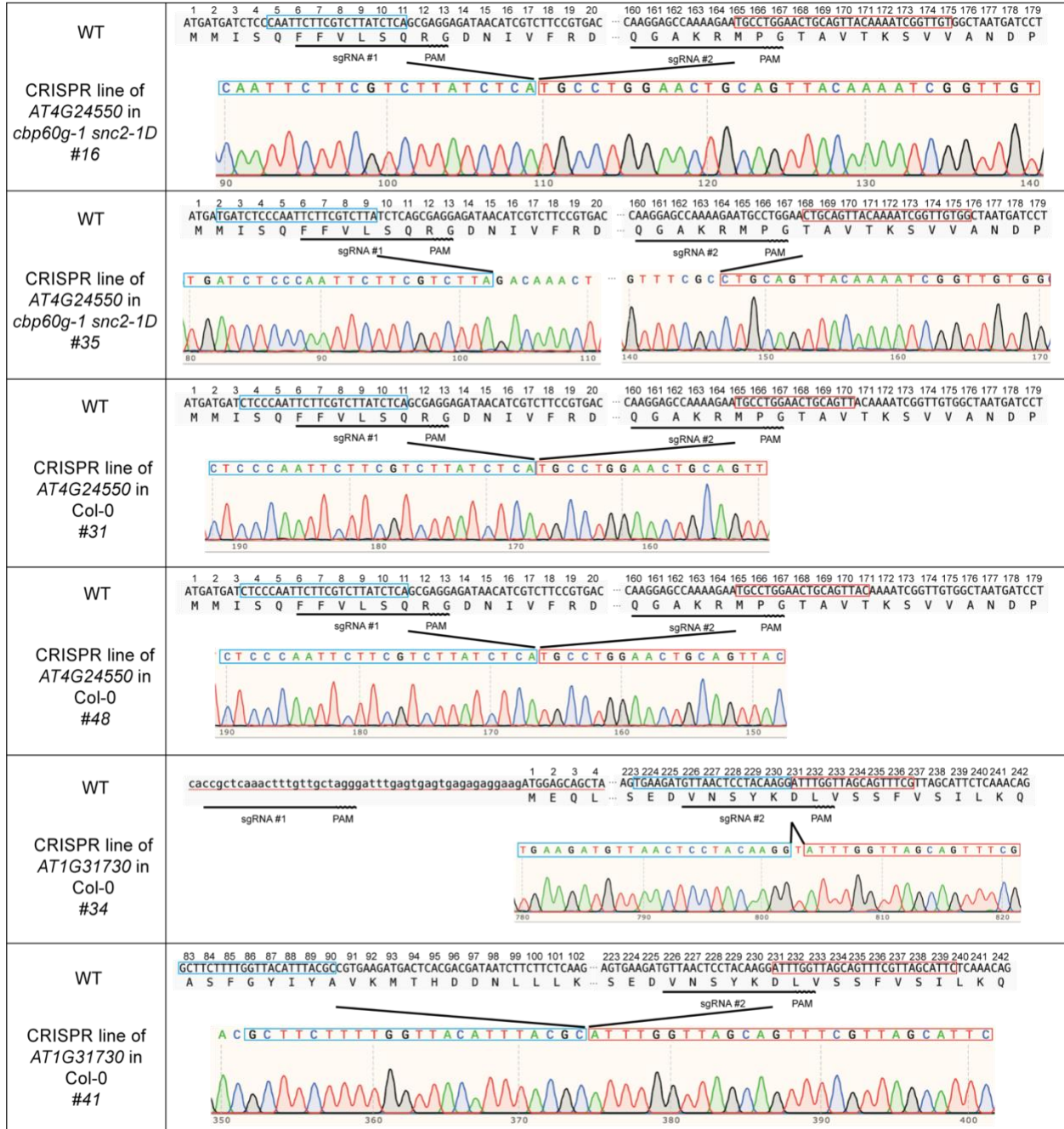


B.3 Dot plots of frequency (f) of SNP mutations on five chromosomes in *bda6-3 cbp60g-1 snc2-ID*, as derived from Illumina sequencing.

The red dot indicates the mutation in *AT4G24550*.



B.4 Sequences of deletion mutations in *AP4M* and *AP4E* generated by CRISPR/Cas9.



B.5 List of primers used in the study described in Chapter 3. Information is assorted by different applications of the primers.

Primers for quantitative PCR:

Gene ID	Forward primer	Reverse primer
AT2G37620	ACT1-F: cgatgaagctcaatccaaacga	ACT1-R: cagagtcgagcacaataaccg
AT2G14610	PR1-RT-F2: AGGCAACTGCAGACTCATAC	PR1-RT-R2: TTGTTACACCTCACTTTGGC
AT1G74710	ICS1-F101-RT: GTCGTTCCGGTTACAGGTTCC	ICS1-R102-RT: ATTAAACTCAACCTGAGGGAC

Primers for genotyping:

Gene ID	Forward primer	Reverse primer	Usage
AT4G24550	AT4G24550-dele-F: acctcaccaccagacacaca	AT4G24550-dele-R: cttgccatatcaaaccacc	AP4M deletion
AT4G24550	AT4G24550-homo-F: TTGTGCTCGTGTATGAGT TGC	AT4G24550-seq-R2: tgtttgctgaaatttagGCTGA	Sequencing
AT1G31730	At1g31730-dele-F: atttcgcatggtccaatttc	At1g31730-dele-R: TCAATCGACCAAGACCAT CA	AP4E deletion

Primers for cloning:

Purpose	Primer	Sequence

CRISPR-deletion (AP4M)	At4g24550-BsFF0	ATATATGGTCTCGATTGTCTTCGT CTTATCTCAGCGGTTTTAGAGCTA GAAATAGC
CRISPR-deletion (AP4M)	At4g24550-BsRR0	ATTATTGGTCTCGAAACAAGGAG CCAAAAGAATGCCCAATCTCTTA GTCGACTCTAC
CRISPR-deletion (AP4E)	At1g31730-BsFF0	ATATATGGTCTCGATTGccgctcaaact ttgttgctGTTTTAGAGCTAGAAATAG C
CRISPR-deletion (AP4E)	At1g31730-BsRR0	ATTATTGGTCTCGAAACAATCCTT GTAGGAGTTAACCAATCTCTTAGT CGACTCTAC
pBasta-np-AP4M	24550-npStuI-F	gagaAGGCCTtcaatgggcatatgttttg
pBasta-np-AP4M	24550-XbaI-R	TGCtctagaTCATATCCTAGCCACAT AAGAATTCG
pBasta-35S-AP4M-2HA- TurboID	24550-oxXhoI-F	ccgCTCGAGATGATGATCTCCCAA TTCTTCG
pBasta-35S-AP4M-2HA- TurboID	24550-nstop-XbaI-R	TGCtctagaTATCCTAGCCACATAAG AATTCG
pBasta-35s-24550-3flag	24550-oxXhoI-F	ccgCTCGAGATGATGATCTCCCAA TTCTTCG
pBasta-35s-24550-3flag	24550-nstop-XbaI-R	TGCtctagaTATCCTAGCCACATAAG AATTCG

pBasta-35S-BDA1-2HA-TurboID	BDA1-KpnI-F	cggGGTACCgtaagtATGGATTCAAA ATTGCT
pBasta-35S-BDA1-2HA-TurboID	BDA1-BamHI-R	cgcGGATCCggTTAAACCATGTTCT TGAAGTTG
pBasta-35s-BDA1-3flag	BDA1-KpnI-F	cggGGTACCgtaagtATGGATTCAAA ATTGCT
pBasta-35s-BDA1-3flag	BDA1-BamHI-R	cgcGGATCCggTTAAACCATGTTCT TGAAGTTG